AD NUMBER
AD889187
LIMITATION CHANGES
TO: **Approved for public release; distribution is unlimited.**
FROM: **Distribution authorized to U.S. Gov't. agencies only; Test and Evaluation; NOV 1971. Other requests shall be referred to Air Force Armament Laboratory, DLRA, Eglin AFB, FL 32542.**
AUTHORITY
afatl ltr 12 apr 1974

AEDC-TR-71-247
AFATL-TR-71-144

cy. 2

TRANSONIC STATIC STABILITY CHARACTERISTICS OF BOMBLET MUNITION MODELS USED IN THE EVALUATION OF THE ZERO-CONING AERODYNAMIC DISPERSAL TECHNIQUE

T. O. Shadow

ARO, Inc.

November 1971

PROPULSION WIND TUNNEL FACILITY
ARNOLD ENGINEERING DEVELOPMENT CENTER
AIR FORCE SYSTEMS COMMAND
ARNOLD AIR FORCE STATION, TENNESSEE

NOTICES

When U. S. Government drawings specifications, or other data are used for any purpose other than a definitely related Government procurement operation, the Government thereby incurs no responsibility nor any obligation whatsoever, and the fact that the Government may have formulated, furnished, or in any way supplied the said drawings, specifications, or other data, is not to be regarded by implication or otherwise, or in any manner licensing the holder or any other person or corporation, or conveying any rights or permission to manufacture, use, or sell any patented invention that may in any way be related thereto.

Qualified users may obtain copies of this report from the Defense Documentation Center.

References to named commercial products in this report are not to be considered in any sense as an endorsement of the product by the United States Air Force or the Government.

TRANSONIC STATIC STABILITY CHARACTERISTICS OF BOMBLET MUNITION MODELS USED IN THE EVALUATION OF THE ZERO-CONING AERODYNAMIC DISPERSAL TECHNIQUE

T. O. Shadow
ARO, Inc.

FOREWORD

The work reported herein was sponsored by the Air Force Armament Laboratory (DLRA/M. J. Bouffard), Armament Development and Test Center, Air Force Systems Command (AFSC), under Program Element 62602F, Project 2547.

The test results presented were obtained by ARO, Inc. (a subsidiary of Sverdrup & Parcel and Associates, Inc.), contract operator of the Arnold Engineering Development Center (AEDC), AFSC, Arnold Air Force Station, Tennessee, under Contract F40600-72-C-0003. The test was conducted September 16 and 17, 1971, under ARO Project No. PC0205. The manuscript was submitted for publication on October 12, 1971.

This technical report has been reviewed and is approved.

George F. Garey
Lt Colonel, USAF
AF Representative, PWT
Directorate of Test

Duncan W. Rabey, Jr.
Colonel, USAF
Director of Test

ABSTRACT

A wind-tunnel investigation was conducted in the Aerodynamic Wind Tunnel (4T) to determine the static stability characteristics of bomblet munition models designed for the evaluation of the Zero-Coning Aerodynamic Dispersal Technique. Force and moment data were recorded at Mach numbers from 0.3 to 1.2 at a constant Reynolds number of 2.2 x 10^6 per foot. Angle of attack was varied from -8 to 27 deg. Roll angle was varied from 0 to 30 deg on one configuration. The test results indicate that the configurations tested are marginally acceptable to achieve Zero-Coning dispersion.

CONTENTS

APPENDIX
ILLUSTRATIONS

Figure

Figure | Page

NOMENCLATURE

C_A	Axial-force coefficient, measured axial force/$q_\infty S$
C_m	Pitching-moment coefficient (see Fig. 3 for moment reference location), measured pitching moment/$q_\infty Sd$
C_N	Normal-force coefficient, measured normal force/$q_\infty S$
d	Model body diameter (reference diameter). 0.2500 ft
M_∞	Free-stream Mach number
q_∞	Free-stream dynamic pressure, psf
Re/ft	Reynolds number per foot
S	Model cross-sectional area (reference area), 0.0491 sq ft
α	Model angle of attack with respect to tunnel centerline, deg
ϕ	Model roll angle, deg

MODEL NOMENCLATURE

B_S	Cylindrical centerbody, d = 0.2500 ft, S = 0.0491 sq ft
N_{S1}	Blunted nose, 0.750-in. shoulder radius
N_{S2}	Spherical nose, 1.500-in. spherical radius
N_{S3}	Blunted nose, 0.375-in. shoulder radius
N_{S4}	Spherical-segment nose, 2.250-in. spherical radius
A_{S1}	Cylindrical afterbody
A_{S2}	Boattail afterbody

$F_{S2,5}$ Rectangular fins for cylindrical afterbody; 2 and 5 for 3.466- and 3.840-in. spans, respectively

$F_{S3,6}$ Rectangular fins for boattail afterbody; 3 and 6 for 3.466- and 3.840-in. spans, respectively

SECTION I
INTRODUCTION

A wind-tunnel investigation of a group of munition models was conducted in the Aerodynamic Wind Tunnel (4T), Propulsion Wind Tunnel Facility (PWT), to determine the static stability characteristics for use in the evaluation of the Zero-Coning aerodynamic dispersal technique. The tests were conducted at Mach numbers from 0.3 to 1.2 at a constant Reynolds number of 2.2×10^6 per foot.

With the Zero-Coning concept, effective bomblet dispersion attributable to lift is achieved by restriction of the rotation of the angle-of-attack plane in space. A bomblet which is unstable at low angles of attack, stable at high angles of attack, and has lift which is insensitive to roll angle will disperse along a curved flight path.

Previous investigations of the Zero-Coning concept reported in Refs. 1 through 4 have provided static and dynamic stability data on several configurations. The purpose of this investigation was to expand the knowledge of nose shape and fin span effects on static stability characteristics and to investigate configuration modifications to improve stability and reduce the bomblet susceptibility to coning under off-design conditions.

SECTION II
APPARATUS

2.1 TEST FACILITY

The Aerodynamic Wind Tunnel (4T) is a closed-loop, continuous flow, variable density tunnel in which the Mach number can be varied from 0.1 to 1.3. At all Mach numbers, the stagnation pressure can be varied from 300 to 3700 psfa. The test section is 4 ft square and 12.5 ft long with perforated, variable porosity (0.5- to 10-percent open) walls. It is completely enclosed in a plenum chamber from which the air can be evacuated, allowing part of the tunnel airflow to be removed through the perforated walls of the test section. A more thorough description of the tunnel is given in Ref. 5.

The model support system consists of a pitch sector, boom, and sting which provide a pitch capability from -12 to 28 deg with respect to the tunnel centerline. The center of rotation is at tunnel station 108. In addition, a remote controlled roll mechanism allows roll angle variations of ±180 deg. A schematic of the test section, showing the location of the test model, is shown in Fig. 1 (Appendix I). A photograph of the test installation is presented in Fig. 2.

2.2 TEST ARTICLES

Details of the bomblet models are shown in Fig. 3. The models consisted of a 3-in.-diam cylindrical centerbody, four noses with varying bluntness, straight or boattail afterbody, and rectangular fins with two spans for each afterbody.

2.3 INSTRUMENTATION

An internal six-component strain-gage balance was used to measure forces and moments on the models. Differential pressure transducers, referenced to the tunnel plenum pressure, were used to measure the pressure at the base of the models. Electrical signals from the balance, pressure transducers, and standard tunnel instrumentation were processed by the PWT data acquisition system and digital computer.

SECTION III
TEST DESCRIPTION

3.1 TEST CONDITIONS

Data were obtained at nominal Mach numbers from 0.3 to 1.2 at a constant Reynolds number of 2.2 x 10^6 per foot. Stagnation temperature was maintained at approximately 110°F throughout the test. Angle of attack was varied from -8 to 27 deg. One configuration was selected for roll angle variations of 0, 15, and 30 deg. Free transition was used throughout the test.

3.2 PRECISION OF MEASUREMENTS

The estimated precision of the data presented in this report, based on a 95-percent confidence level, is given below and in Fig. 4. The error sources considered for the coefficients were balance uncertainties, Mach number nonuniformities, instrument errors, and Mach number calibration accuracies.

Δa	±0.1
$\Delta \phi$	±0.1

The uncertainties in Mach number include variation of Mach number along the tunnel centerline, instrument errors, and errors in data acquisition techniques.

SECTION IV
RESULTS AND DISCUSSION

4.1 GENERAL

The recorded balance data were reduced to aerodynamic coefficients in the nonrolling body-axis coordinate system with the moment reference point 1.5 cal from the nose of the model.

Base pressure measurements were made on all models; however, no corrections have been made to the data presented. Since the models represent bomblets which are free-dropped with no rocket assist, it is assumed that the pressures acting on the base of the models in the wind tunnel are representative of those in free flight.

4.2 ROLL ANGLE EFFECTS

One essential characteristic that a bomblet must possess to disperse with zero coning is that lift be insensitive to model roll angle. The effects of roll angle on the longitudinal characteristics of a typical bomblet model are presented in Fig. 5. There were essentially no roll angle effects.

4.3 NOSE SHAPE EFFECTS

The effects of nose shape on C_N, C_m, and C_A, for a cylindrical and a boattail afterbody, are shown in Figs. 6 and 7, respectively. The small-radius blunt nose produced the highest normal-force coefficients and the spherical nose the lowest at the high angles of attack throughout the Mach number range with the cylindrical afterbody (Fig. 6a). The criteria for zero-coning dispersal (unstable at low angles of attack, stable at high angles of attack) is obviously violated by the spherical-segment nose configuration for $M_\infty < 1.1$ (Fig. 6b). In addition, the spherical-nose configuration, which comes nearest to meeting the requirements, is at best marginal at the subsonic Mach numbers. Axial-force coefficients were highest with the spherical-segment nose configuration and lowest with the spherical-nose configuration (Fig. 6c).

Normal-force coefficients were essentially insensitive to nose shape with the boattail afterbody except at supersonic Mach numbers and high angles of attack where the coefficients were highest with the large-radius blunt nose and lowest with the spherical nose (Fig. 7a). Again, the low angle-of-attack stability characteristics are less desirable with the spherical-segment nose (Fig. 7b). Other nose shapes are marginally unstable near $\alpha = 0$ deg with no highly stable trim angles. Axial-force coefficients show the same trends as with the cylindrical afterbody (Fig. 7c).

4.4 AFTERBODY EFFECTS

Comparisons are made of the effects of cylindrical and boattail afterbodies on the longitudinal characteristics of models with spherical and spherical-segment noses in Figs. 8 and 9, respectively. Normal-force coefficients for the configuration with spherical nose were highest with the boatttail afterbody at all Mach numbers except 0.8 and 0.9 where they were equal or greater with the cylindrical afterbody (Fig. 8a). The comparisons in pitching-moment coefficients (Fig. 8b) show that both afterbodies had approximately the same stability characteristics near $\alpha = 0$ for $M_\infty < 0.8$. At $M_\infty = 0.9$, the boattail base was slightly more unstable near $\alpha = 0$ deg; however, there were no strongly stable trim angles. In Fig. 8c, it can be seen that the cylindrical afterbody produced the higher axial force but to a lesser extent as Mach number was increased.

For the configuration with the spherical-segment nose, normal-force coefficients were highest with the boattail afterbody except in the region $0.7 \leqslant M_\infty \leqslant 0.9$ where the coefficients were highest with the cylindrical afterbody (Fig. 9a). Both afterbody configurations showed stable characteristics at angles of attack near zero and subsonic Mach numbers with the spherical-segment nose. At supersonic Mach numbers, both configurations

became slightly unstable near α = 0 deg (Fig. 9b). The same trends in axial-force coefficients, as seen with the spherical nose, were obtained with the spherical-segment nose (Fig. 9c).

4.5 FIN SPAN EFFECTS

The effects of the variation of fin span on model longitudinal characteristics are presented in Figs. 10 through 13 for various nose and afterbody configurations. In general, the larger fin span produced the largest normal-force coefficient for all configurations (Figs. 10a, 11a, 12a, and 13a). The fins with the shortest span caused the models to be more unstable near α = 0 deg (Figs. 10b, 11b, 12b, and 13b); however, only two of the configurations showed unstable characteristics near α = 0 deg and a high angle-of-attack trim point. At supersonic Mach numbers with the cylindrical afterbody, short-span fins, blunt- and spherical-segment noses, trim angles of approximately 12 deg were noted (Figs. 10b and 11b). Fin span had negligible effect on axial-force coefficients (Figs. 10c, 11c, 12c, and 13c).

SECTION V
CONCLUSIONS

The following conclusions were made from the results of the investigation:

1. Increasing fin span makes the bomblet models more stable near zero angle of attack, at which there is no lift for dispersion.

2. Making the model nose more blunt causes the models to be more stable near zero angle of attack.

3. Neither the cylindrical nor the boattail afterbody shape produces the desired instability near zero angle of attack.

4. The normal-force coefficients for the bomblet models are insensitive to roll angle.

REFERENCES

1. Shadow, T. O. "Wind Tunnel Investigation of the Transonic Static Stability Characteristics of Three Bomblet Munition Models Used in the Evaluation of Aerodynamic Dispersion Techniques." AEDC-TR-70-233 (AD875110L), September 1970.

2. Shadow, T. O. "Transonic Roll-Damping and Magnus Characteristics of Three Bomblet Munition Models Used in the Evaluation of Aerodynamic Dispersal Techniques." AEDC-TR-71-33 (AD880981L), March 1971.

3. Uselton, Bob, Carman, Jack, and Shadow, Tom. "Dynamic Stability Characteristics of Axisymmetric Bomblet Munition Models at Mach Numbers 0.3 to 1.2." AEDC-TR-70-270 (AD884281L), December 1970.

4. Carman, J. B., Uselton, B. L., and Burt, G. E. "Roll-Damping, Static Stability, and Damping-in-Pitch Characteristics of Axisymmetric Bomblet Munition Models at Supersonic Mach Numbers." AEDC-TR-71-88 (AD882636L), April 1971.

5. Test Facilities Handbook (Ninth Edition). "Propulsion Wind Tunnel Facility, Vol. 4." Arnold Engineering Development Center, July 1971.

APPENDIX
ILLUSTRATIONS

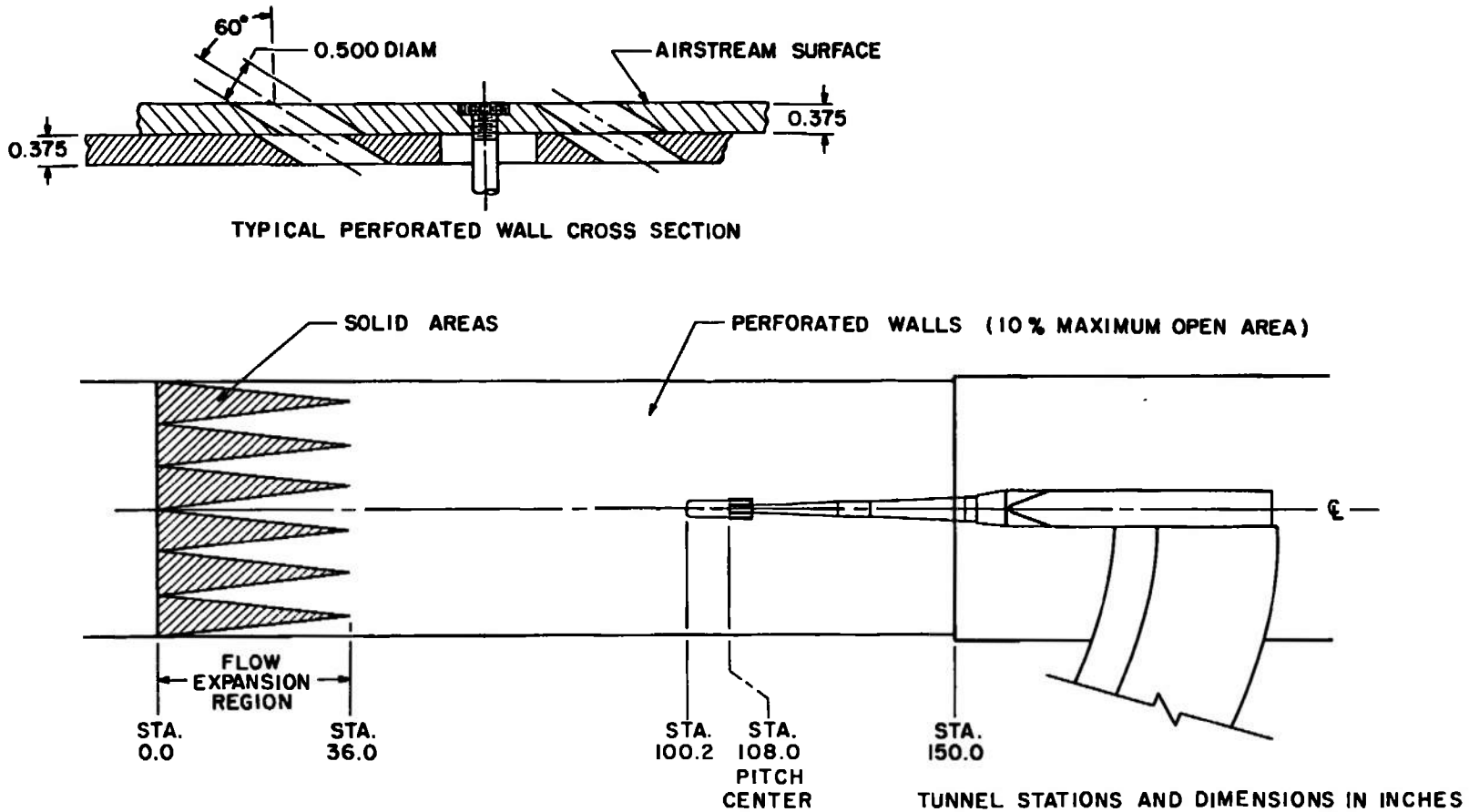

Fig. 1 Schematic of Tunnel Installation

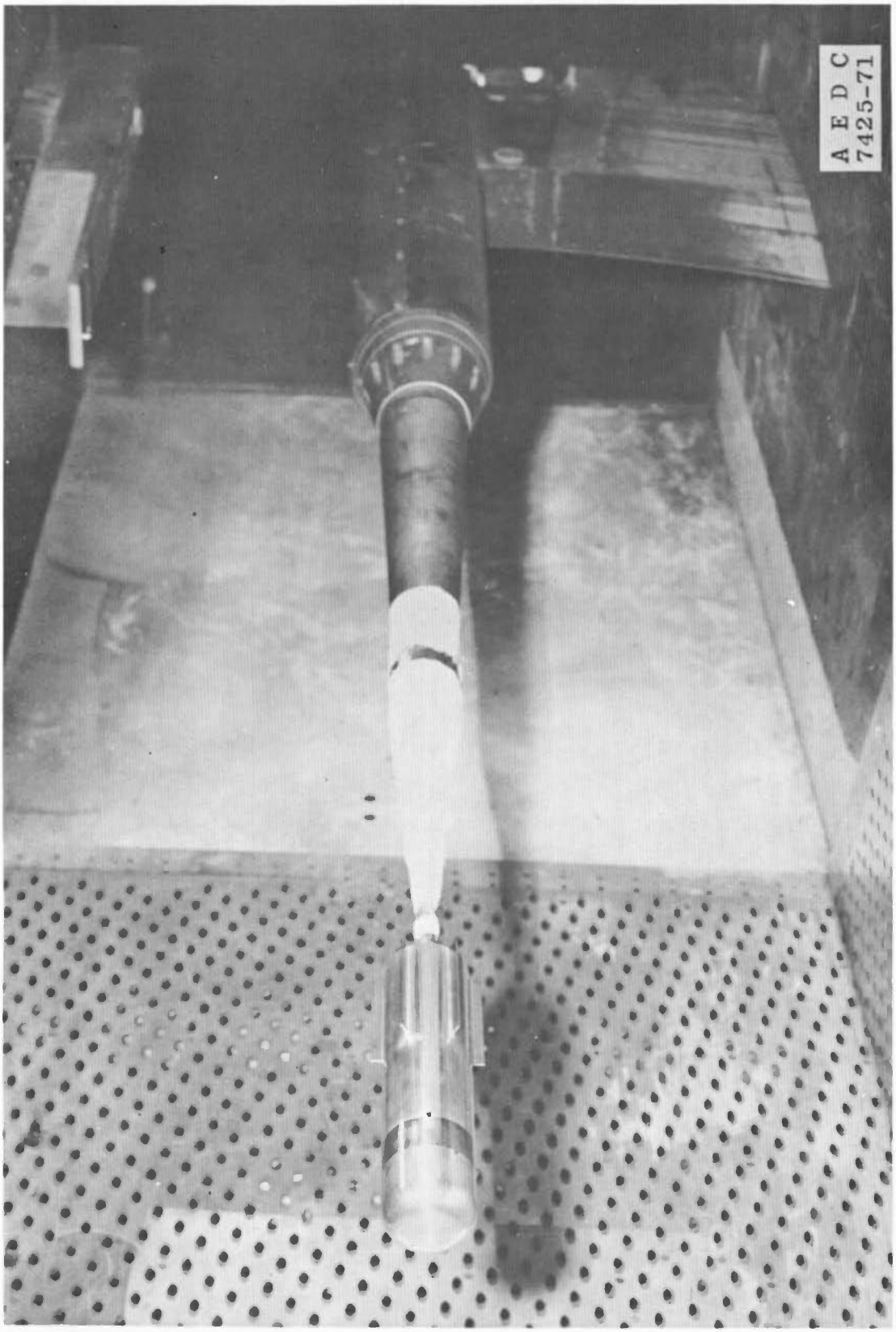

Fig. 2 Photograph of Tunnel Installation

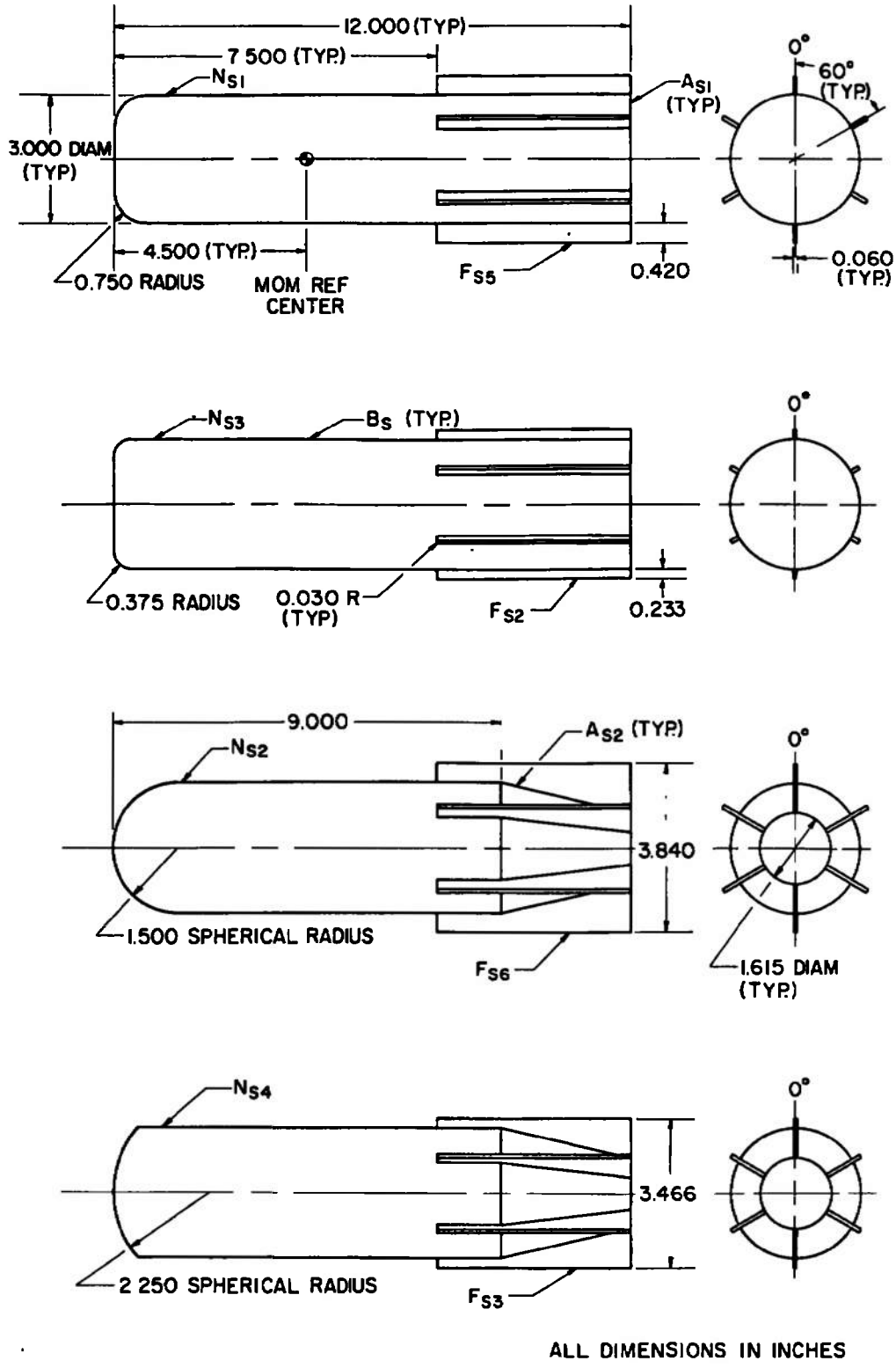

Fig. 3 Details and Dimensions of Bomblet Models

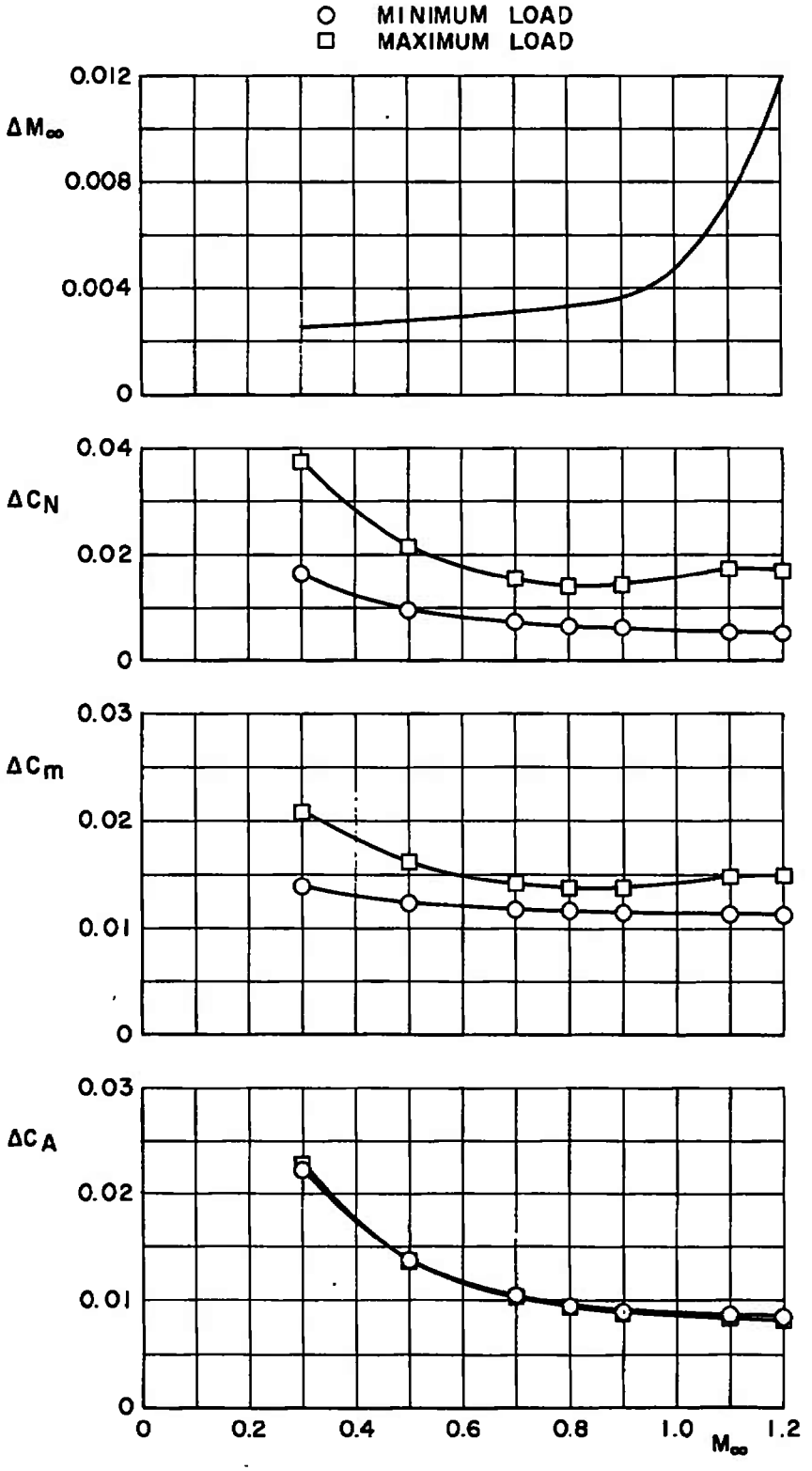

Fig. 4 Estimated Precision of Data

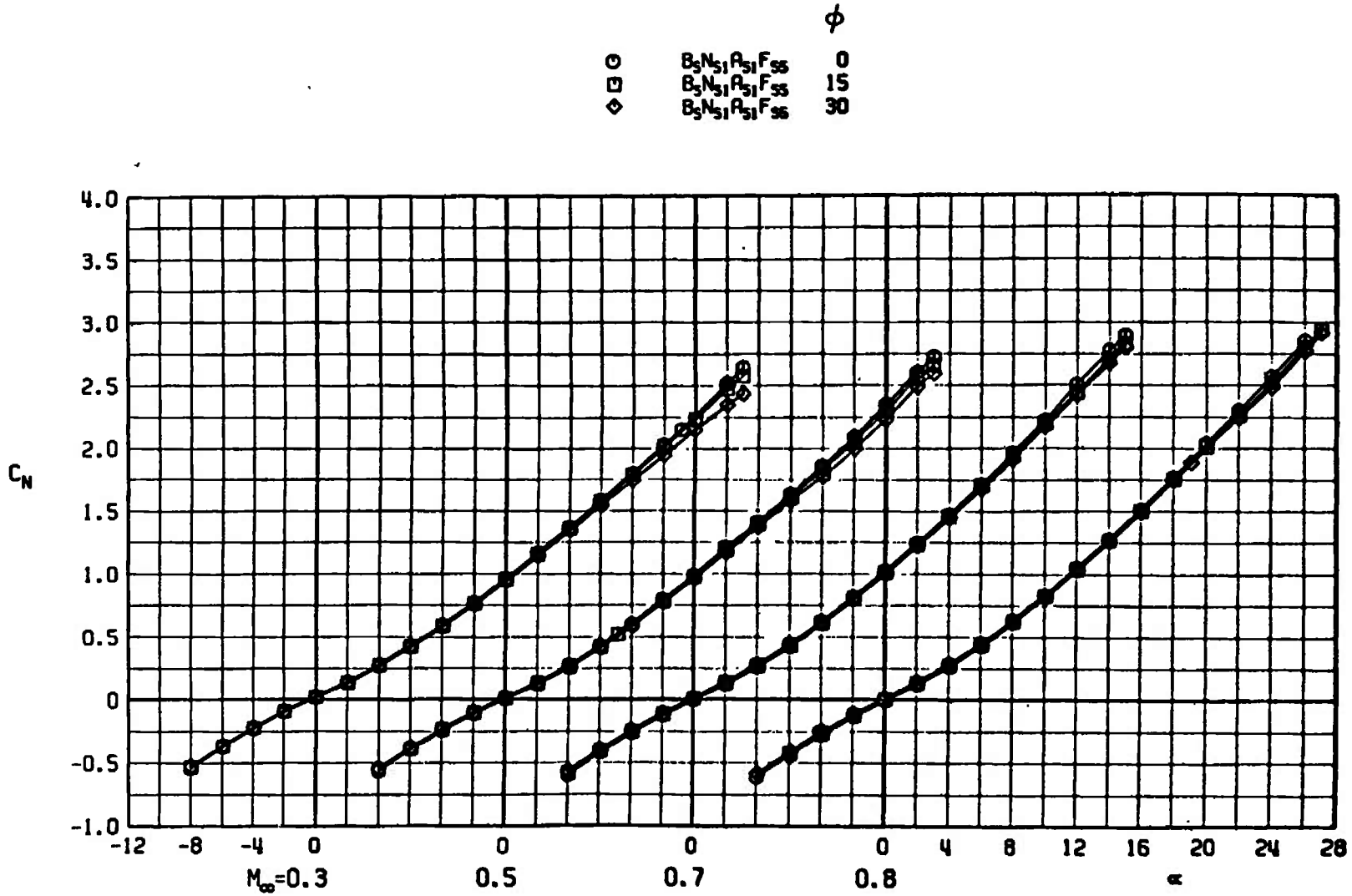

a. C_N versus α

Fig. 5 Effects of Roll Angle on Model Longitudinal Characteristics, $B_S N_{S1} A_{S1} F_{S5}$

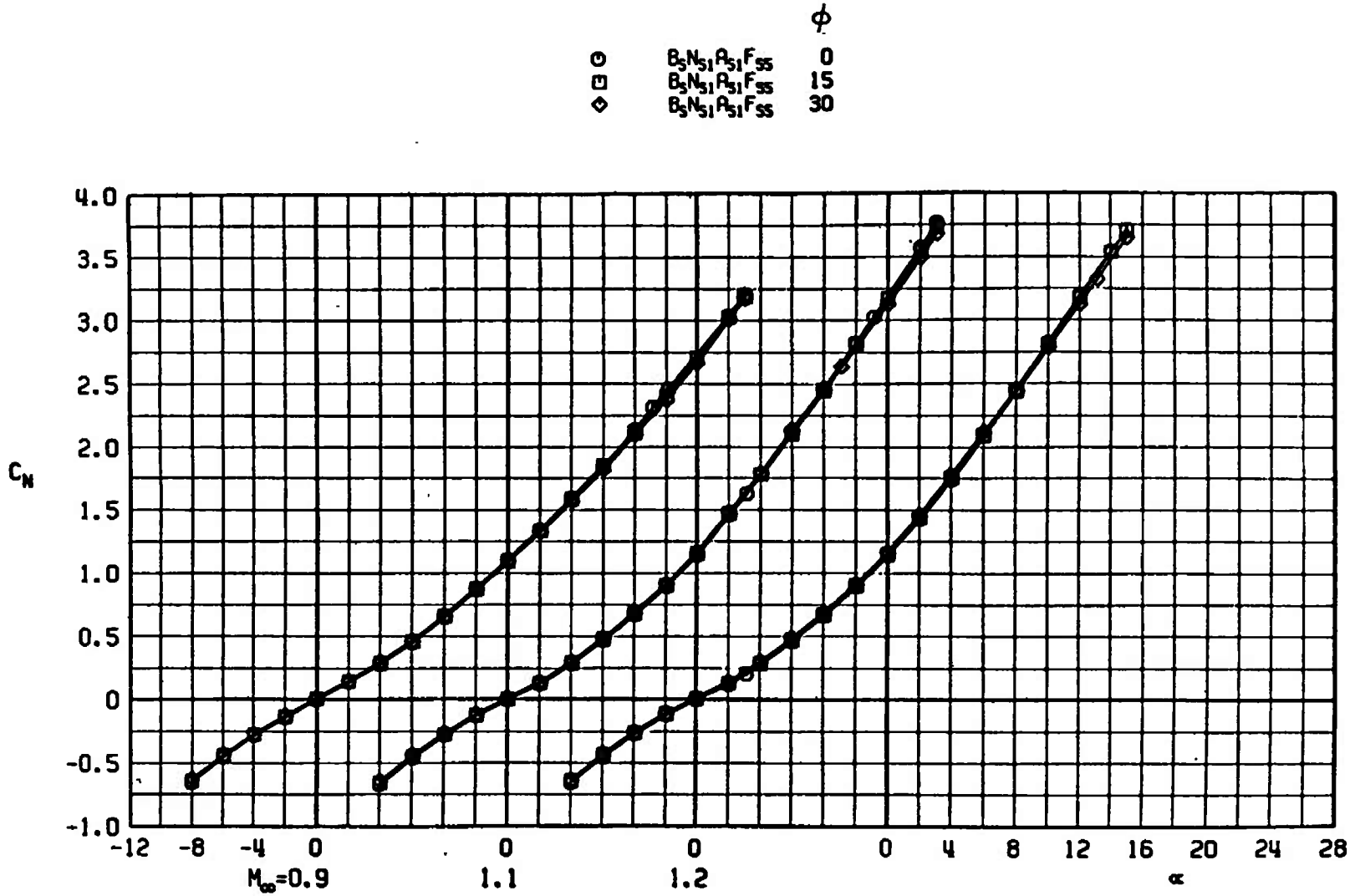

a. Concluded
Fig. 5 Continued

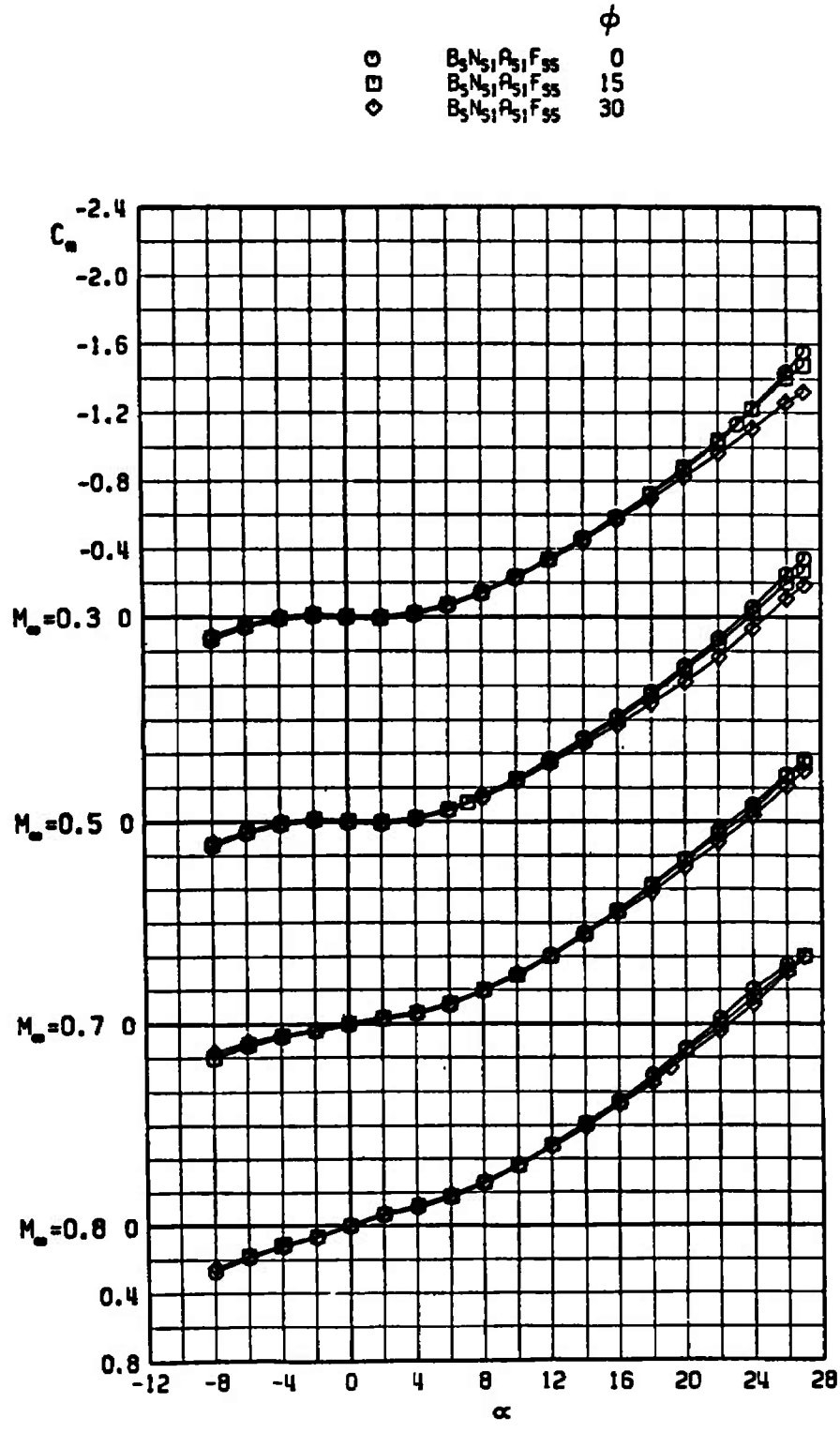

b. C_m versus α

Fig. 5 Continued

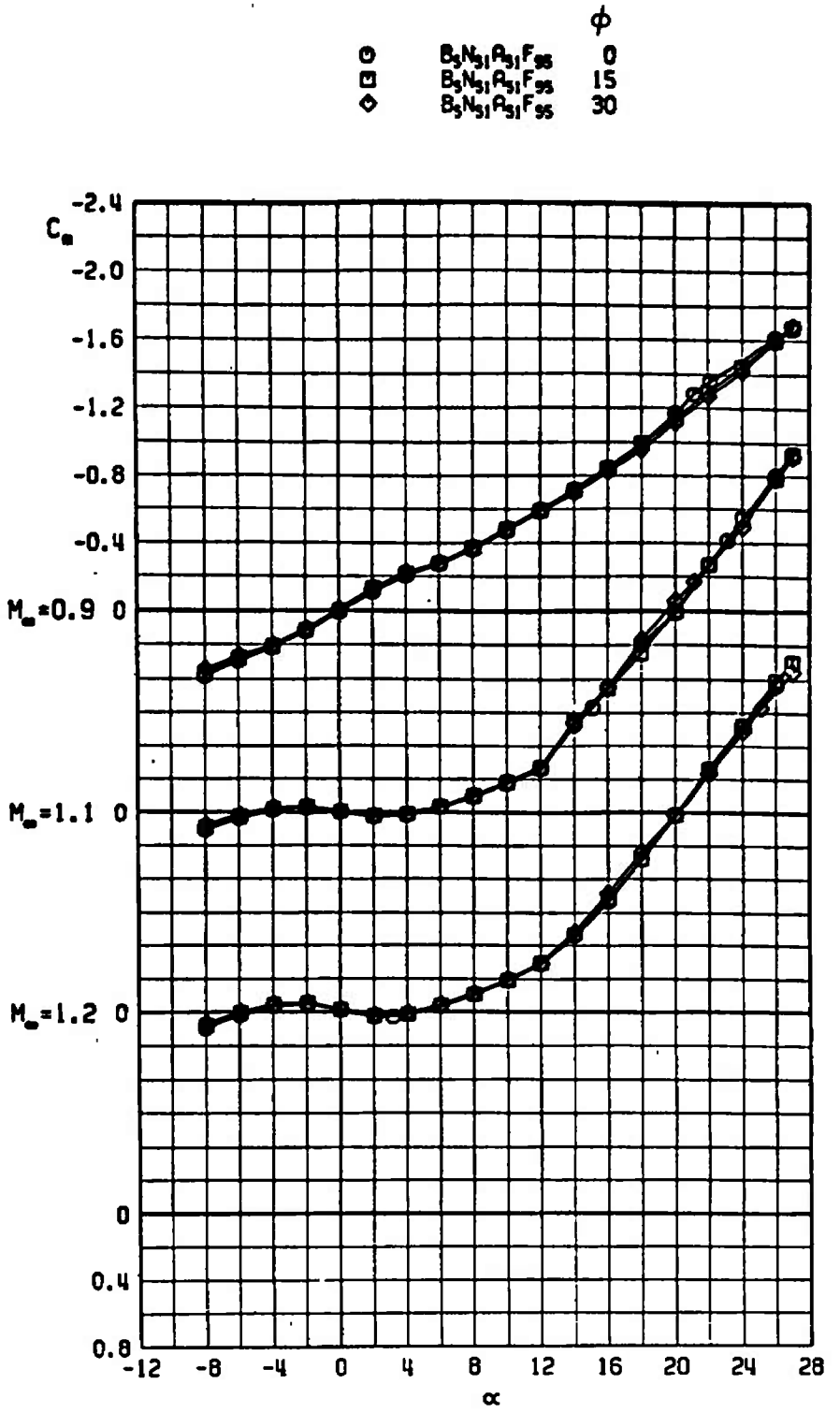

b. Concluded
Fig. 5 Continued

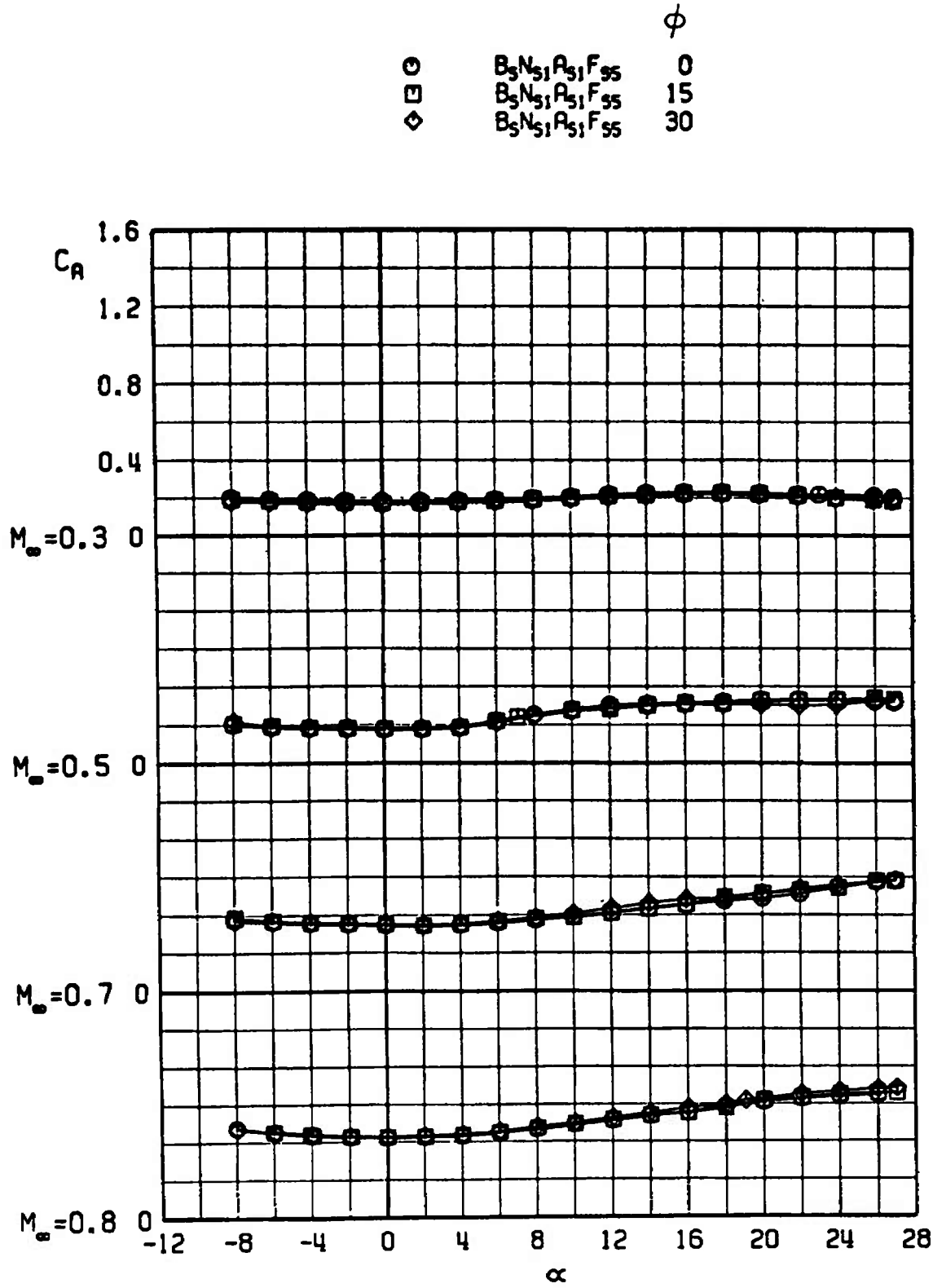

c. C_A versus α

Fig. 5 Continued

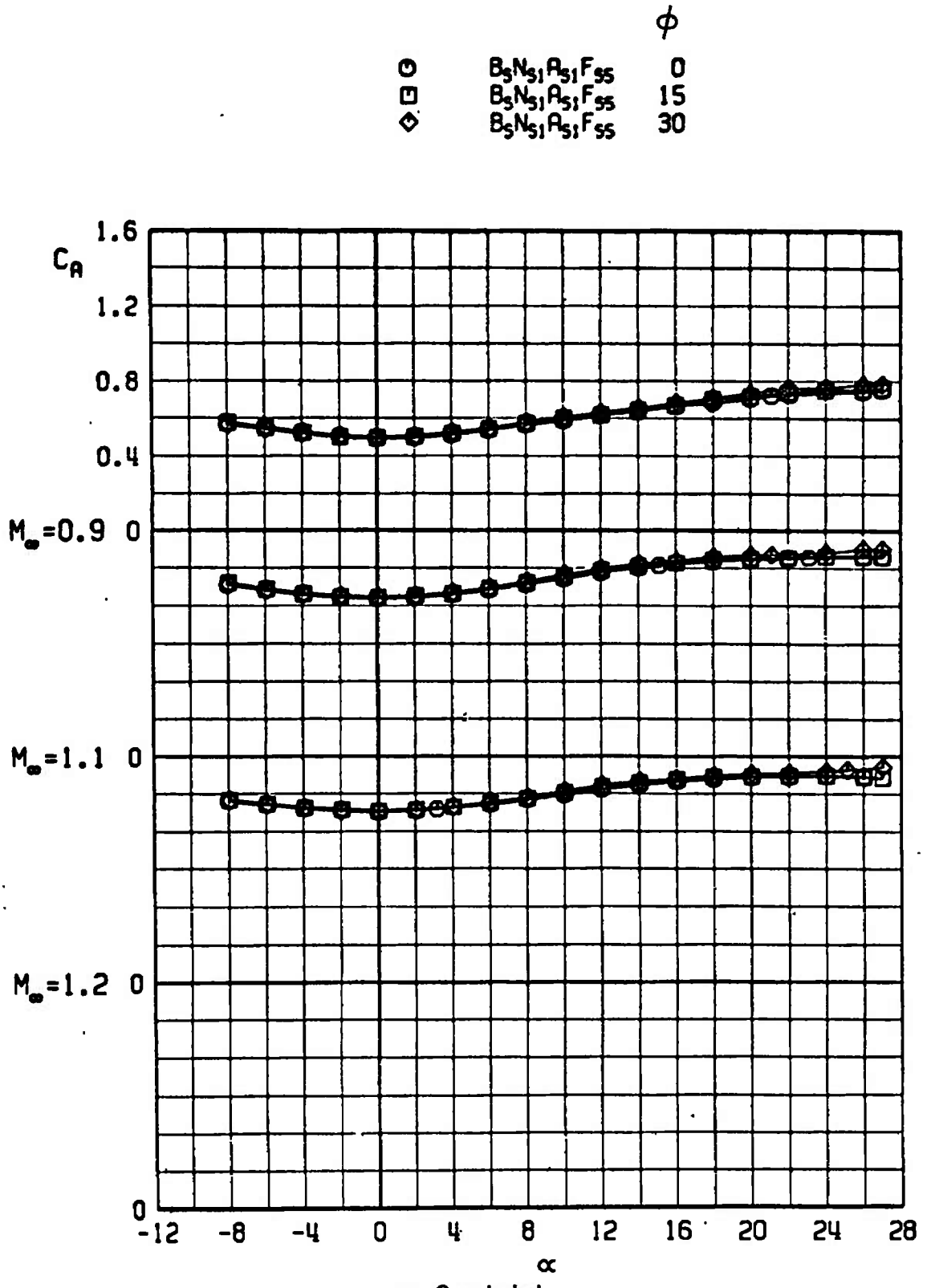

c. Concluded
Fig. 5 Concluded

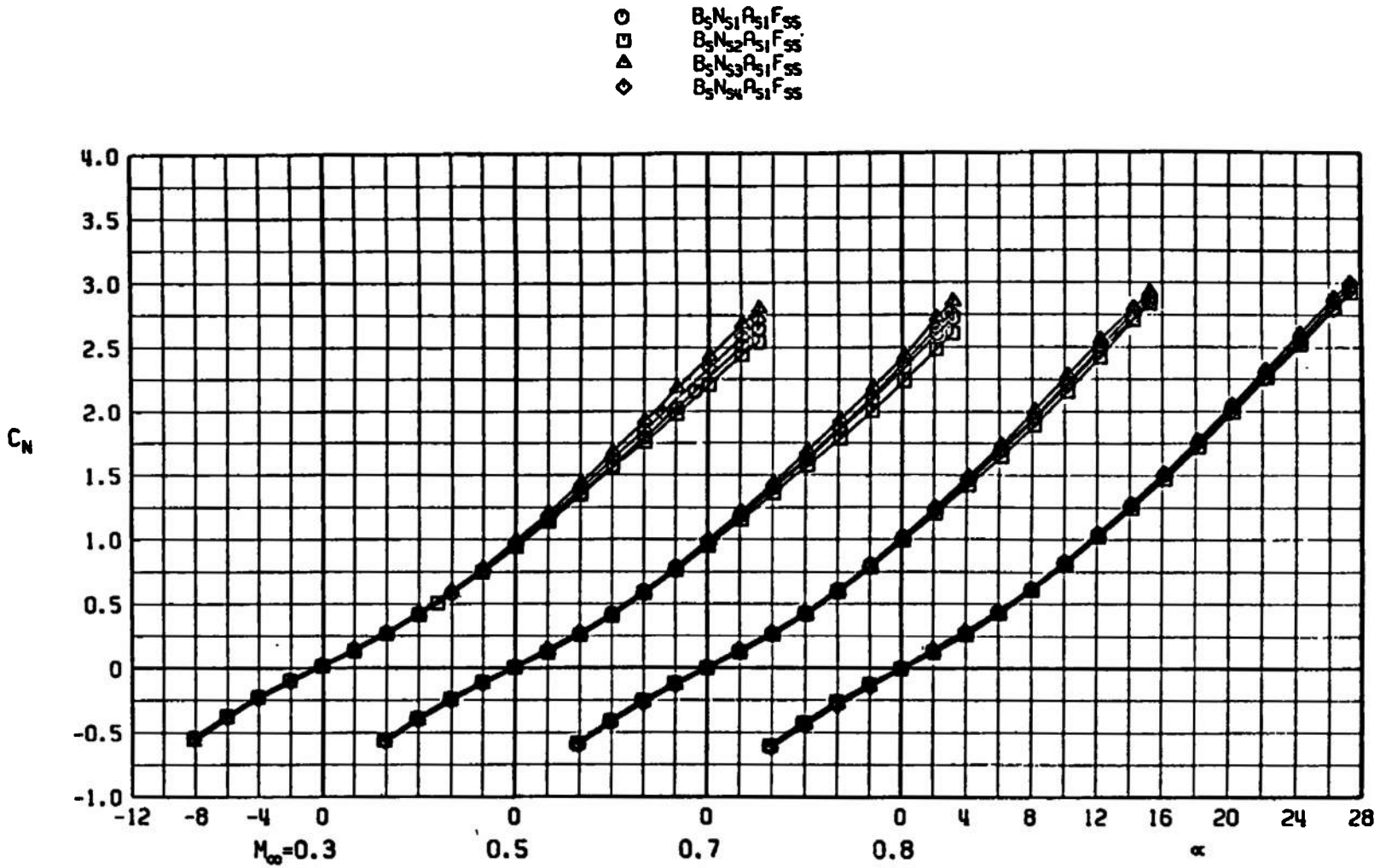

a. C_N versus α

Fig. 6 Effects of Nose Shape on Longitudinal Characteristics of Model with Cylindrical Afterbody, $B_S N_{SX} A_{S1} F_{S5}$, $\phi = 0$

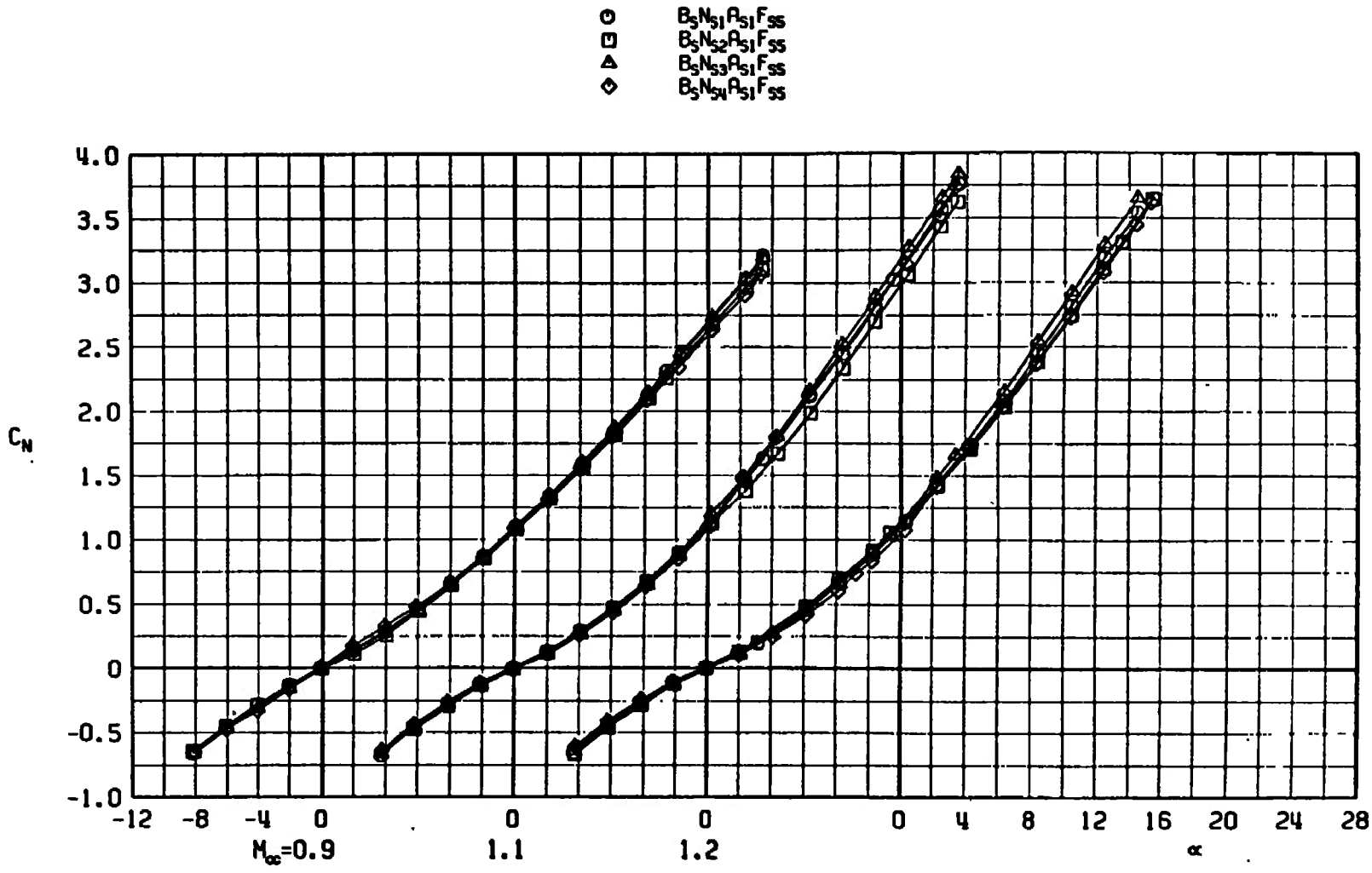

a. Concluded

Fig. 6 Continued

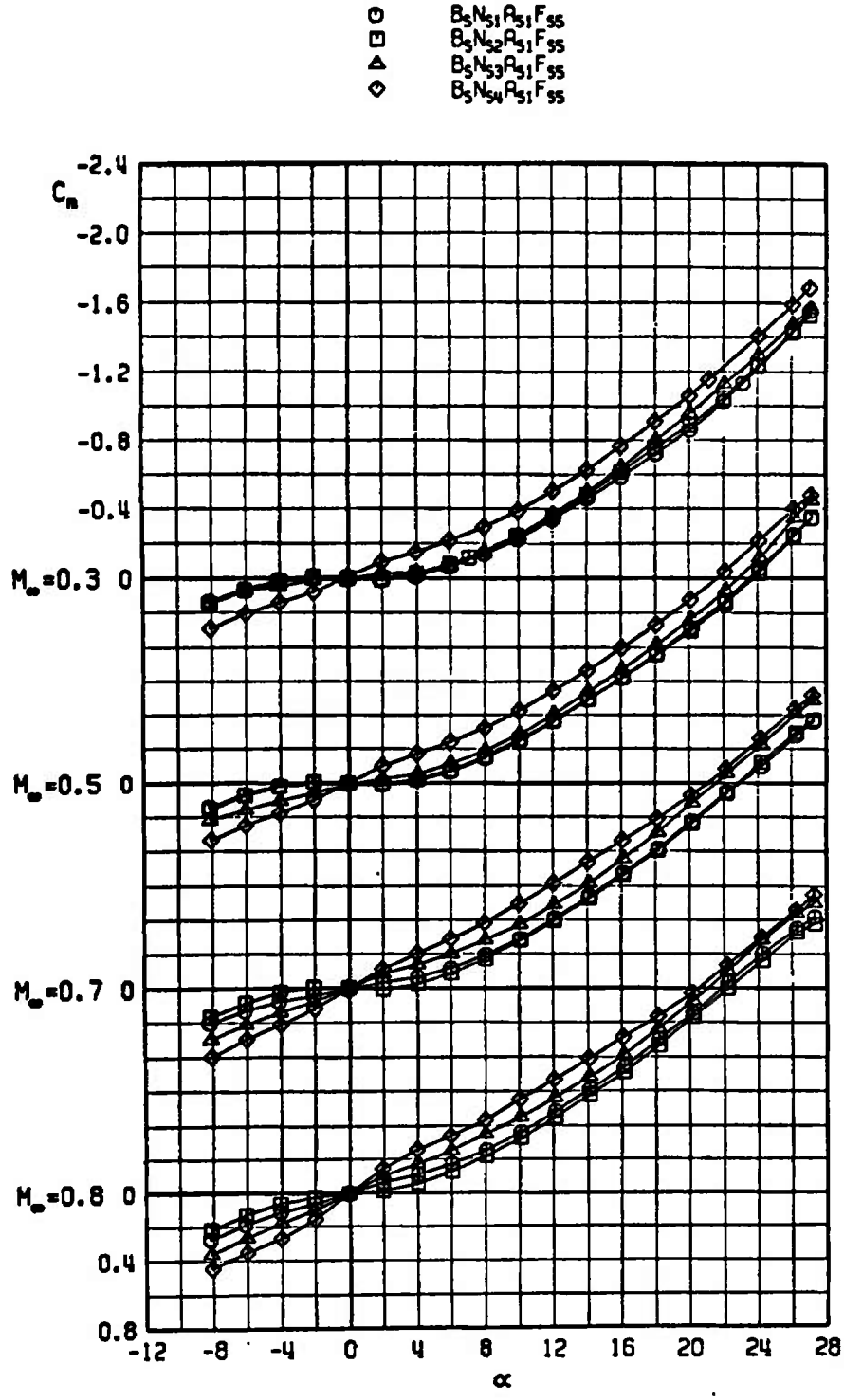

b. C_m versus α

Fig. 6 Continued

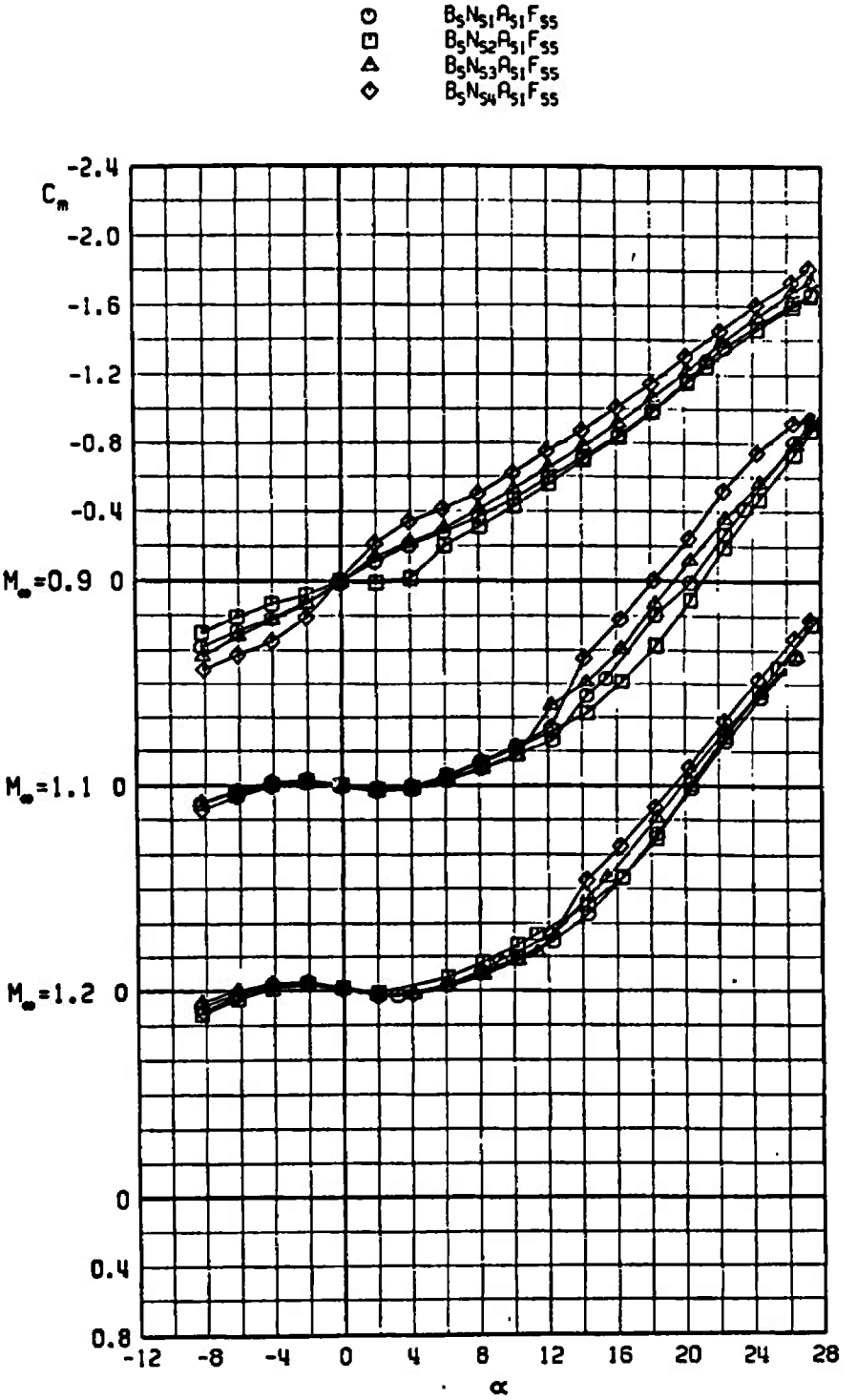

b. Concluded
Fig. 6 Continued

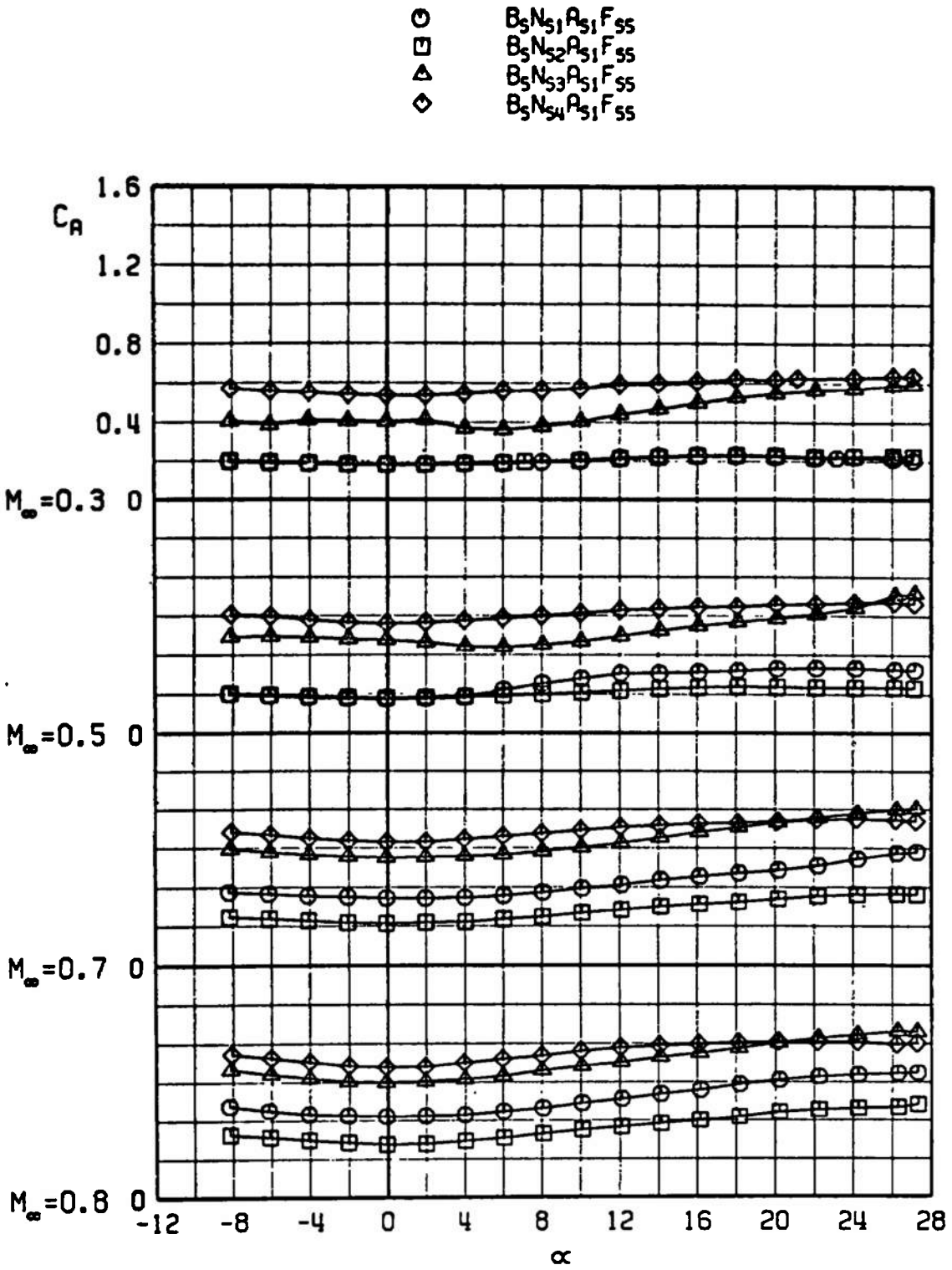

c. C_A versus α
Fig. 6 Continued

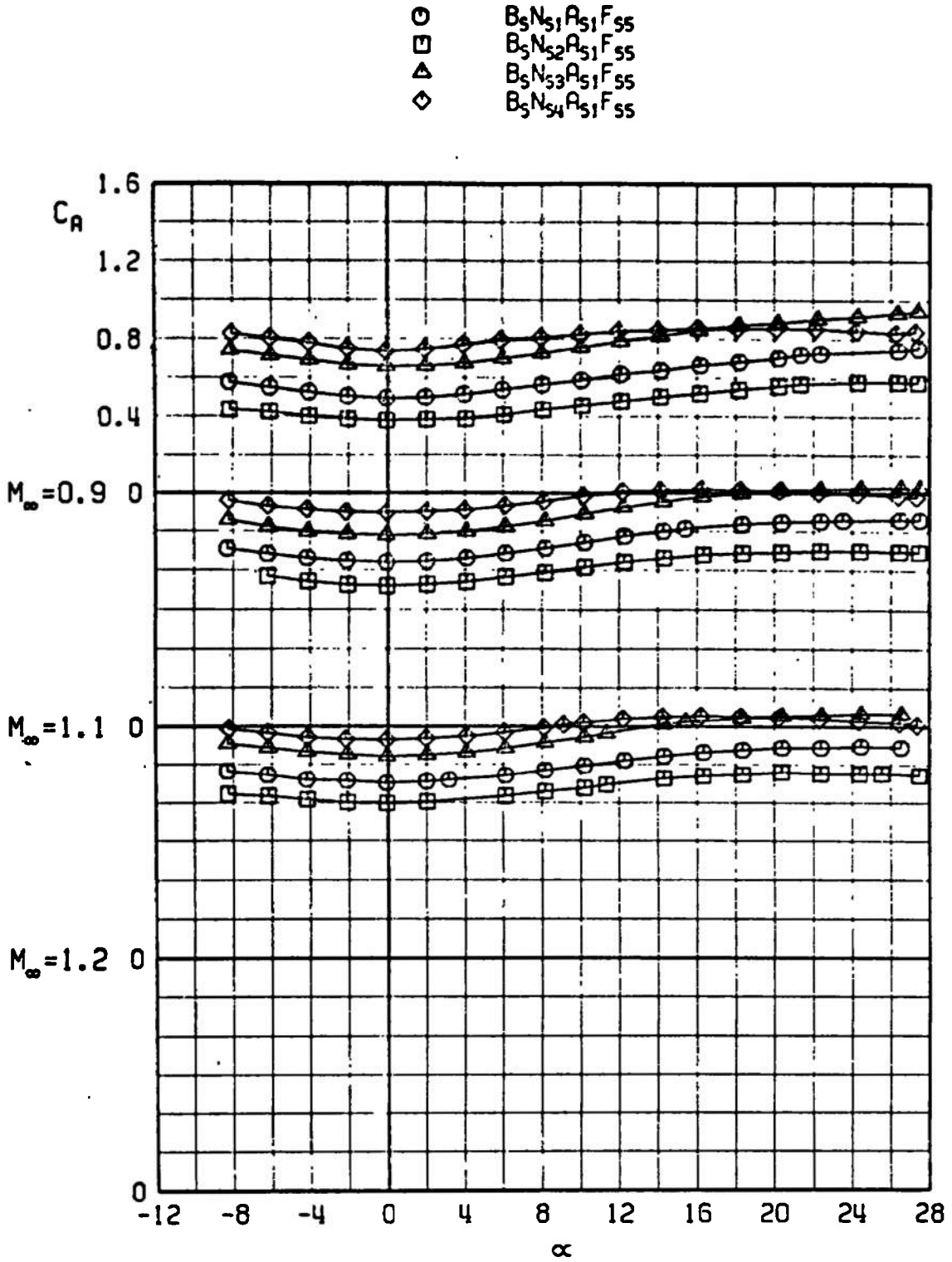

c. Concluded
Fig. 6 Concluded

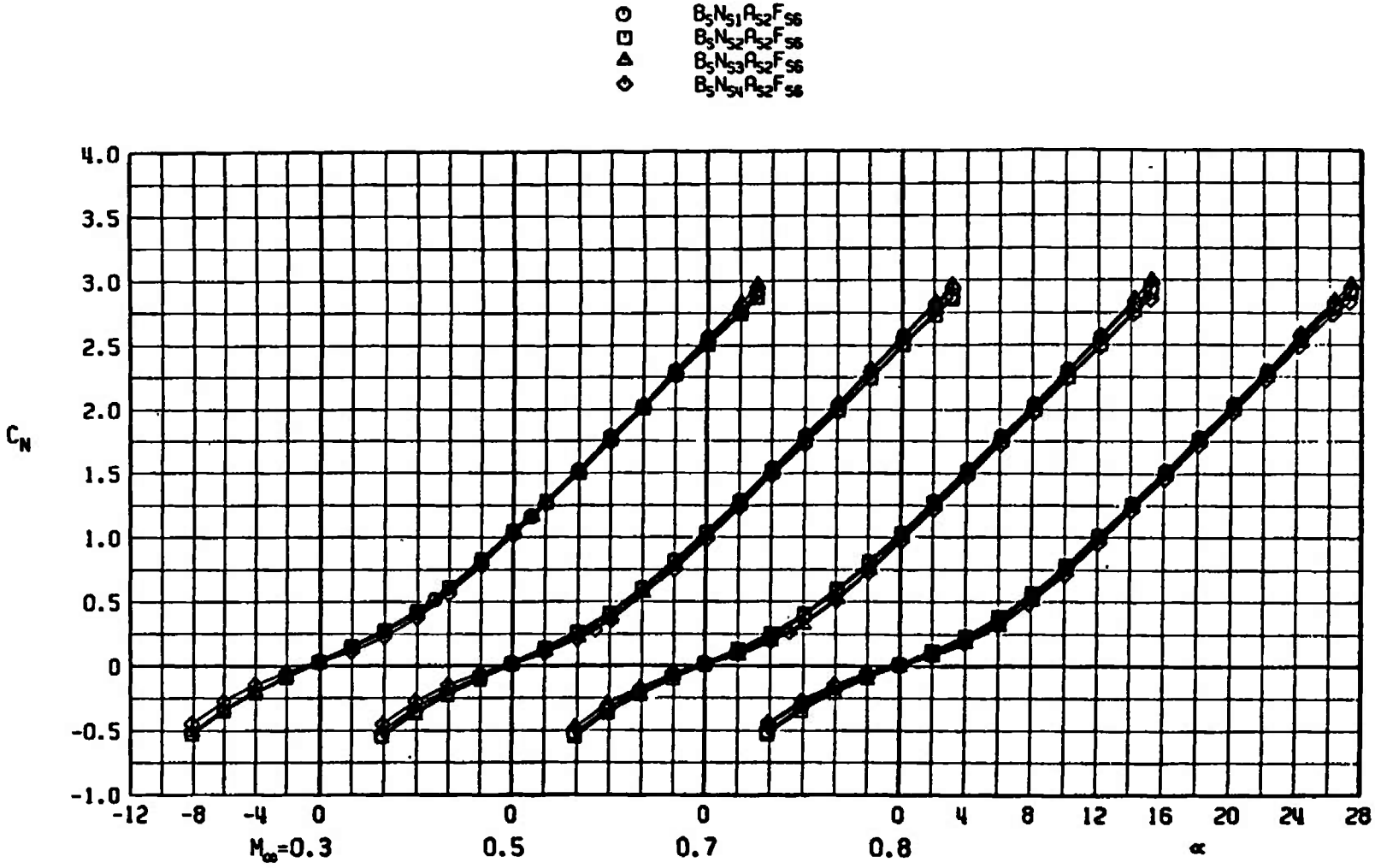

a. C_N versus α

Fig. 7 Effects of Nose Shape on Longitudinal Characteristics of Model with Boattail Afterbody, $B_5 N_{5x}\ A_{52} F_{56}$, $\phi = 0$

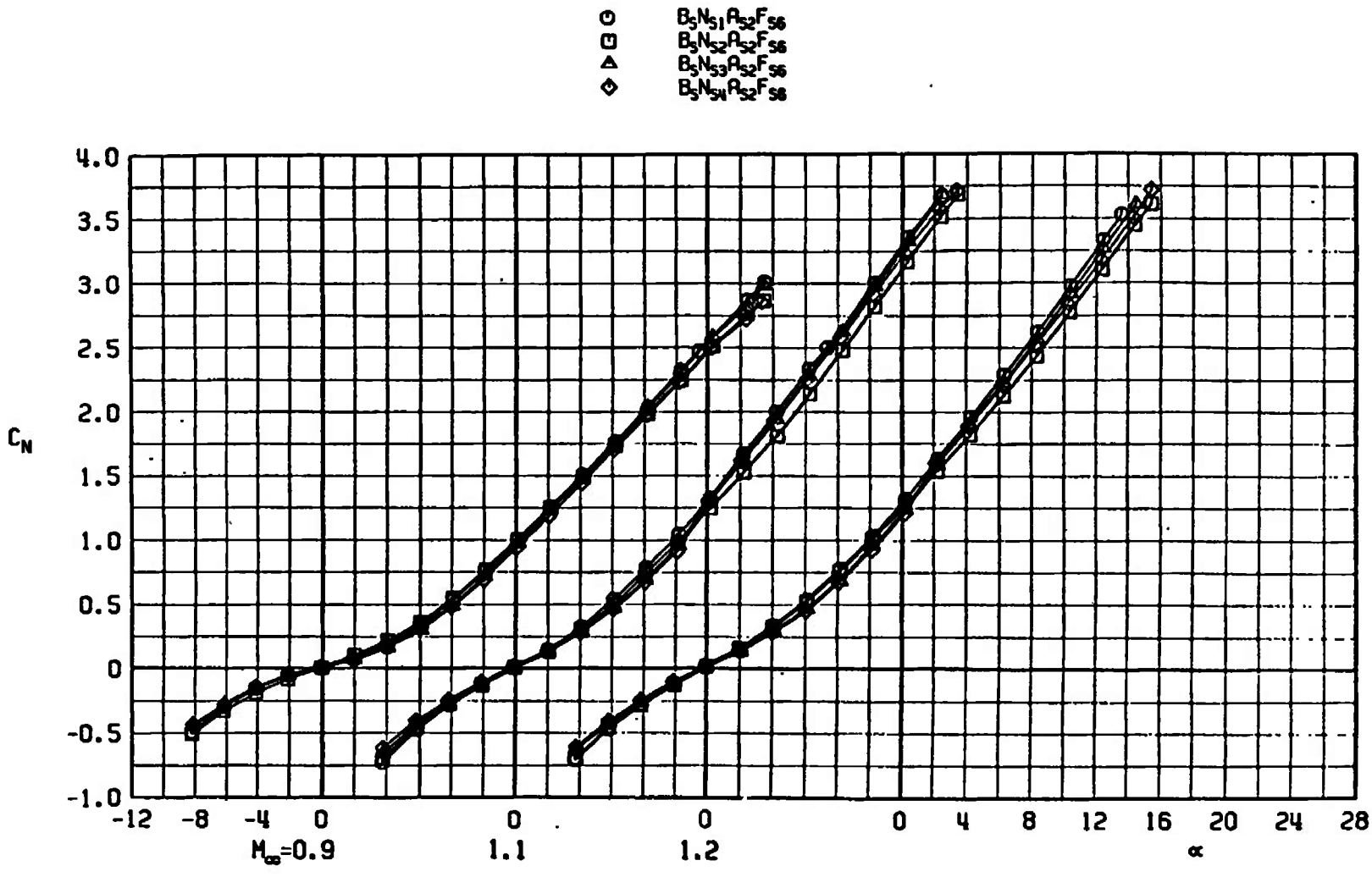

a. Concluded

Fig. 7 Continued

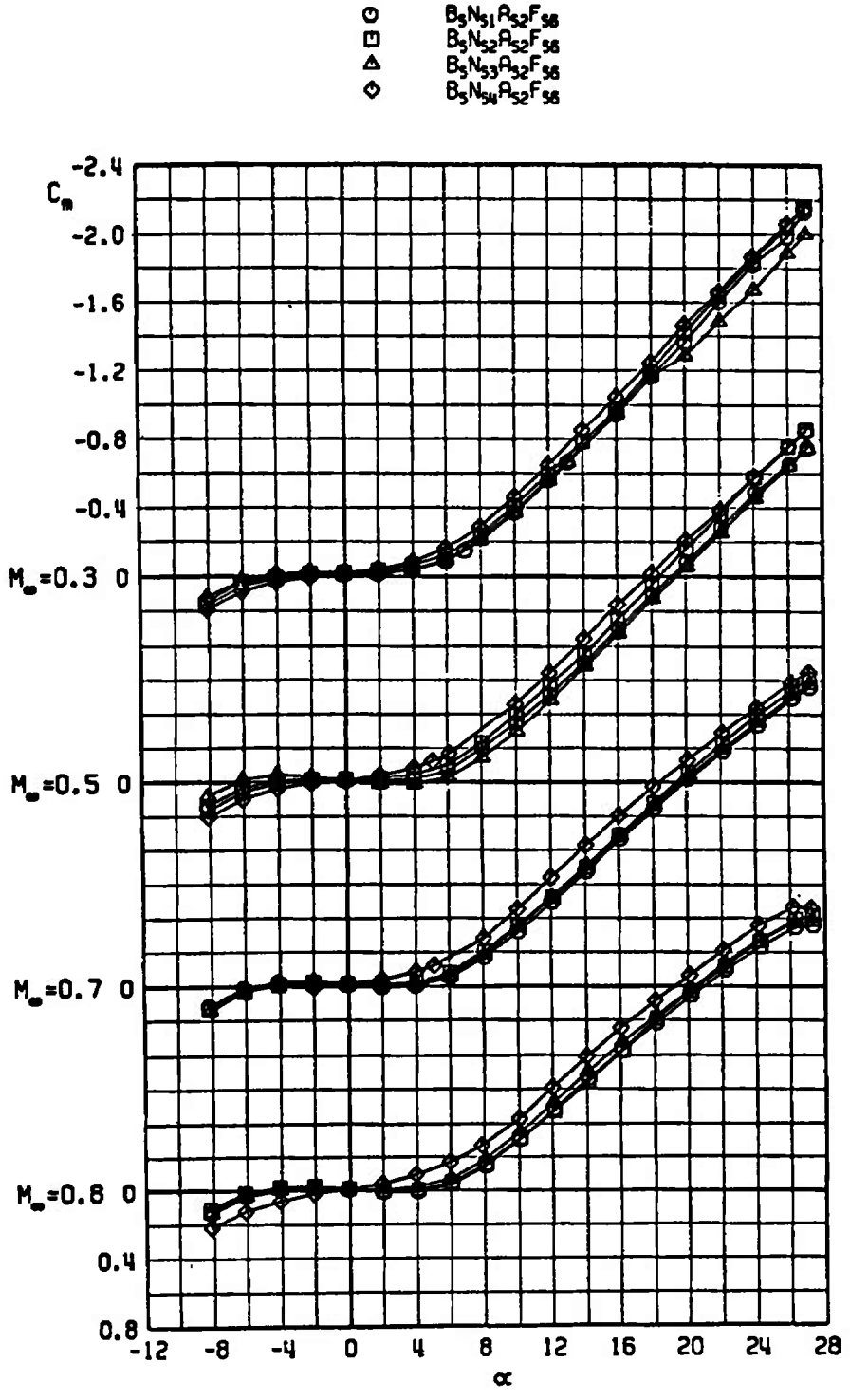

b. C_m versus α

Fig. 7 Continued

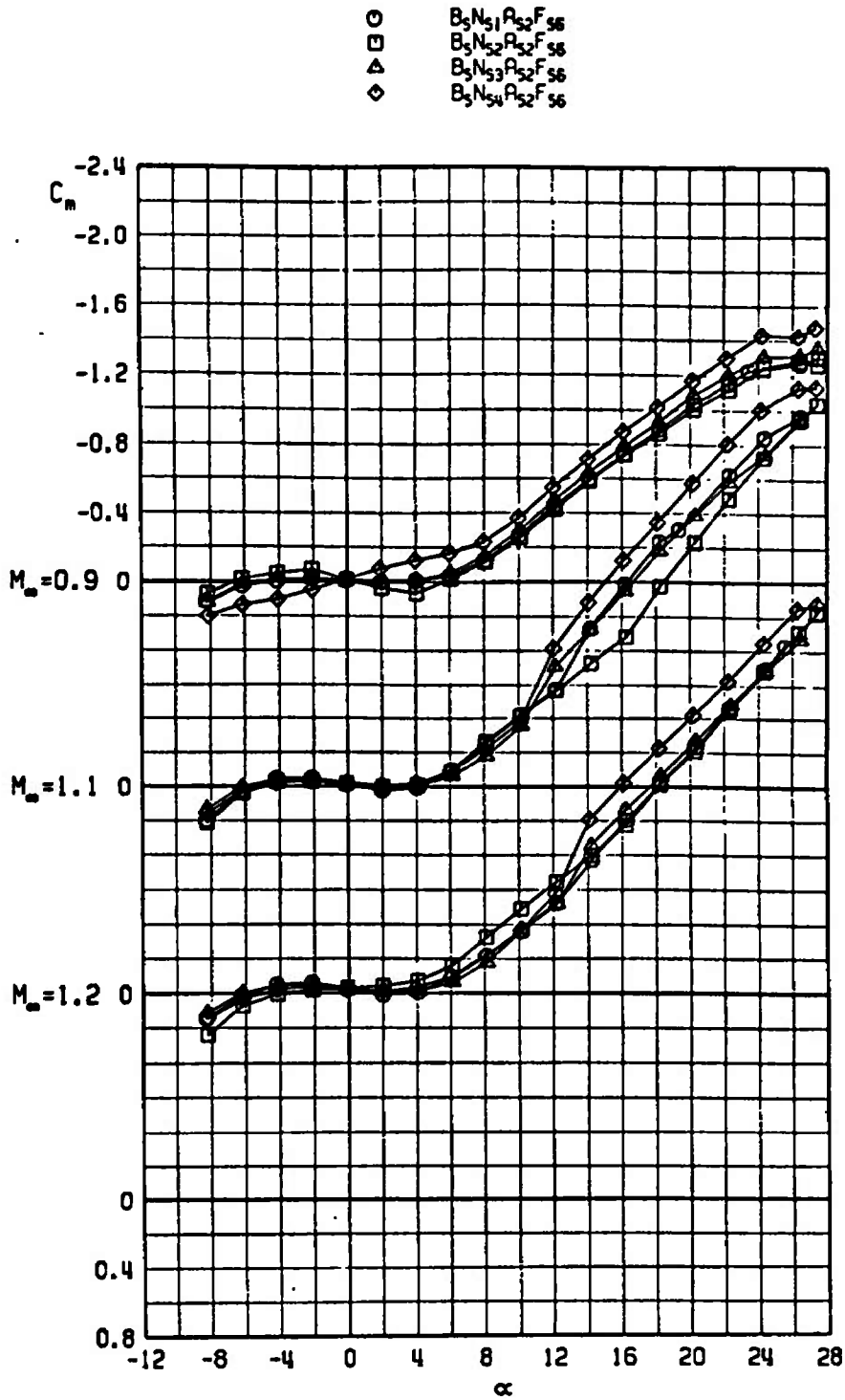

b. Concluded
Fig. 7 Continued

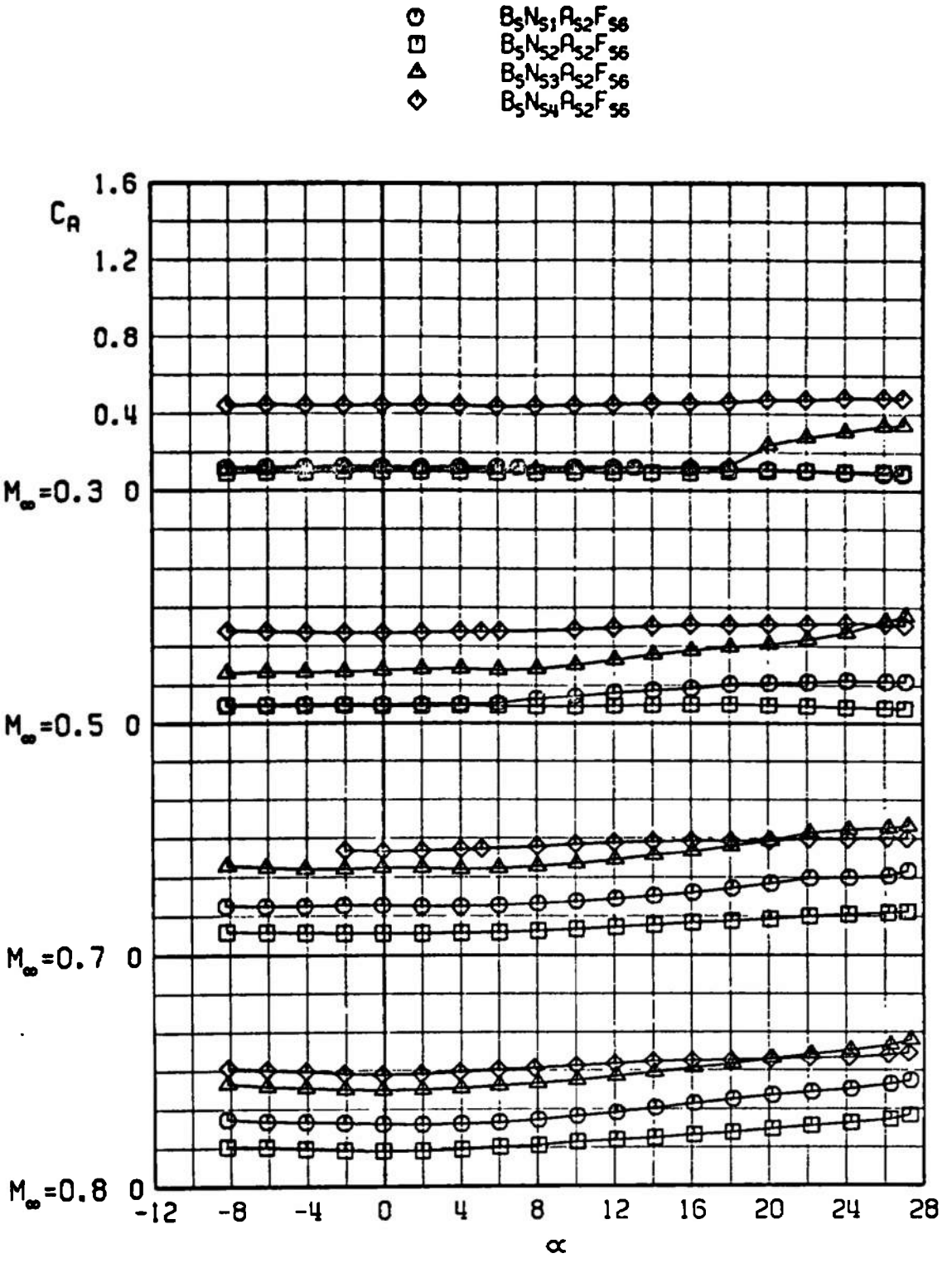

c. C_A versus α
Fig. 7 Continued

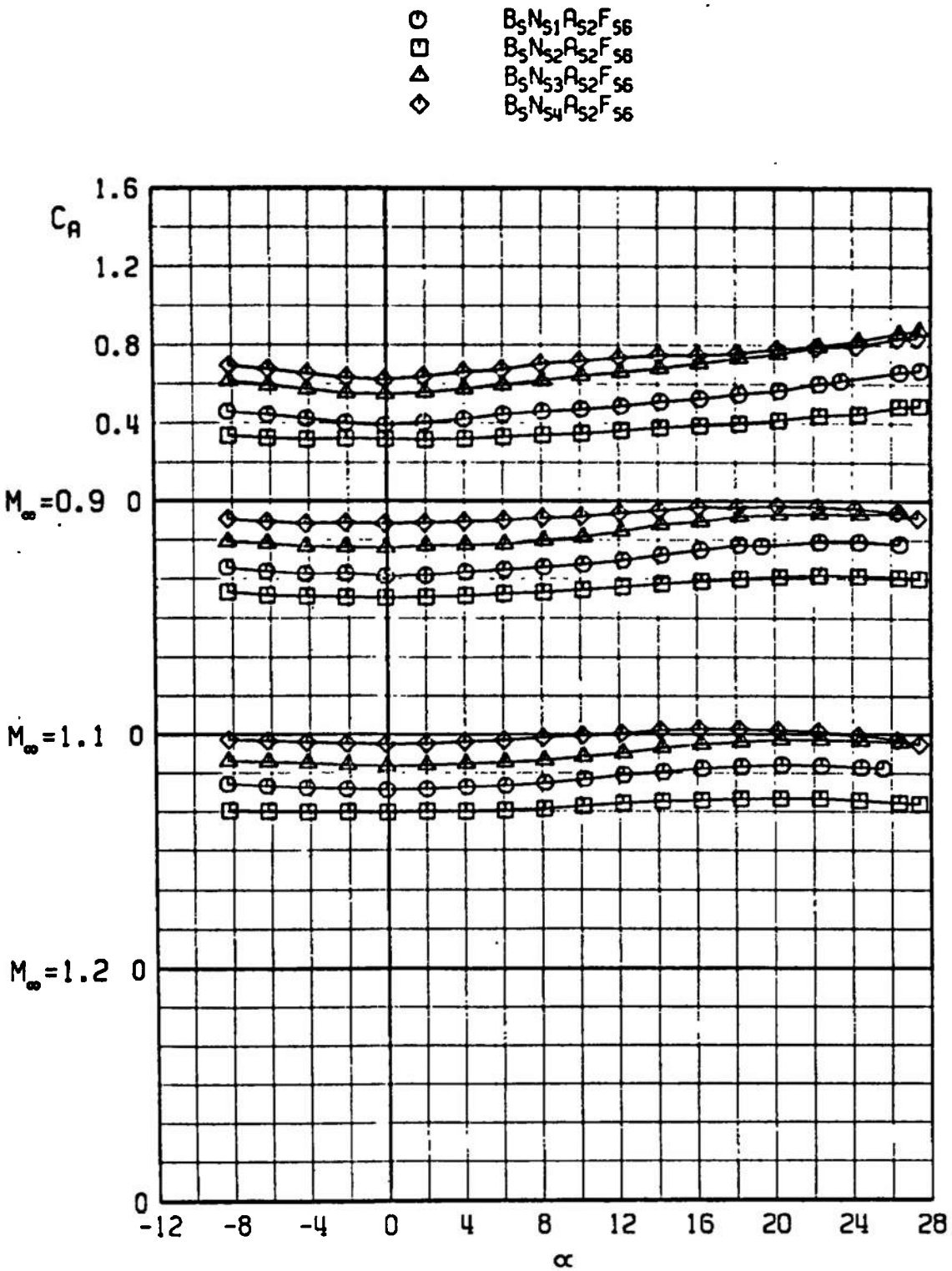

c. Concluded
Fig. 7 Concluded

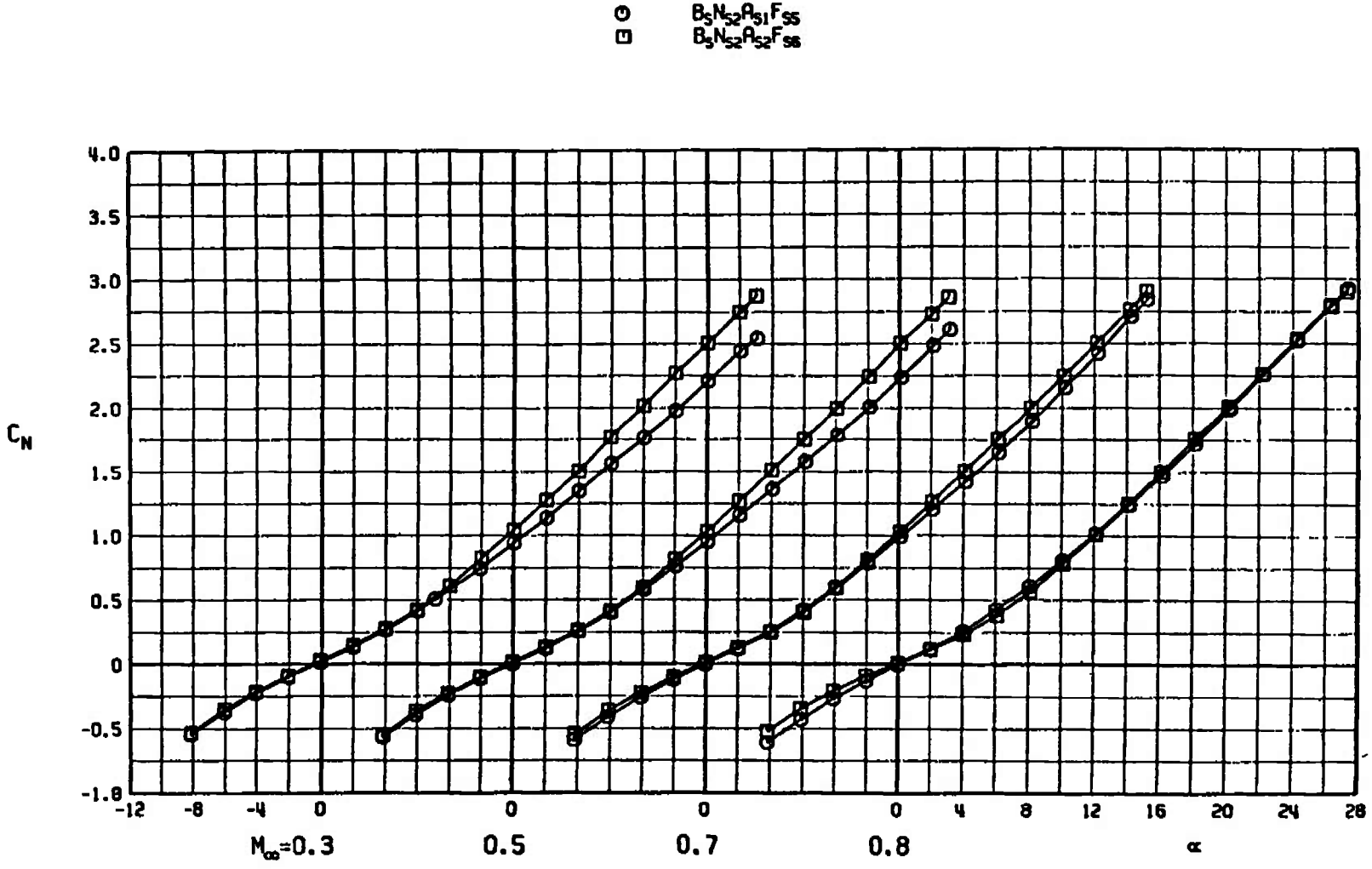

a. C_N versus α

Fig. 8 Effects of Afterbody Shape on Longitudinal Characteristics of Model with Spherical Nose, $B_S N_{S2} A_{SX} F_{SX}$, $\phi = 0$

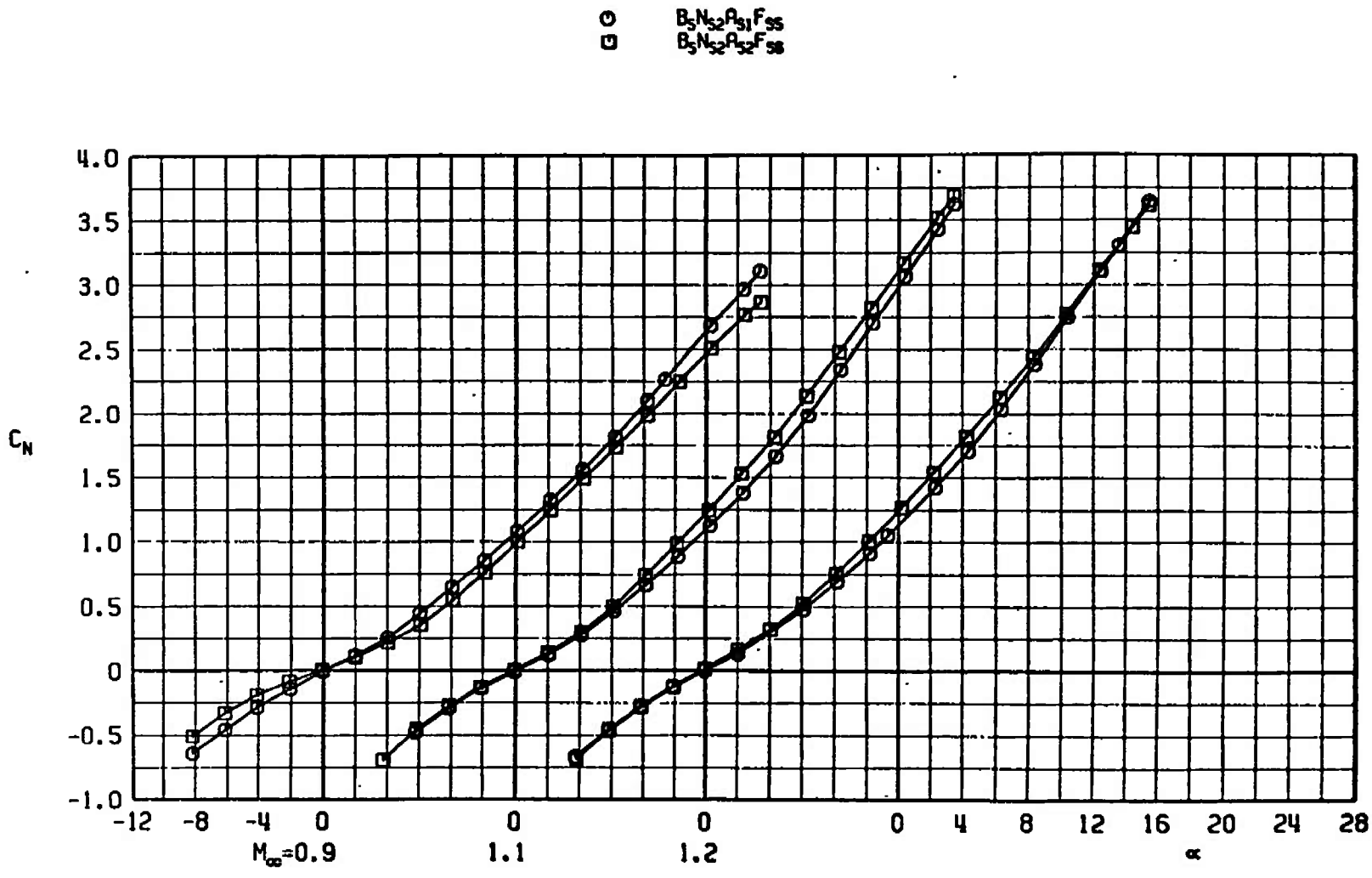

a. Concluded

Fig. 8 Continued

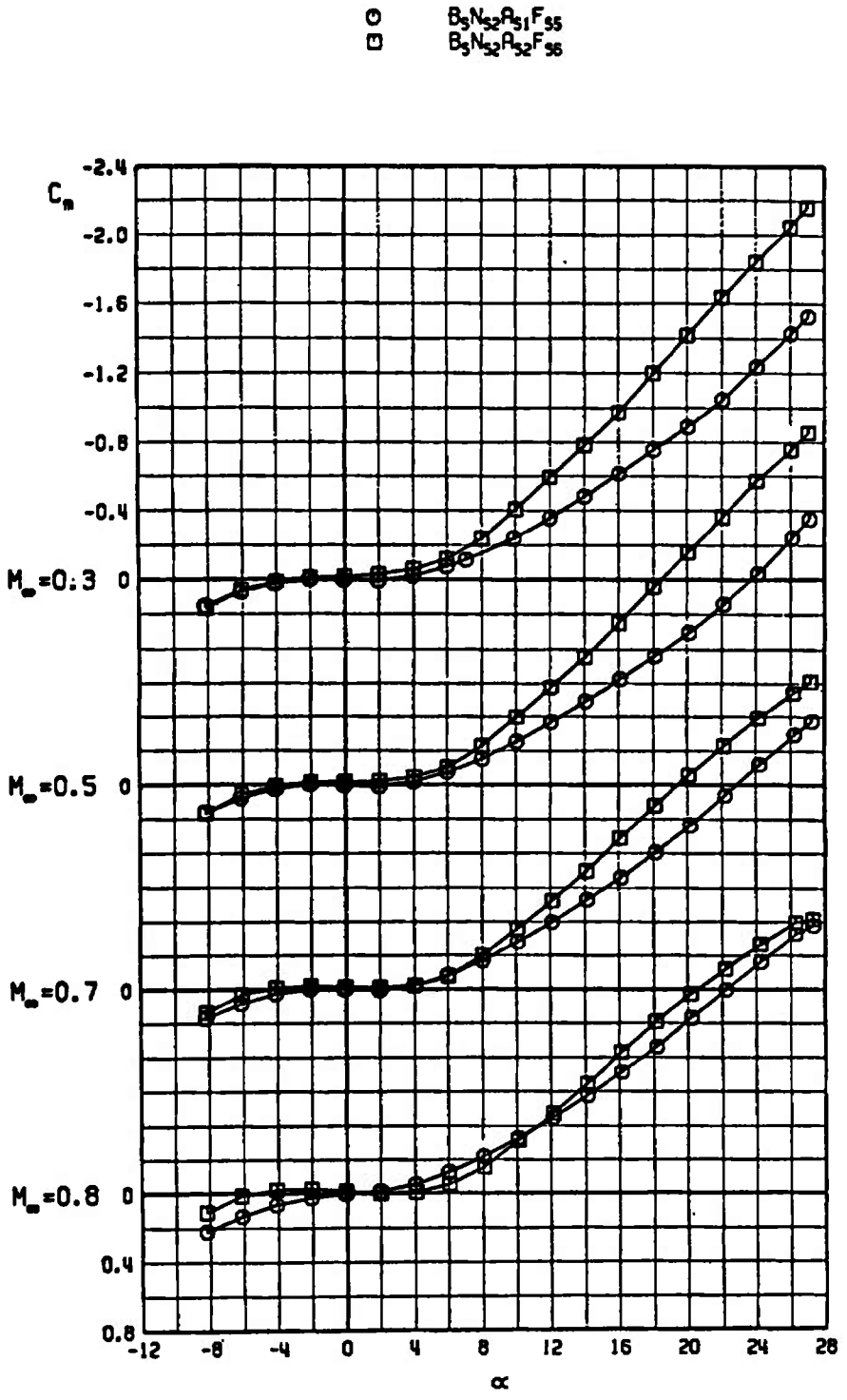

b. C_m versus α
Fig. 8 Continued

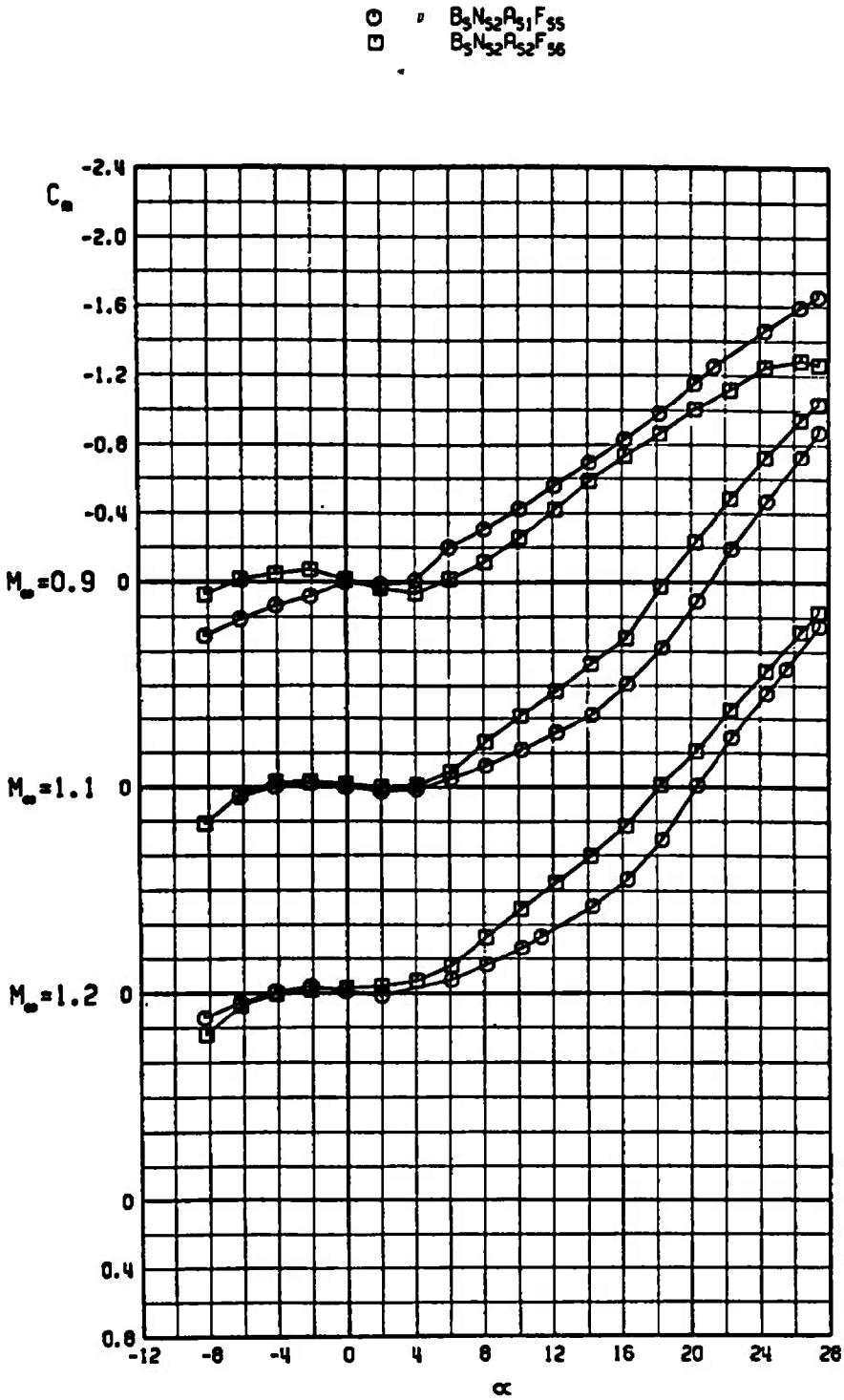

b. Concluded
Fig. 8 Continued

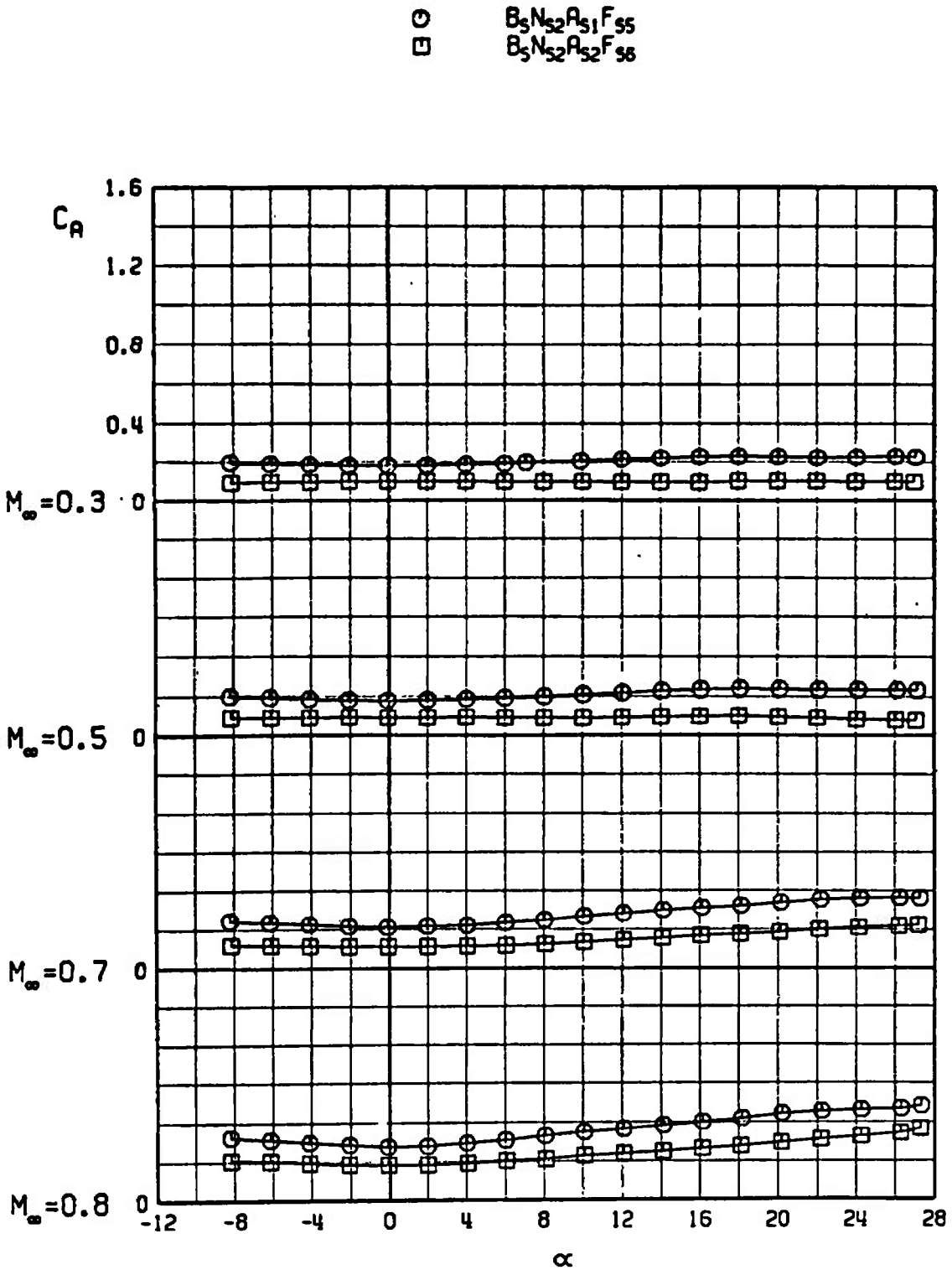

c. C_A versus α
Fig. 8 Continued

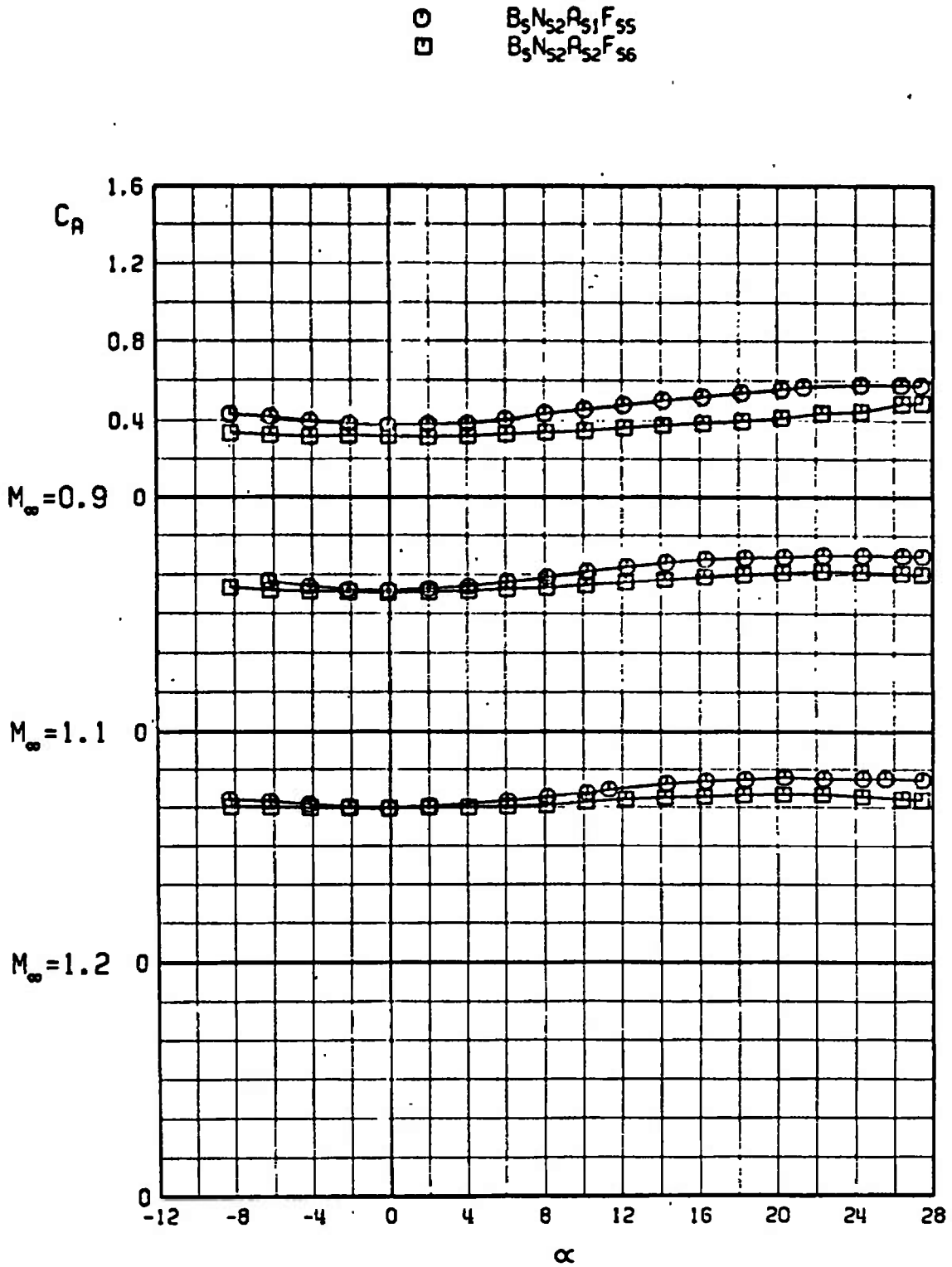

c. Concluded
Fig. 8 Concluded

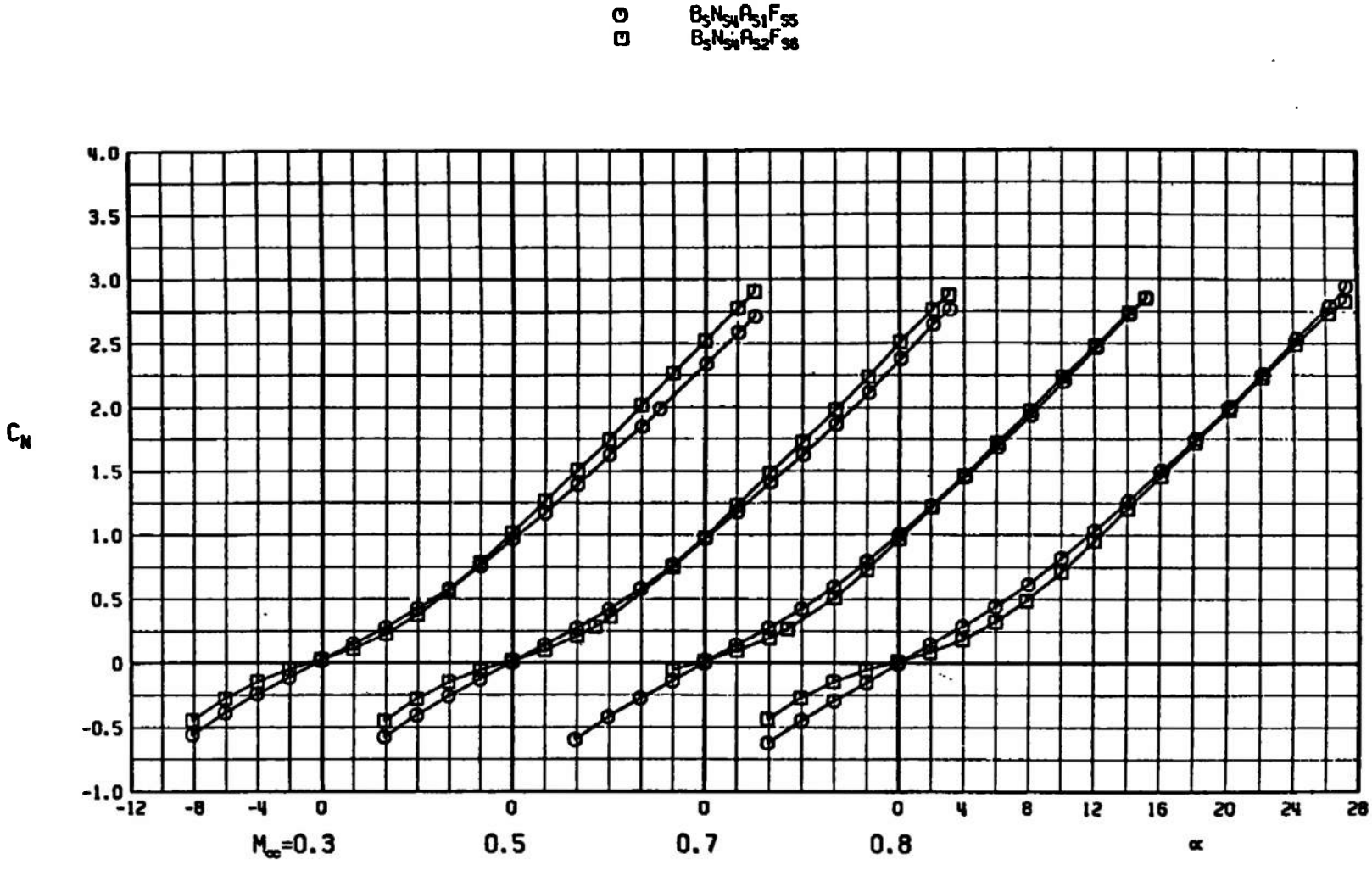

a. C_N versus α

Fig. 9 Effects of Afterbody Shape on Longitudinal Characteristics of Model with Spherical-Segment Nose, $B_S N_{S4} A_{SX} F_{SX}$, $\phi = 0$

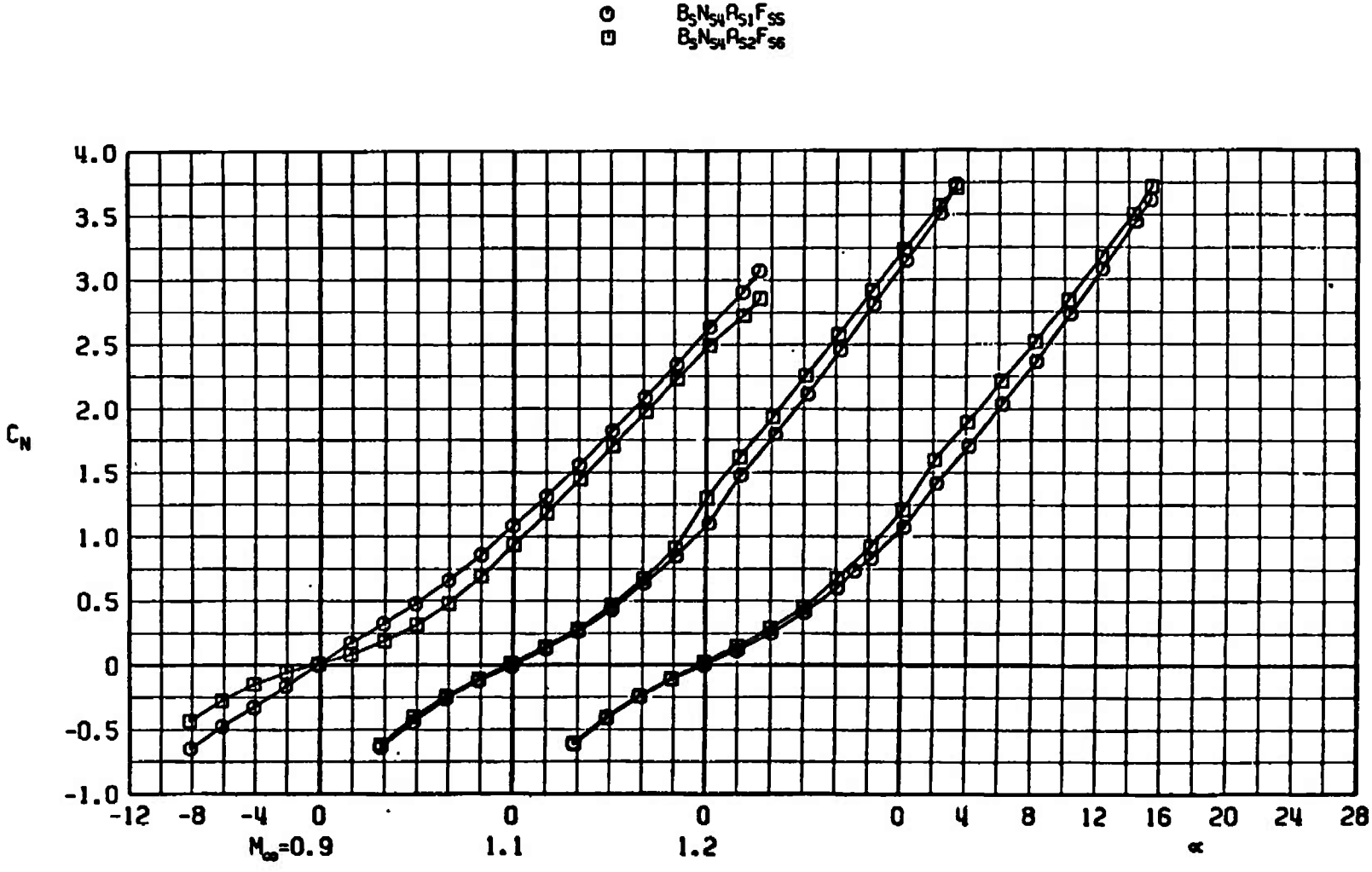

a. Concluded
Fig. 9 Continued

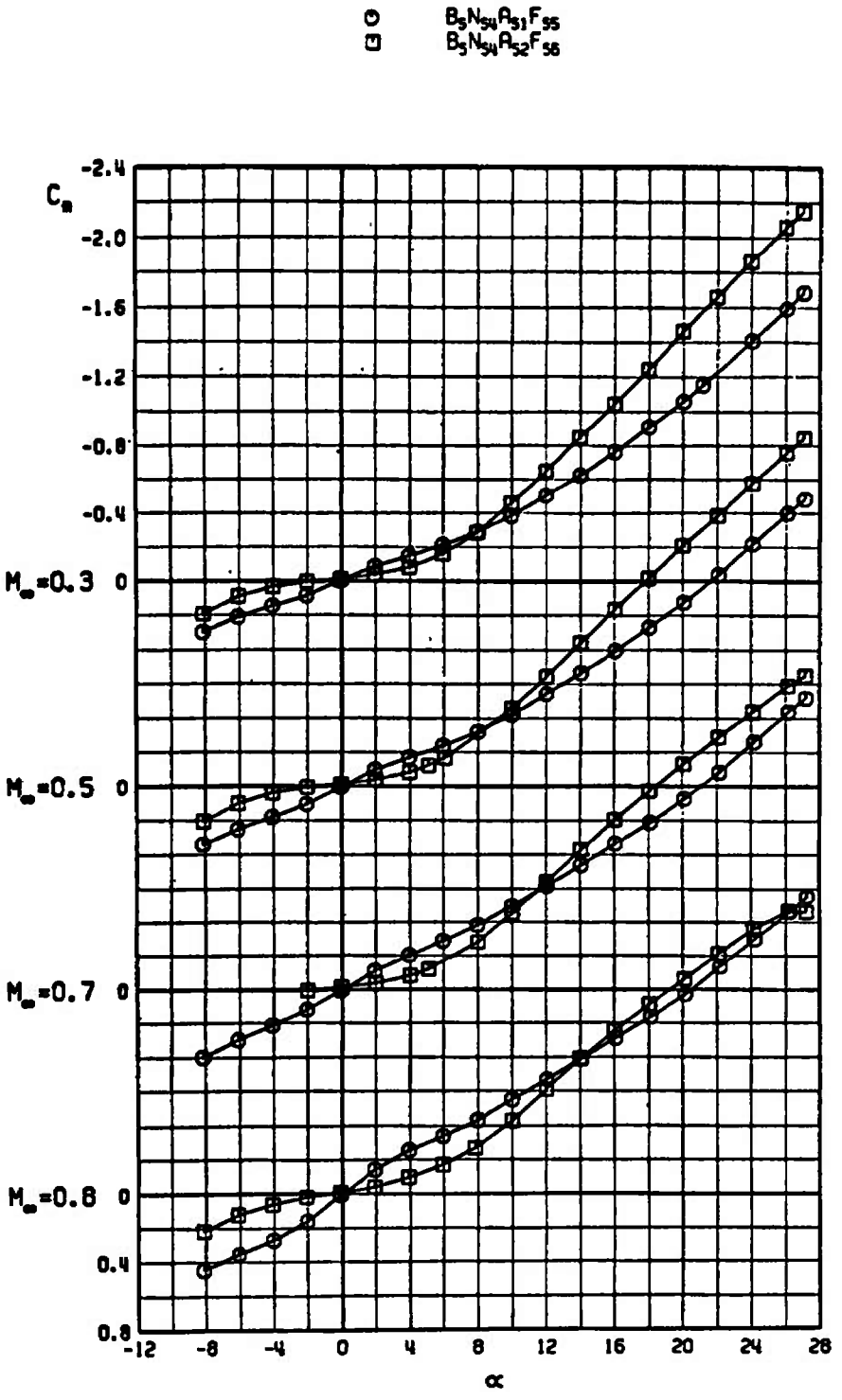

b. C_m versus α
Fig. 9 Continued

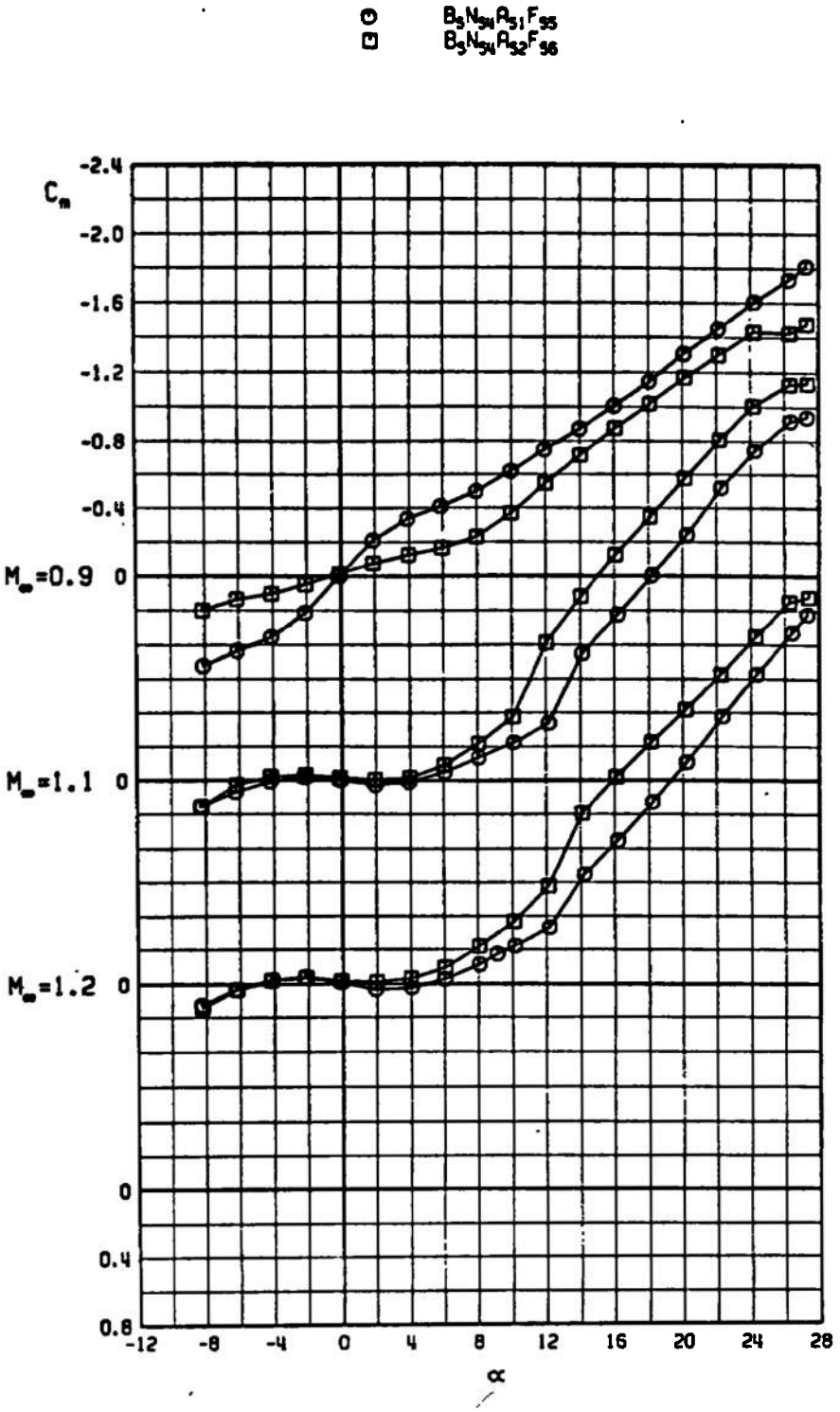

b. Concluded
Fig. 9 Continued

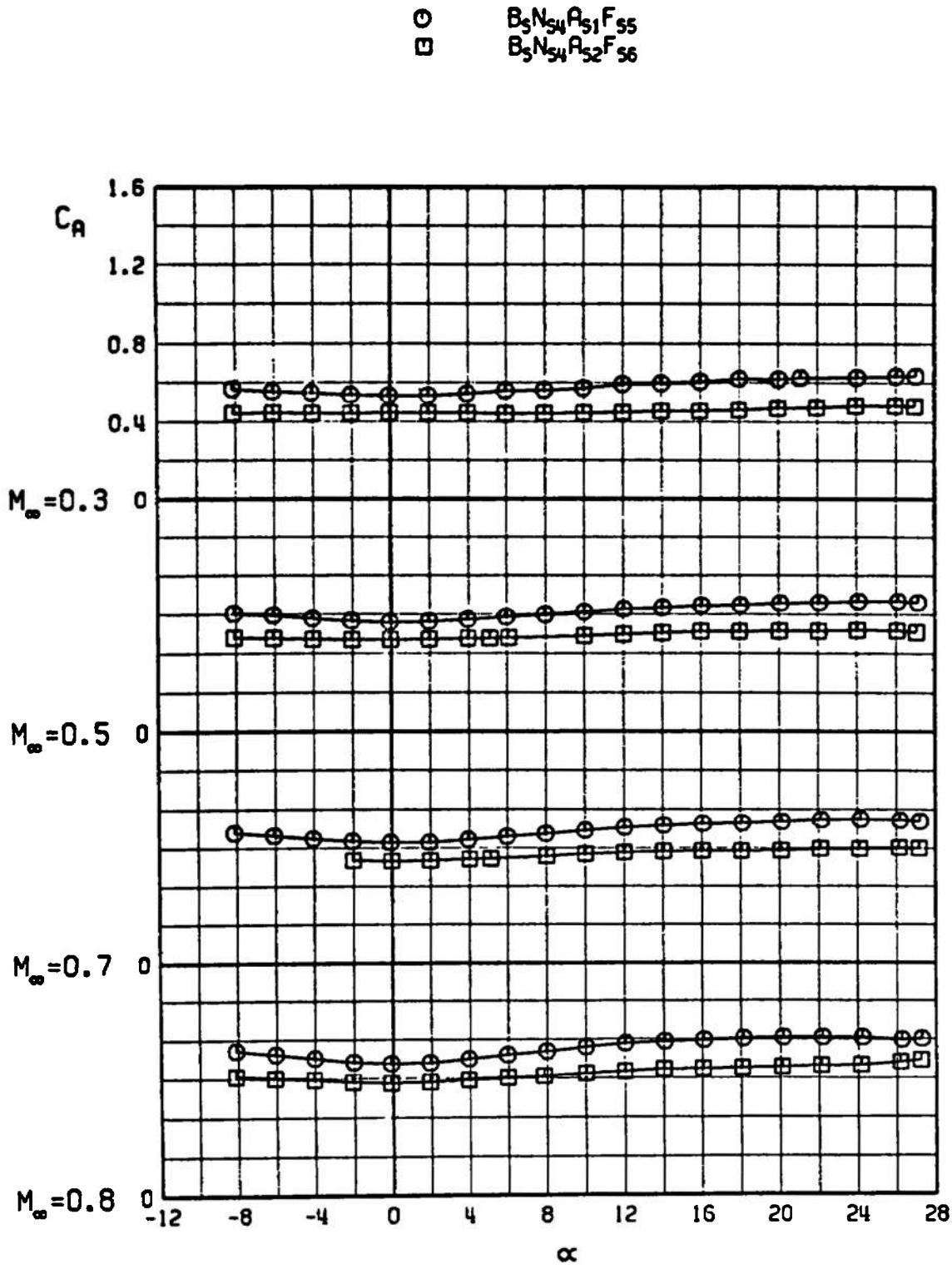

c. C_A versus α
Fig. 9 Continued

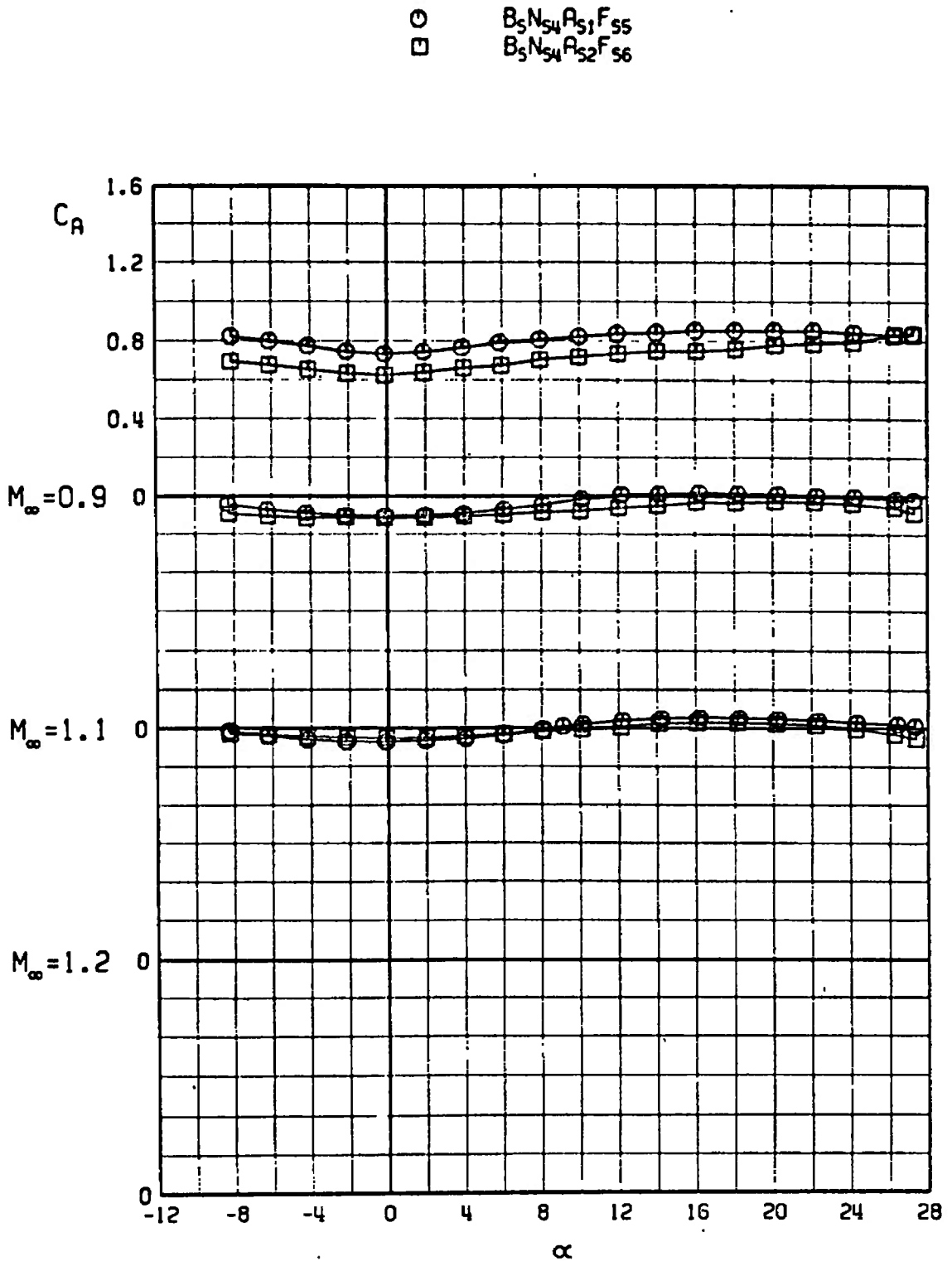

c. Concluded

Fig. 9 Concluded

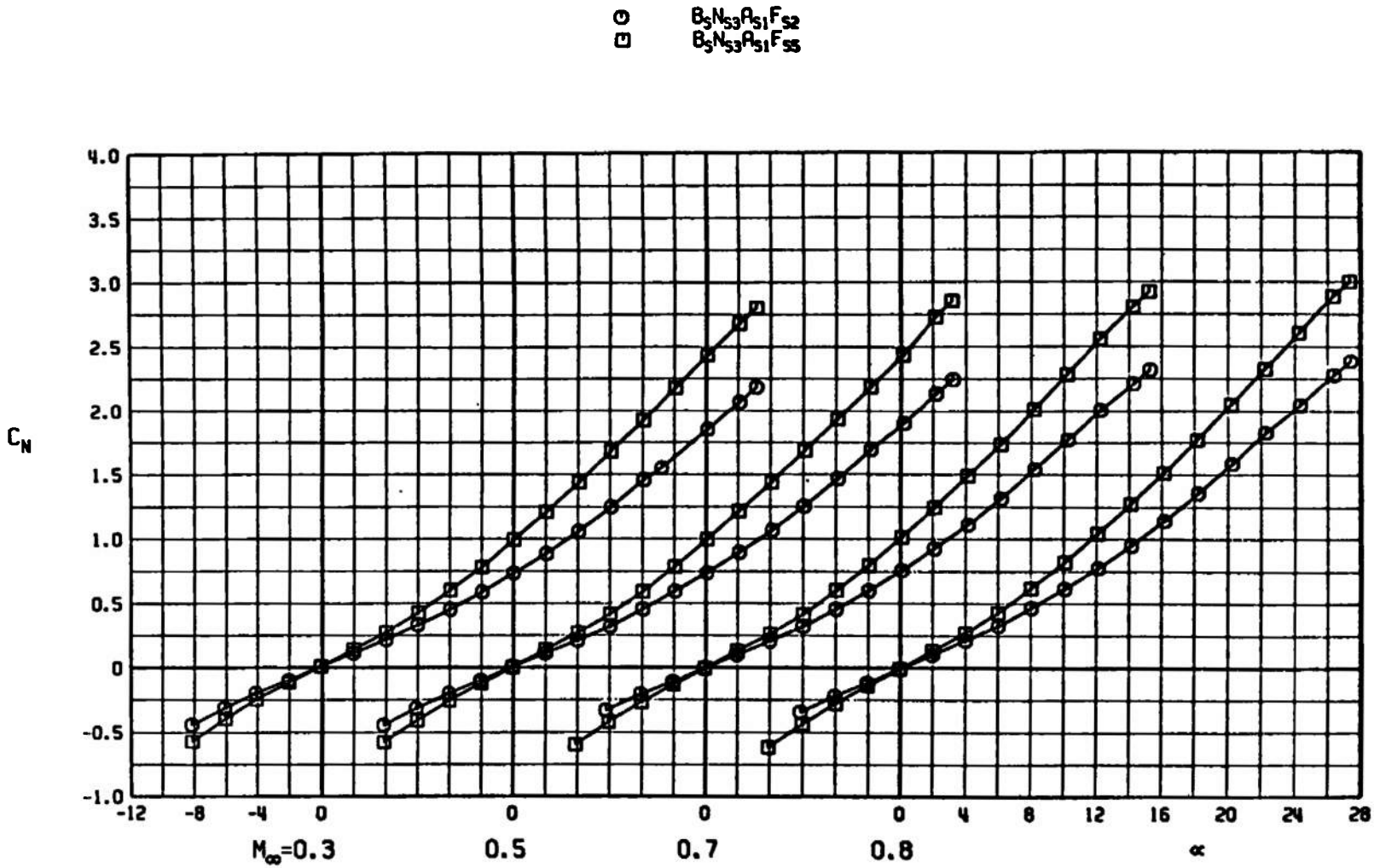

a. C_N versus α

Fig. 10 Effects of Fin Span on Longitudinal Characteristics of Model with Cylindrical Afterbody and Blunted Nose, $B_S N_{S3} A_{S1} F_{SX}$, $\phi = 0$

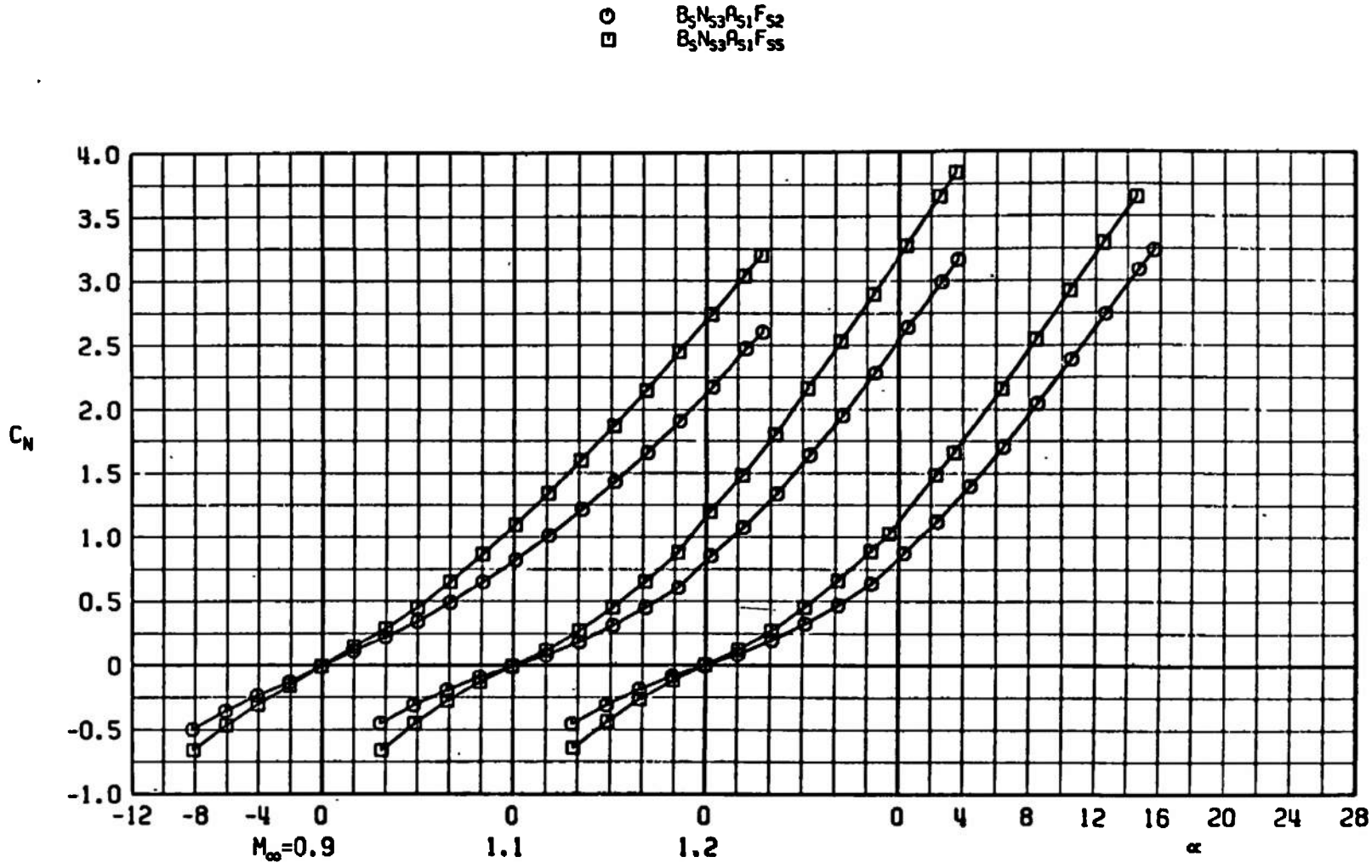

a. Concluded
Fig. 10 Continued

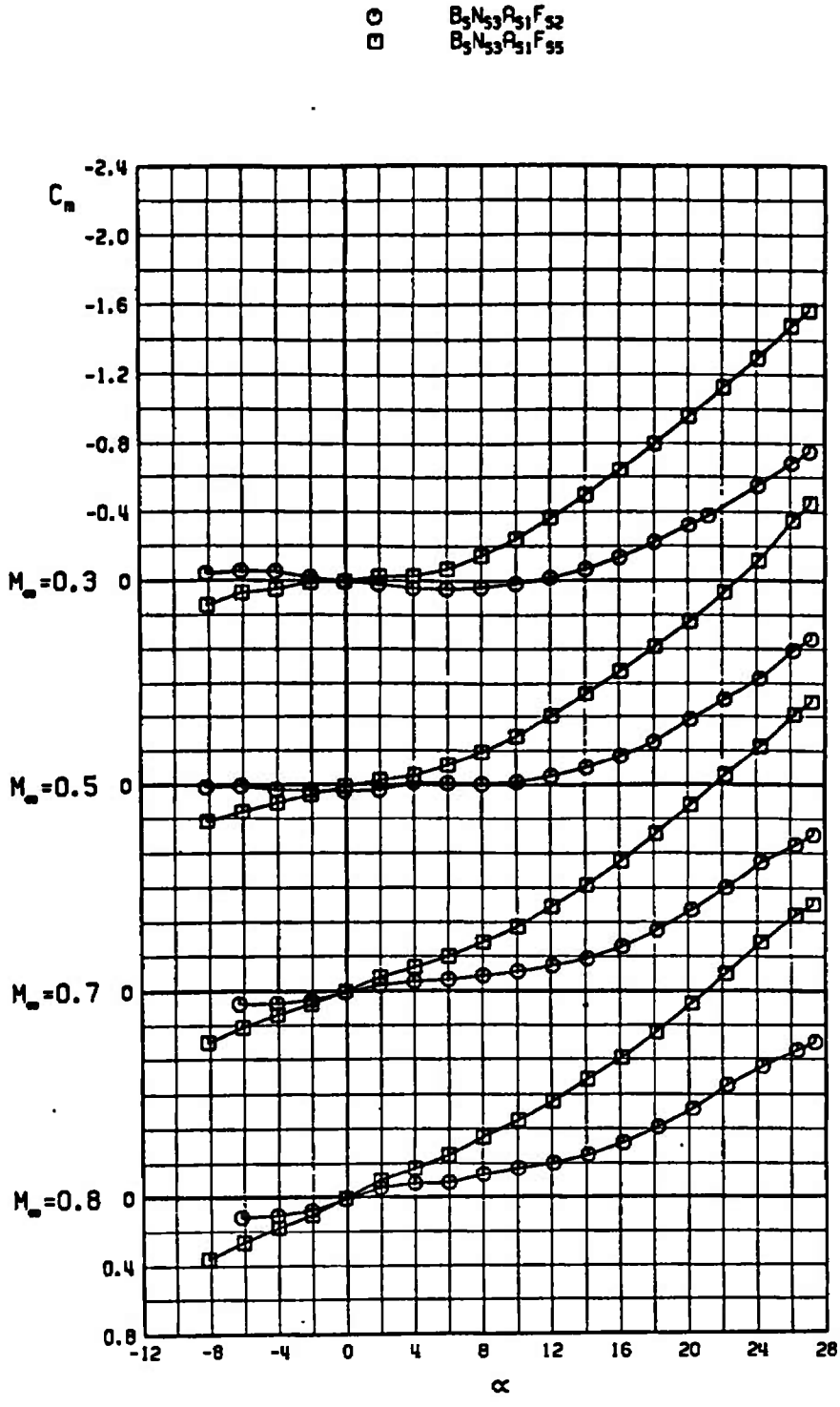

b. C_m versus α

Fig. 10 Continued

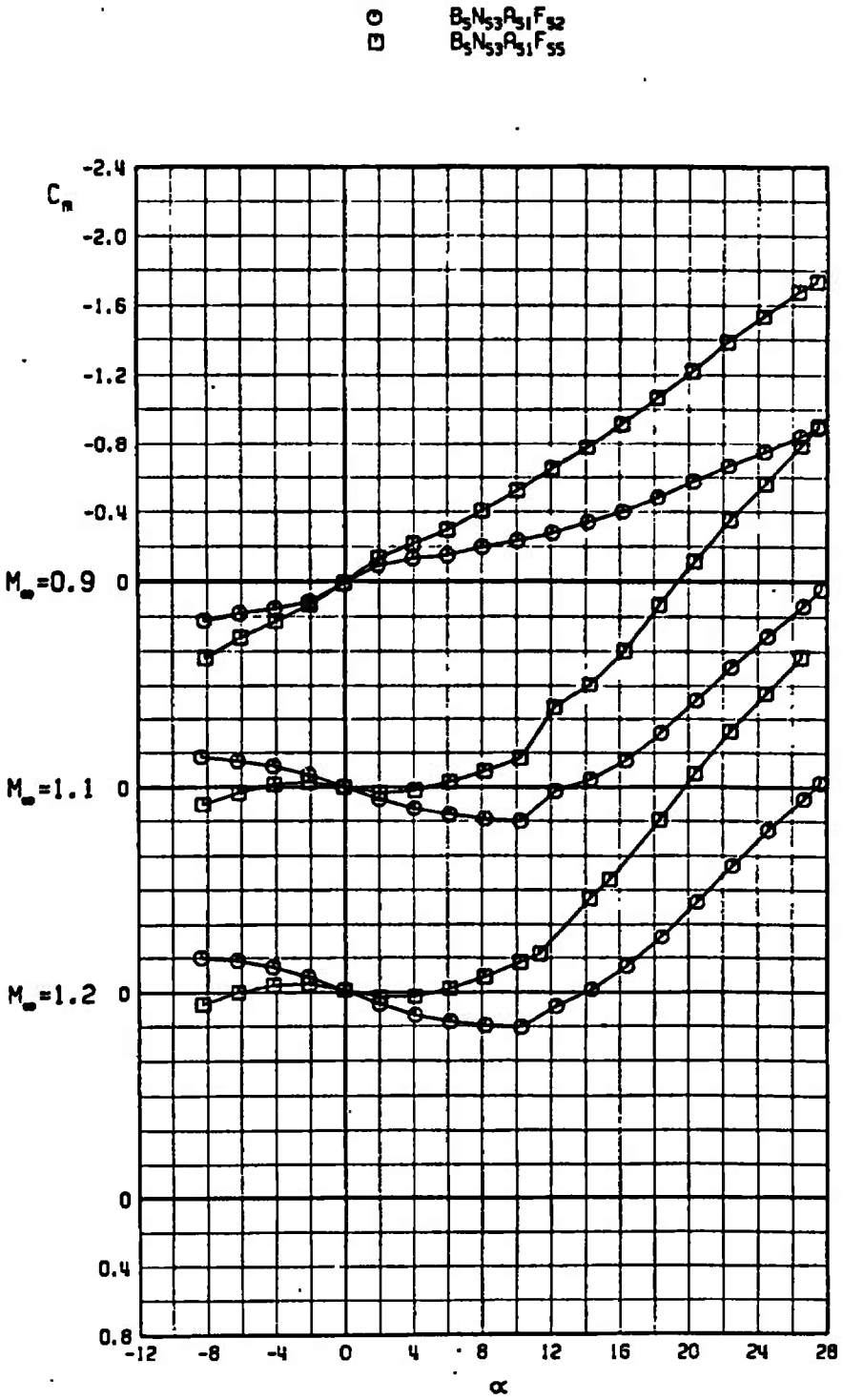

b. Concluded
Fig. 10 Continued

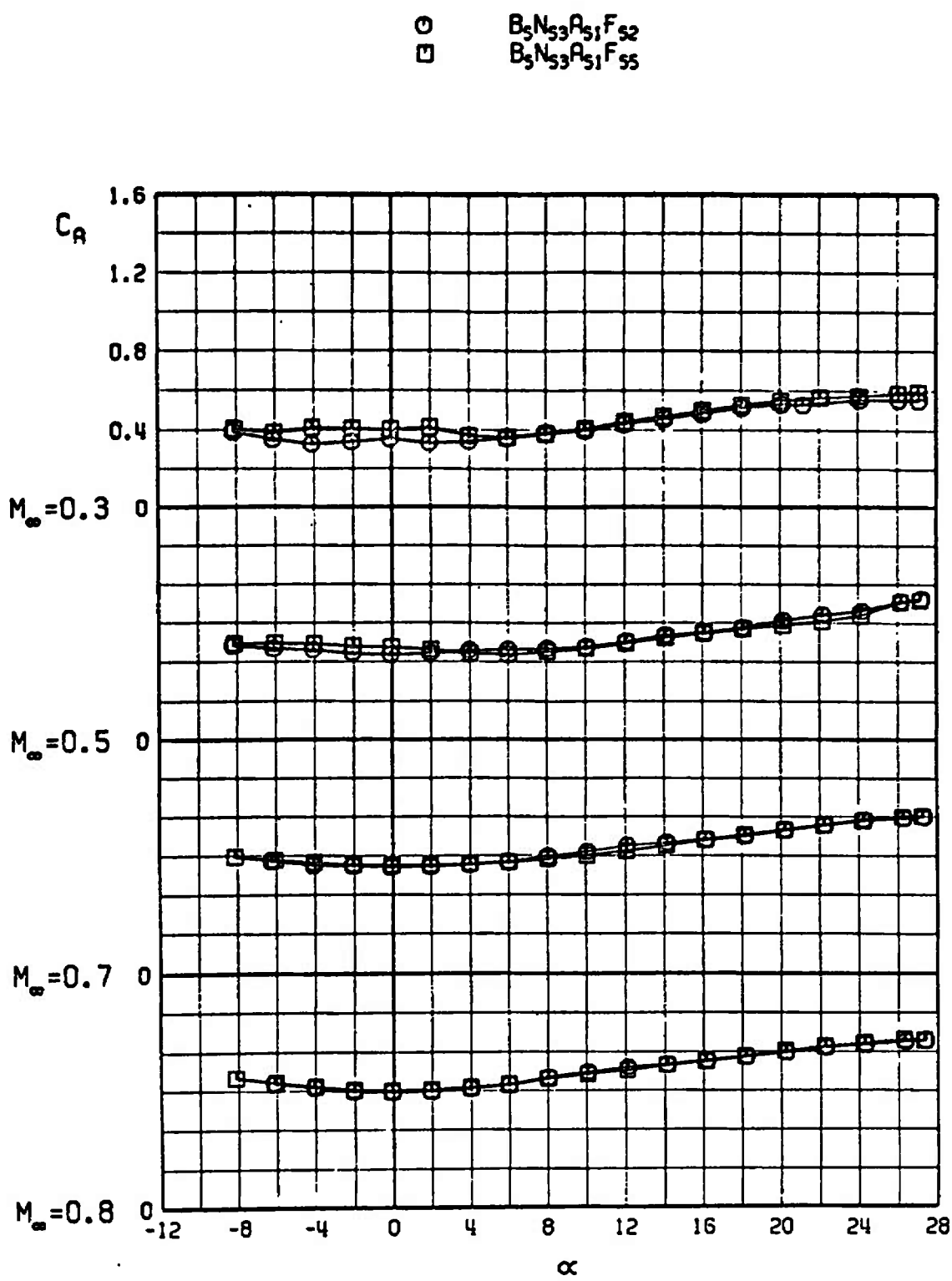

c. C_A versus α
Fig. 10 Continued

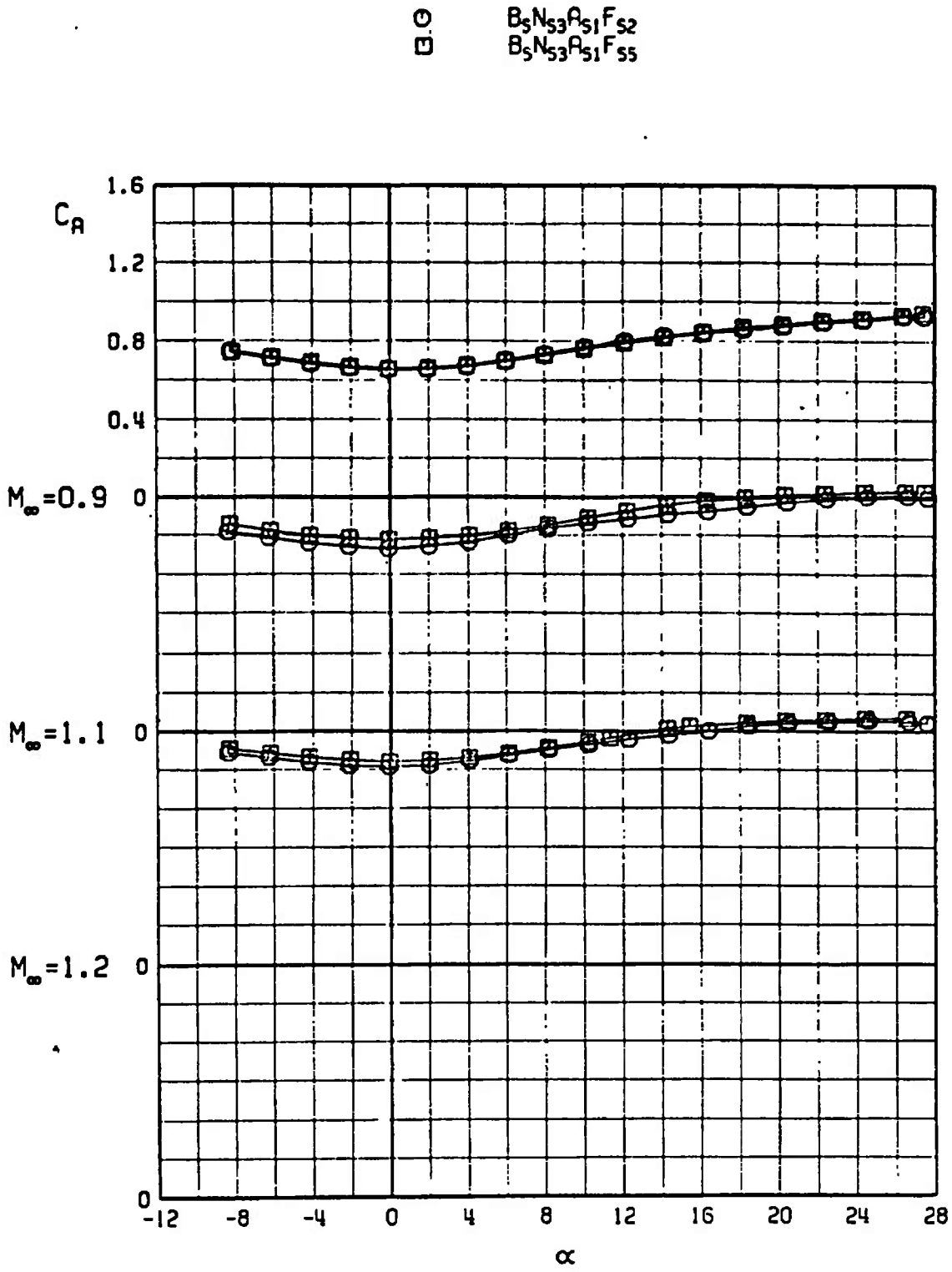

c. Concluded
Fig. 10 Concluded

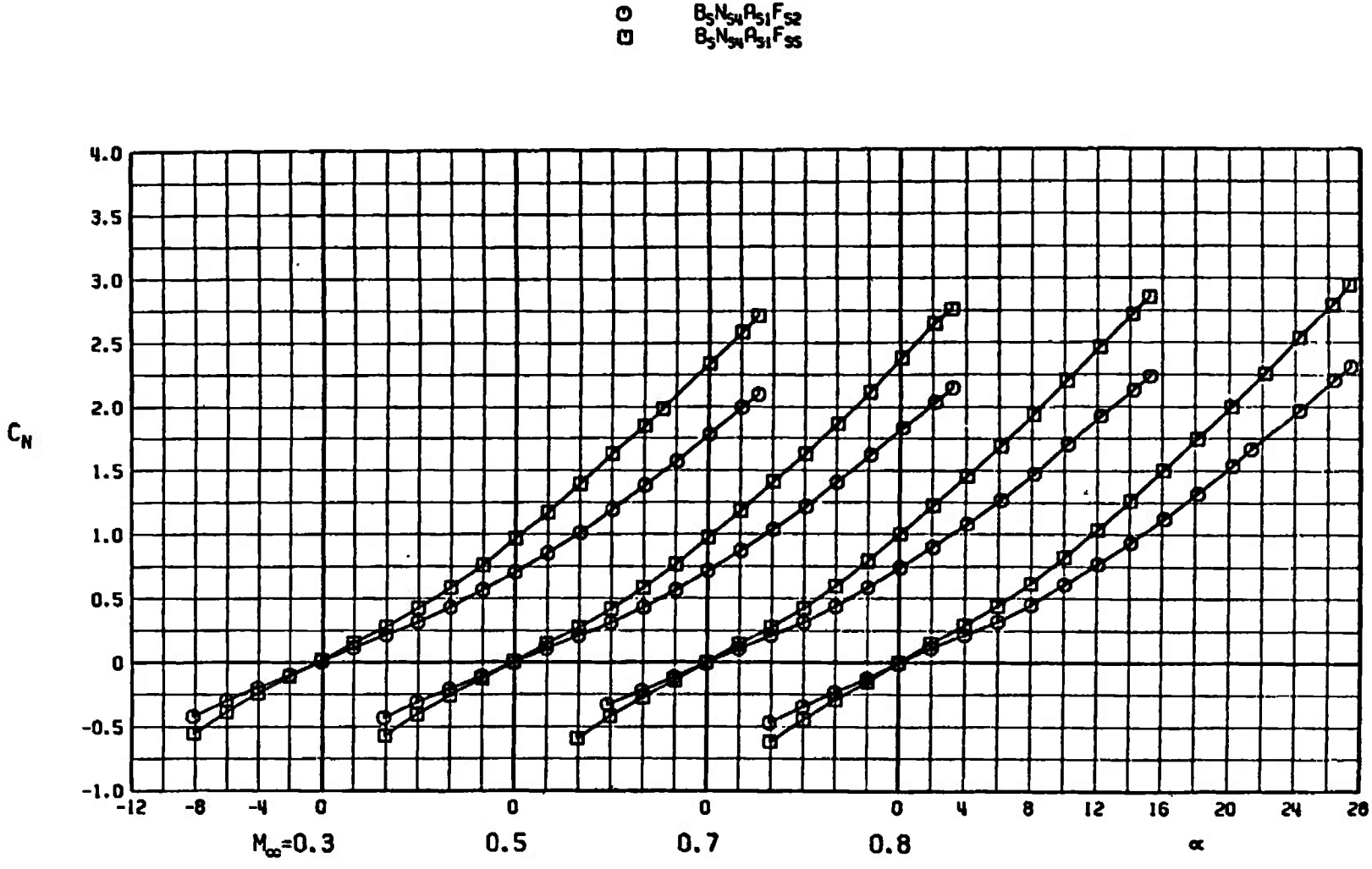

a. C_N versus α

Fig. 11 Effects of Fin Span on Longitudinal Characteristics of Model with Cylindrical Afterbody and Spherical-Segment Nose, $B_S N_{S4} A_{S1} F_{SX}$, $\phi = 0$

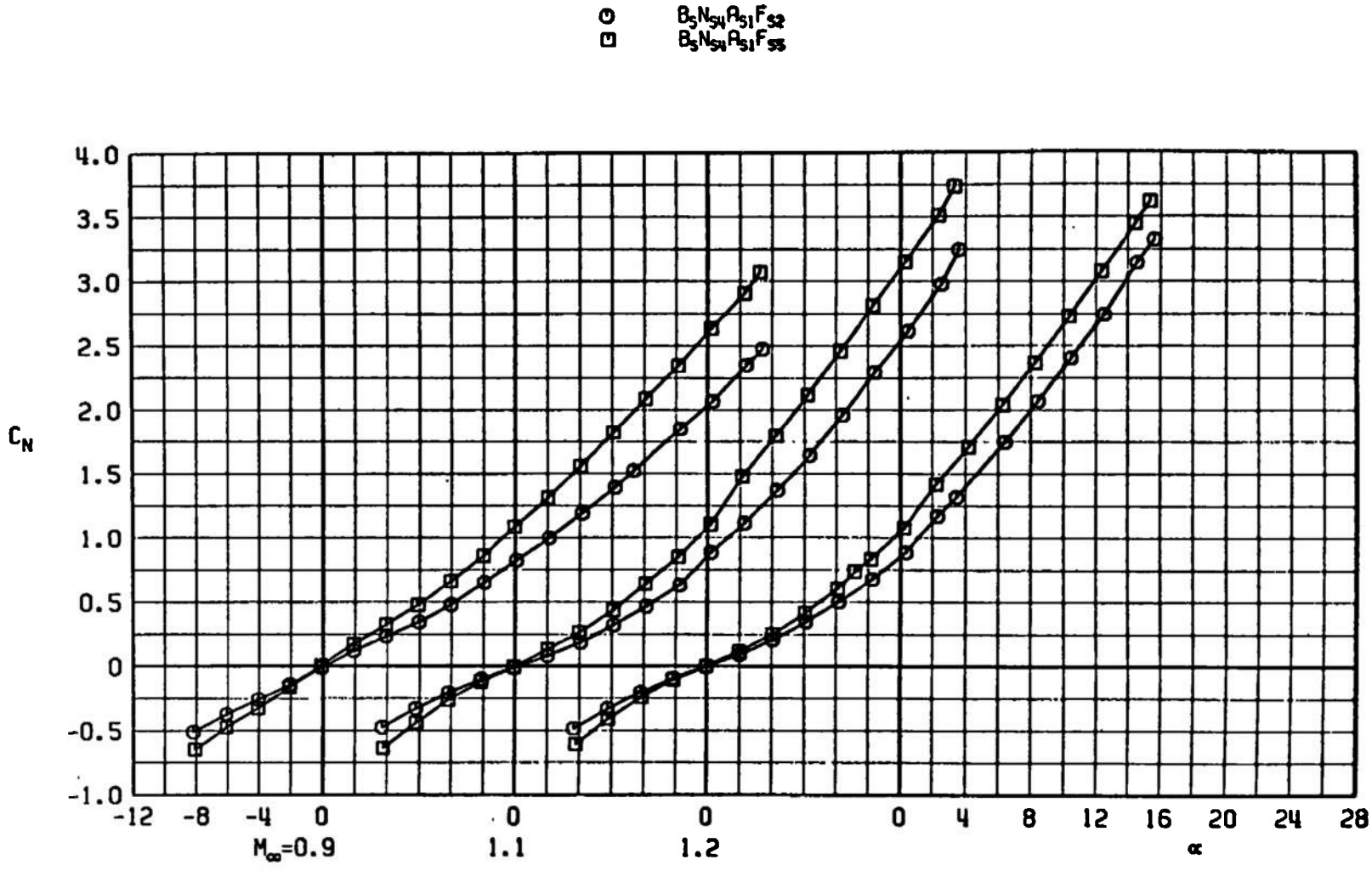

a. Concluded

Fig. 11 Continued

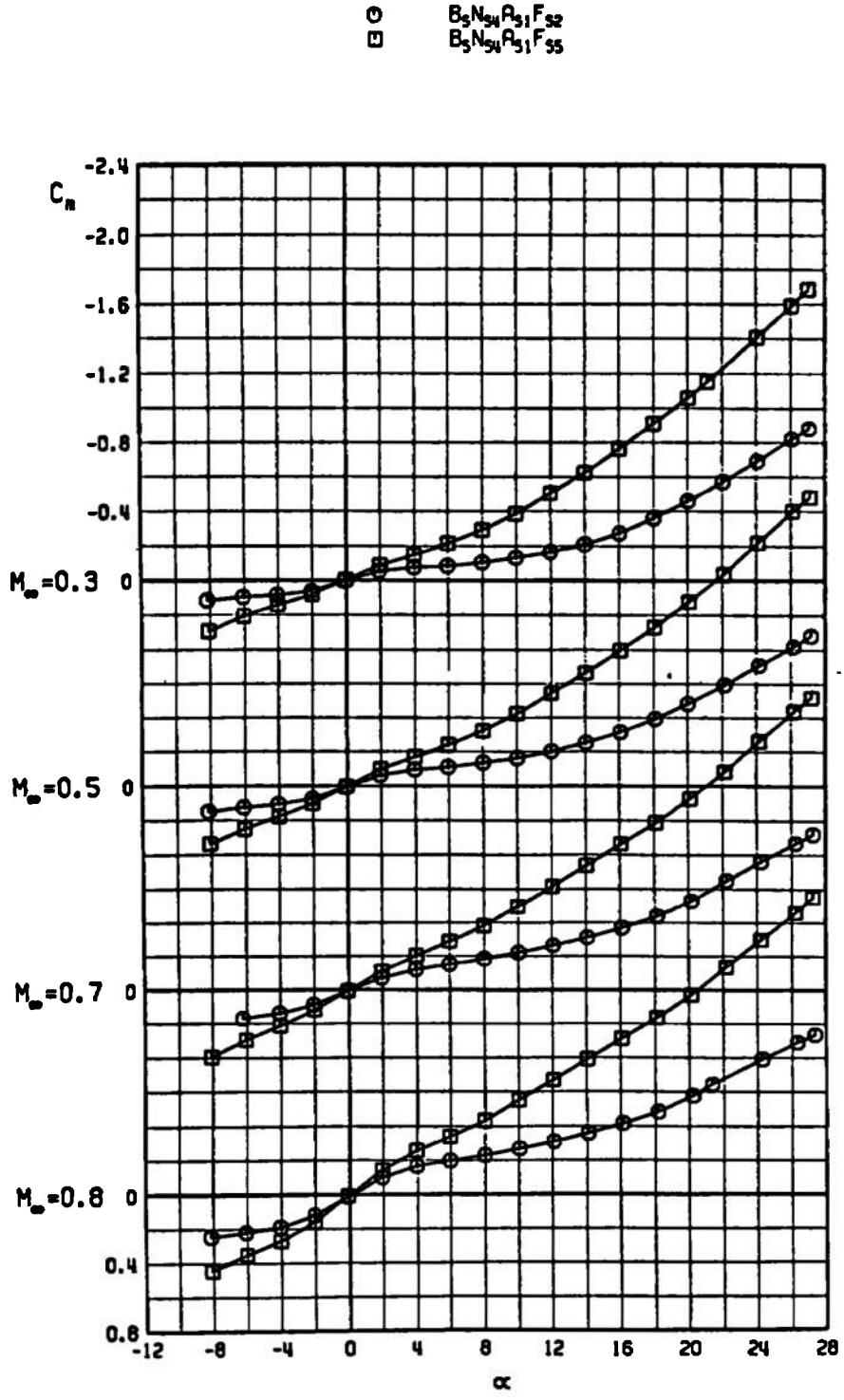

b. C_m versus α

Fig. 11 Continued

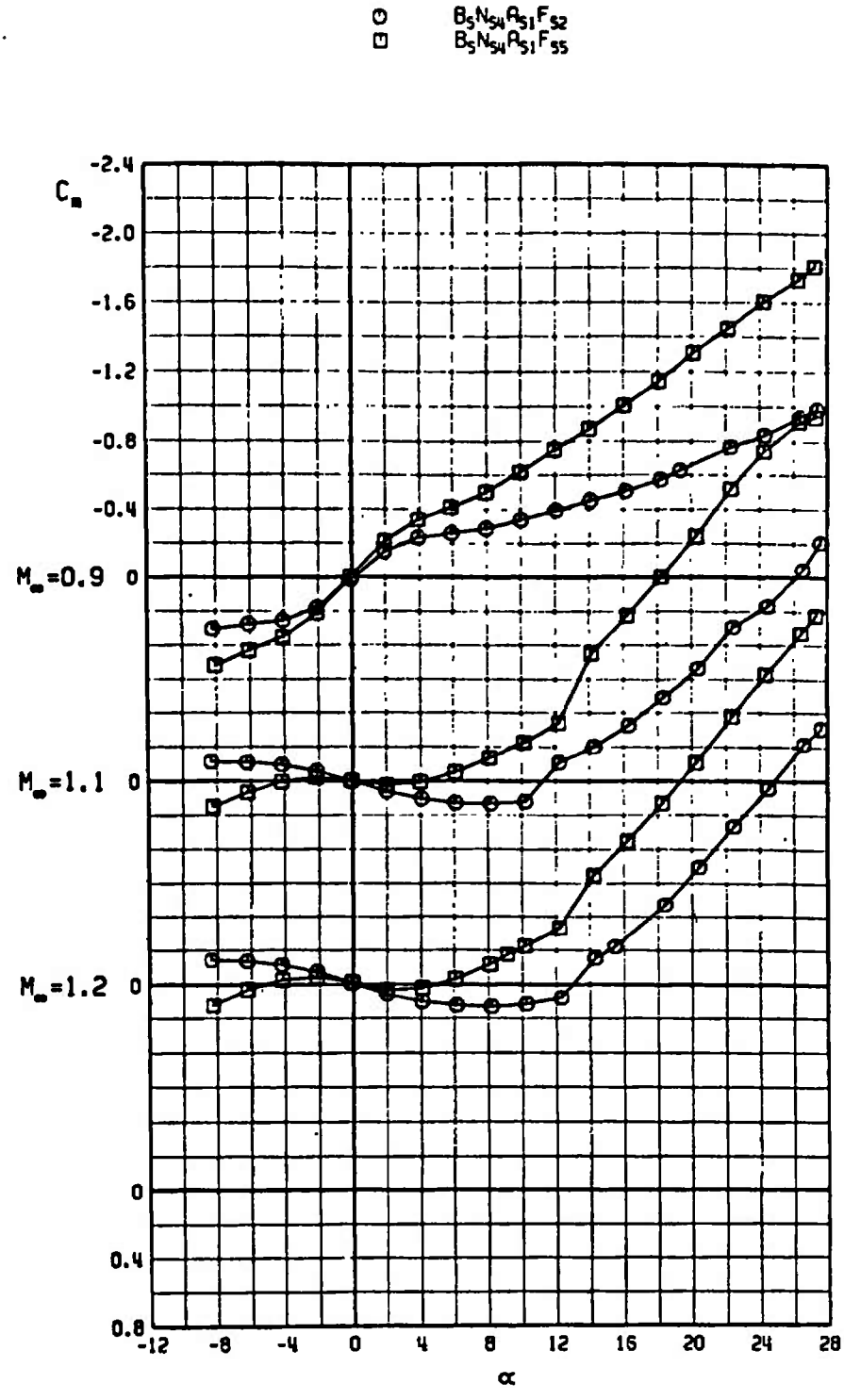

b. Concluded
Fig. 11 Continued

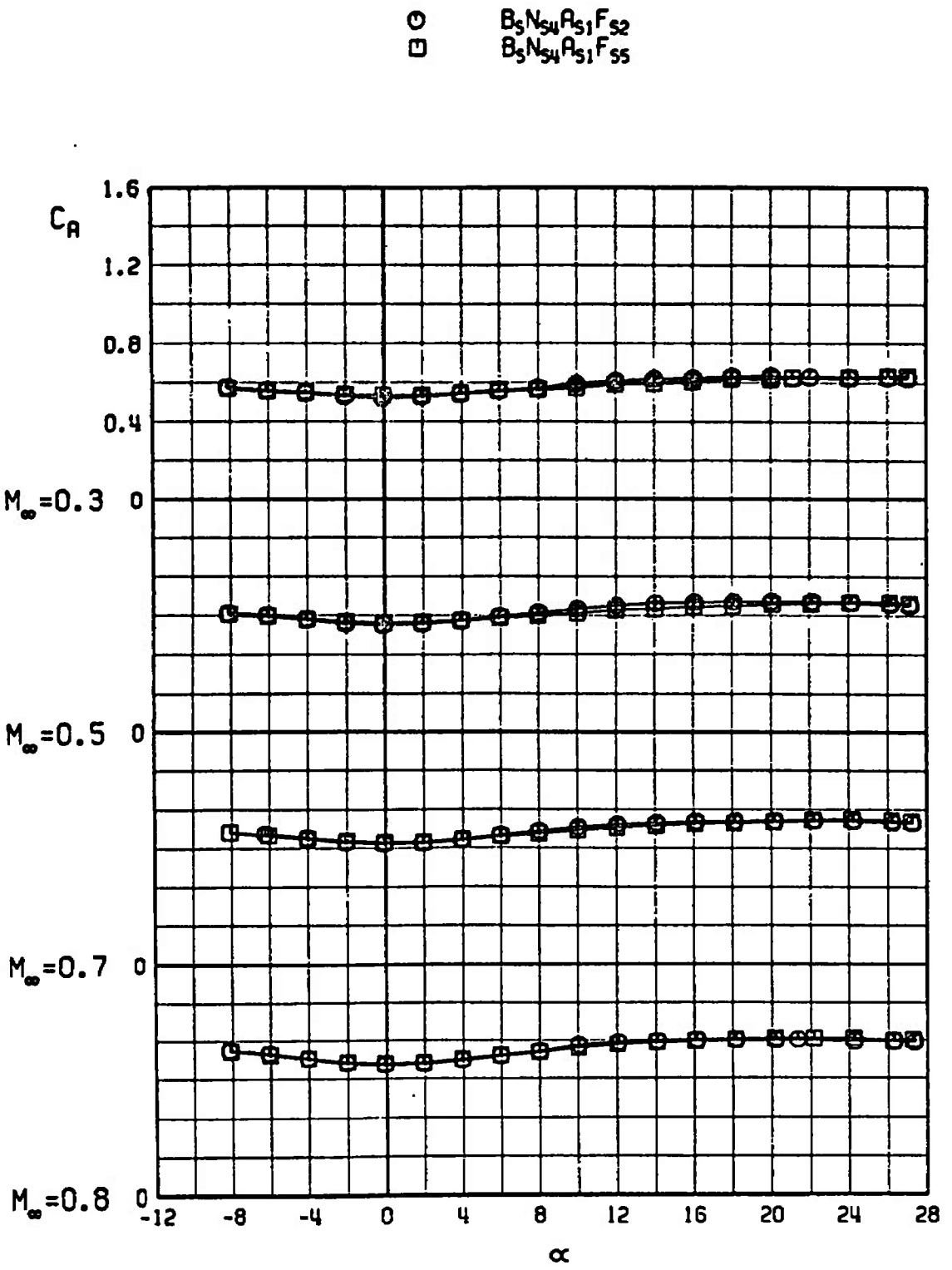

c. C_A versus α
Fig. 11 Continued

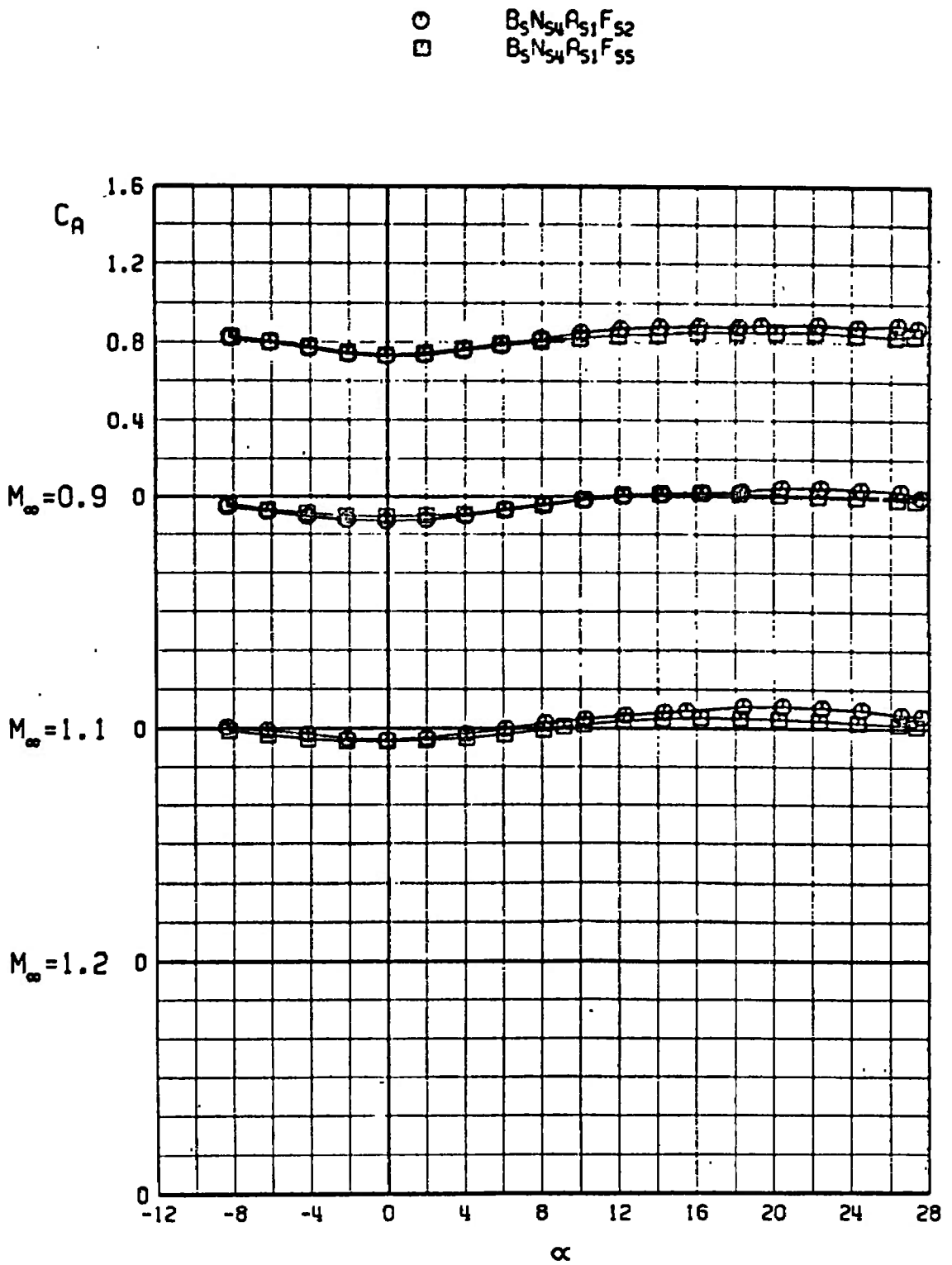

c. Concluded
Fig. 11 Concluded

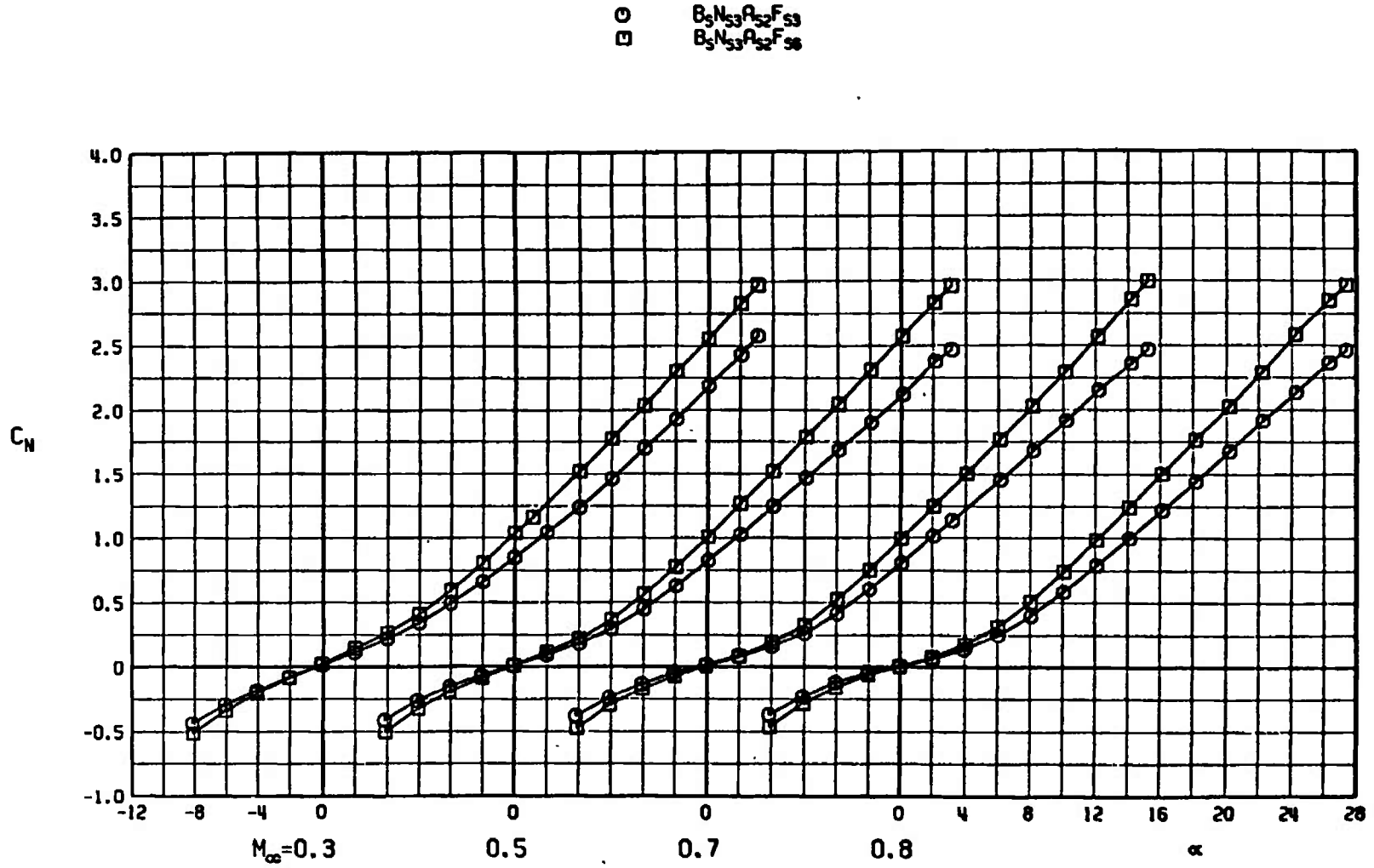

a. C_N versus α

Fig. 12 Effects of Fin Span on Longitudinal Characteristics of Model with Boattail Afterbody and Blunted Nose, $B_S N_{S3} A_{S2} F_{Sx}$, $\phi = 0$

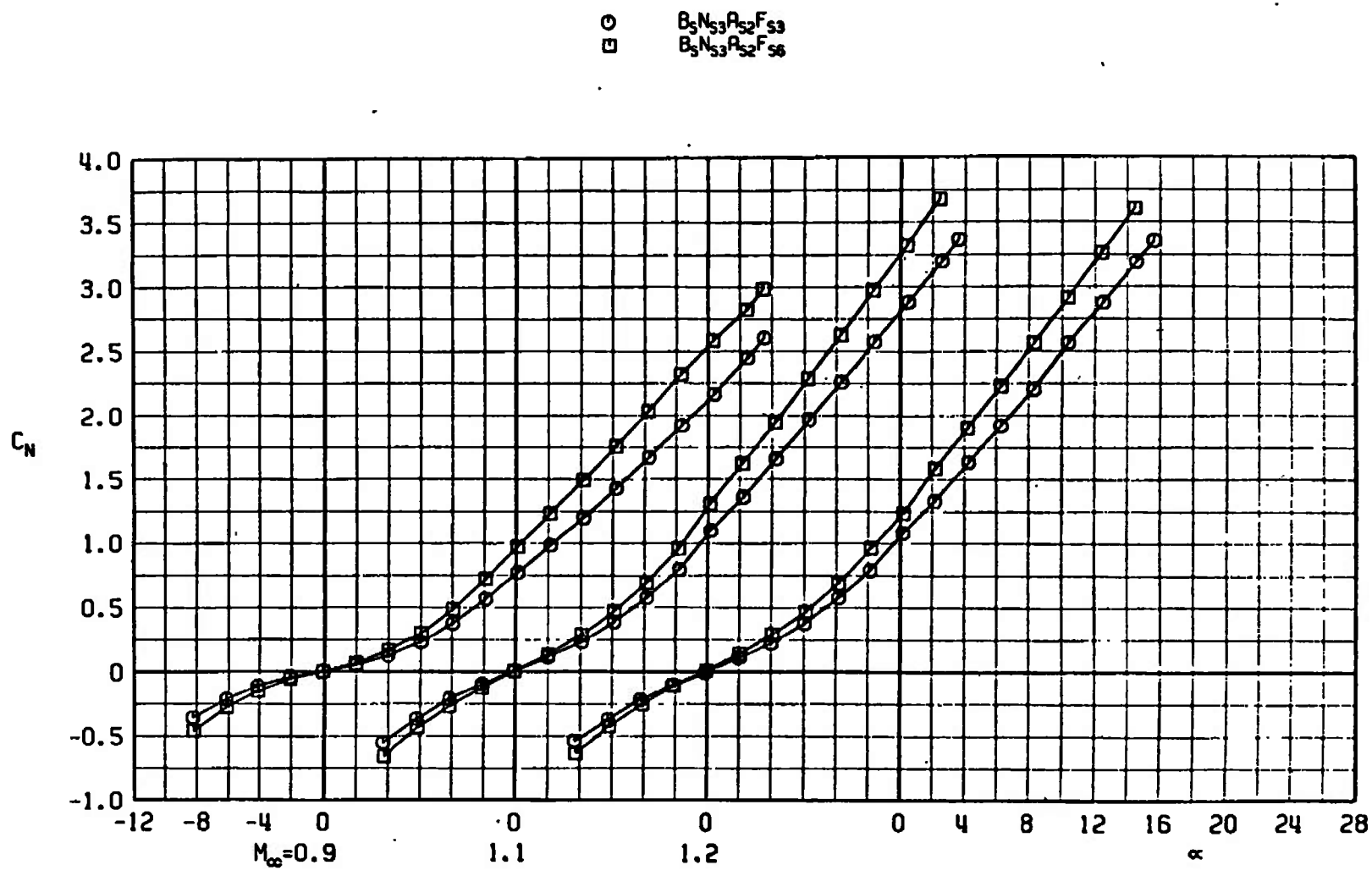

a. Concluded

Fig. 12 Continued

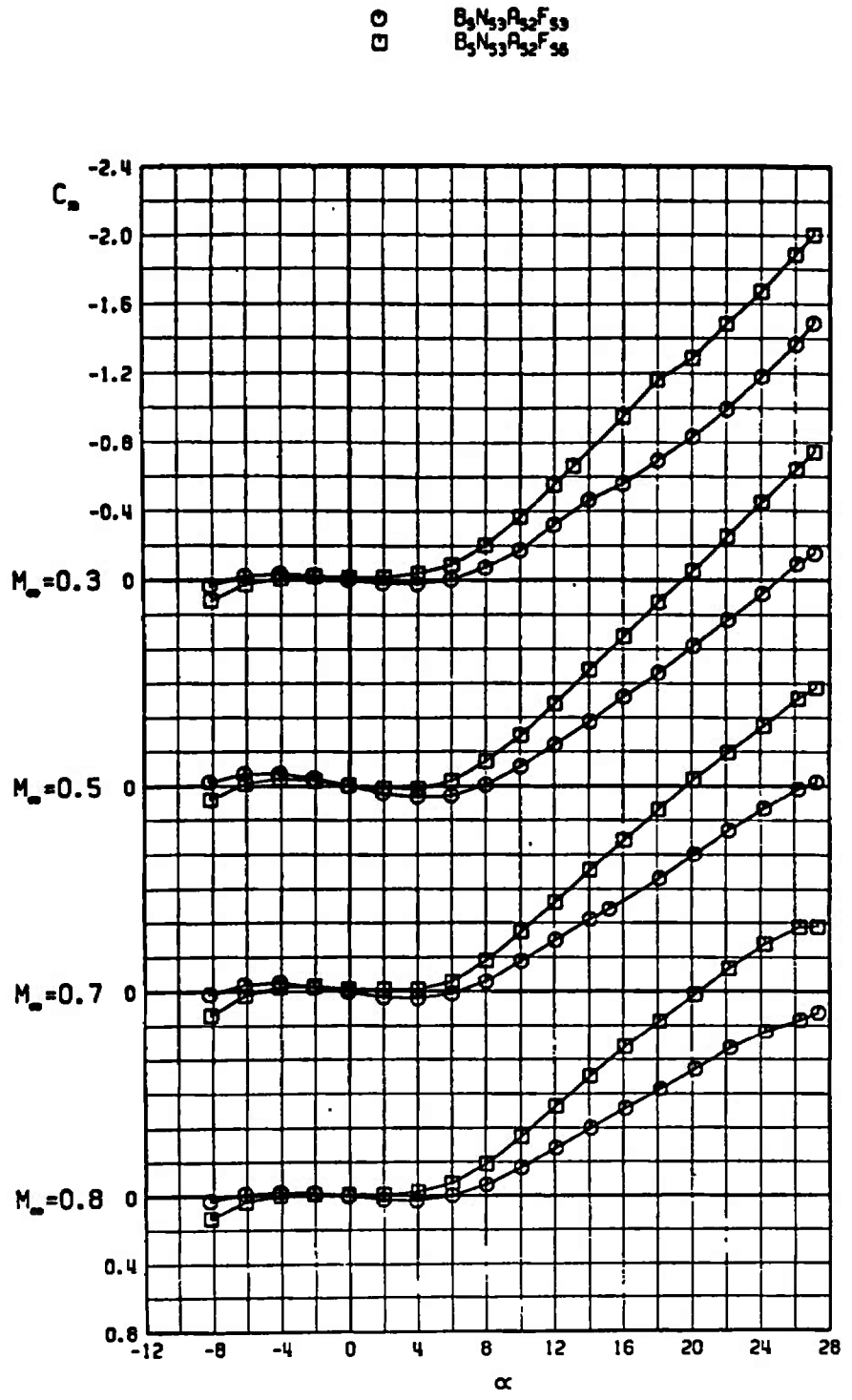

b. C_m versus α

Fig. 12 Continued

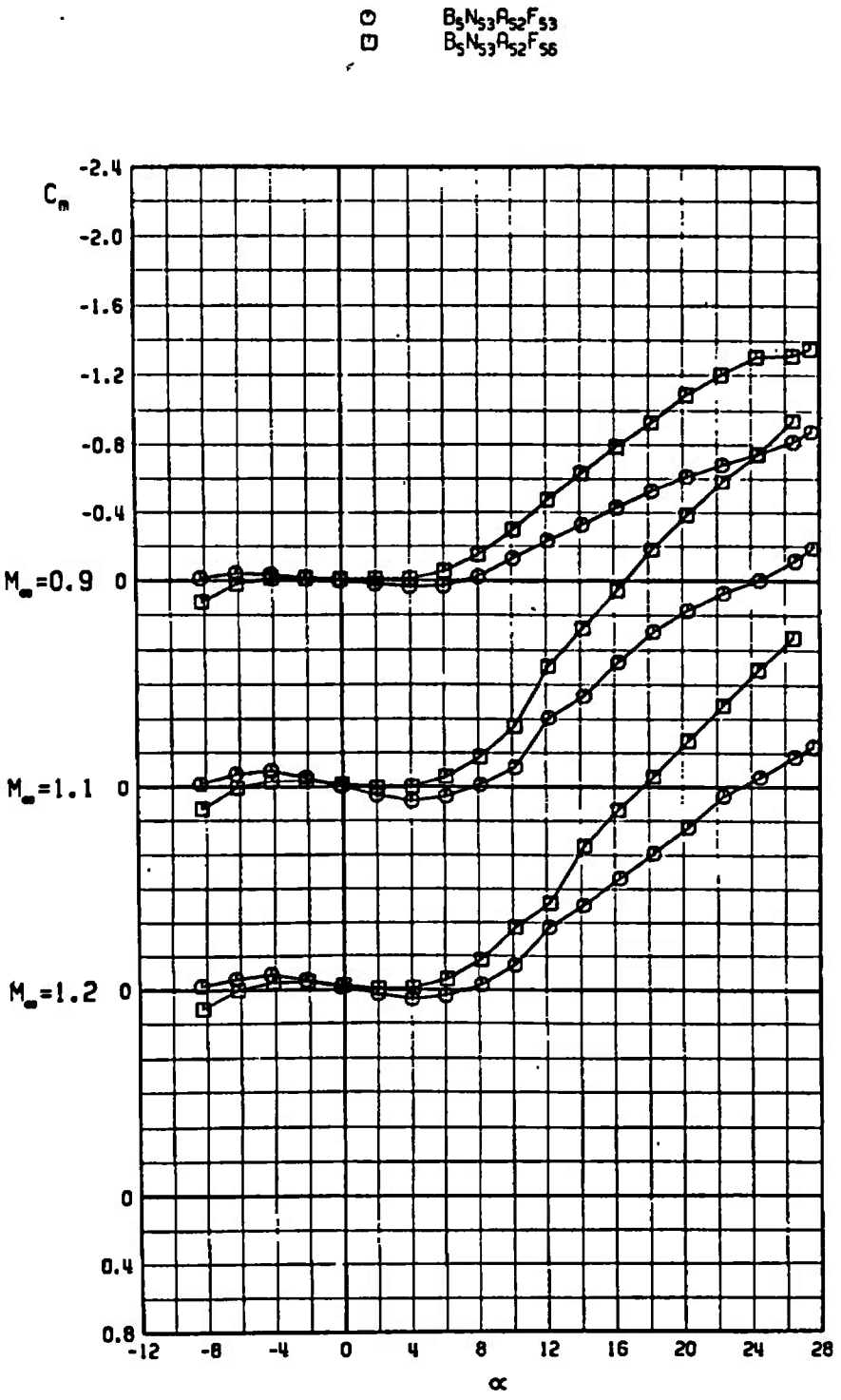

b. Concluded
Fig. 12 Continued

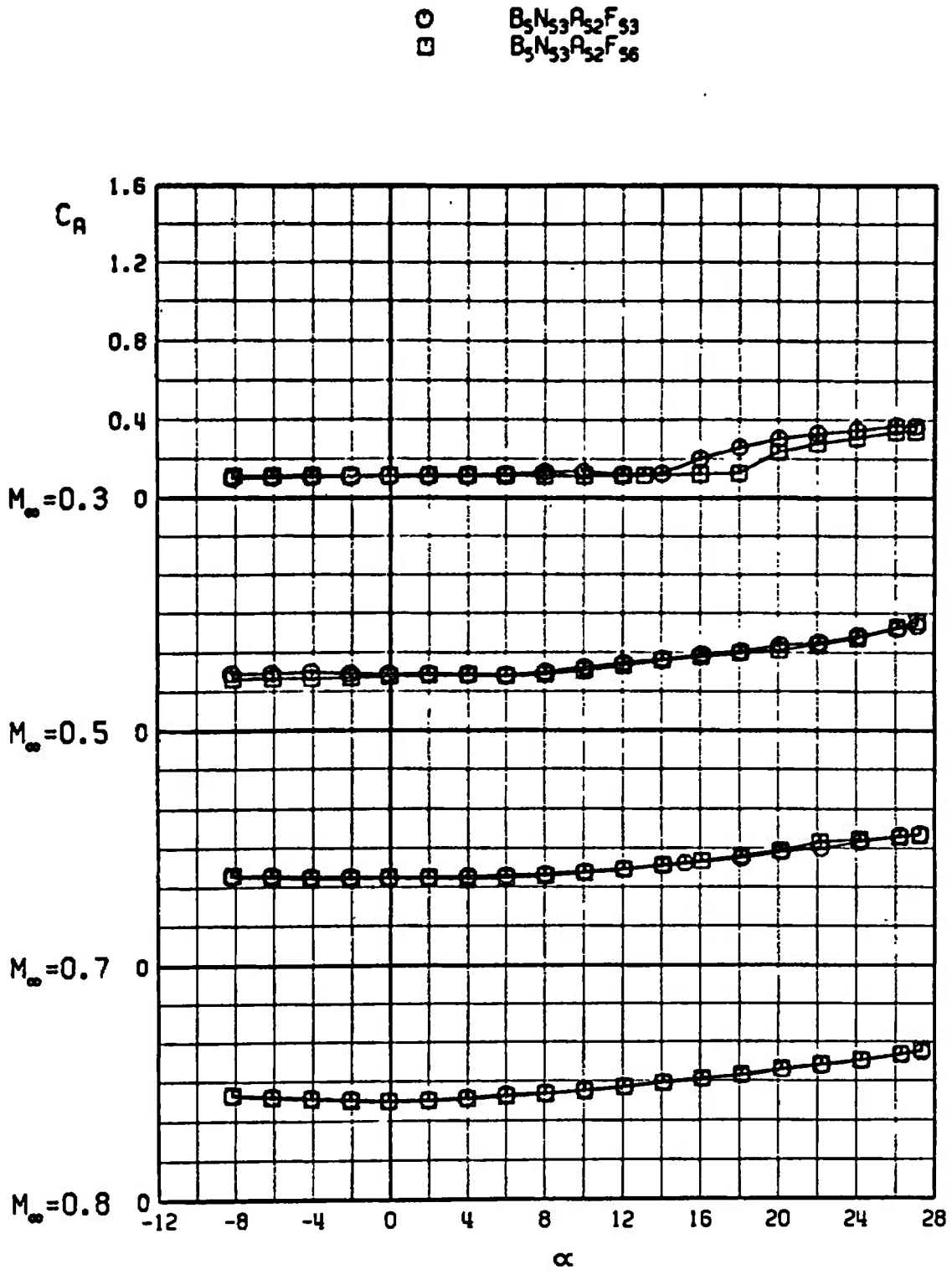

c. C_A versus α

Fig. 12 Continued

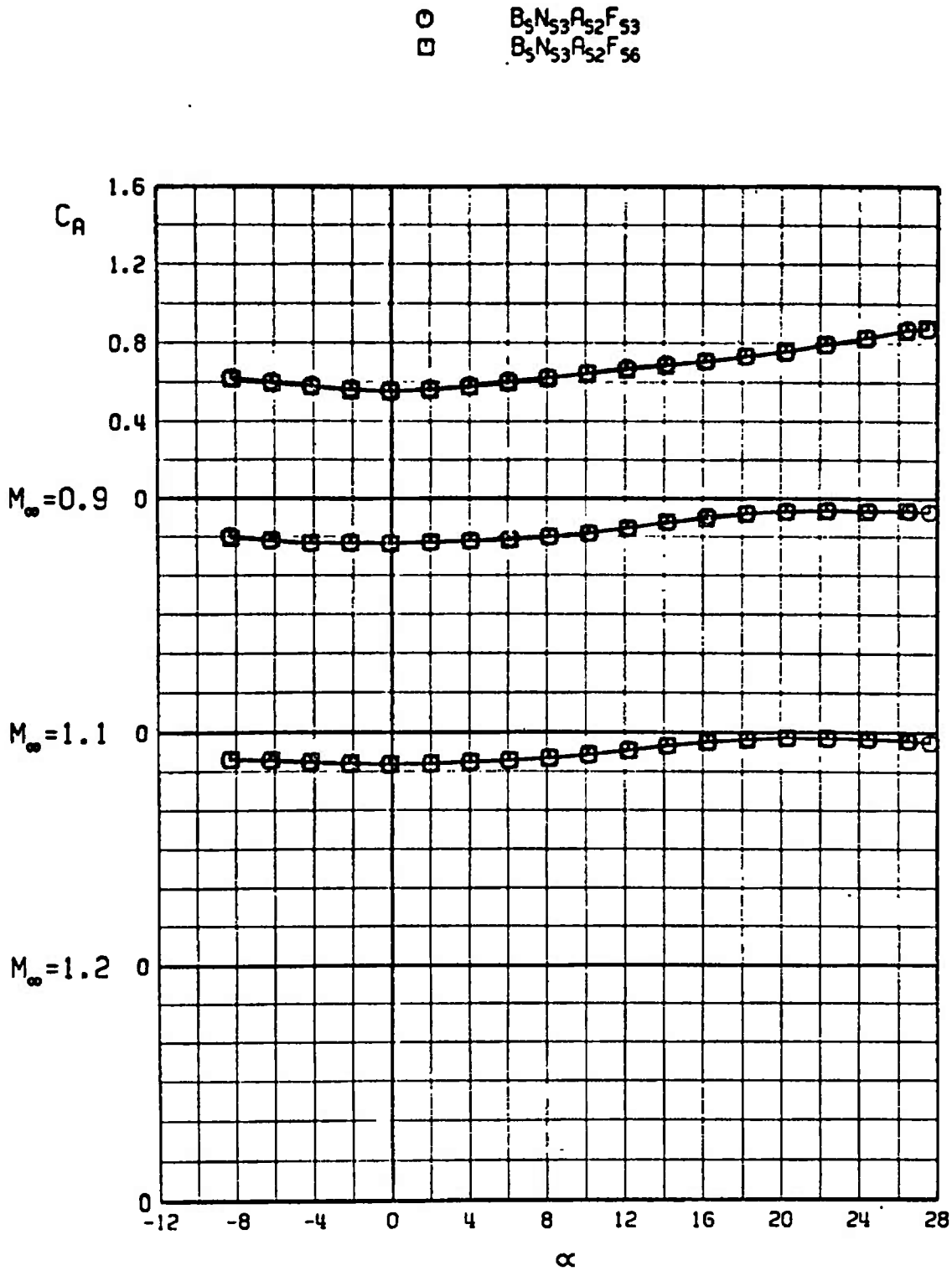

c. Concluded
Fig. 12 Concluded

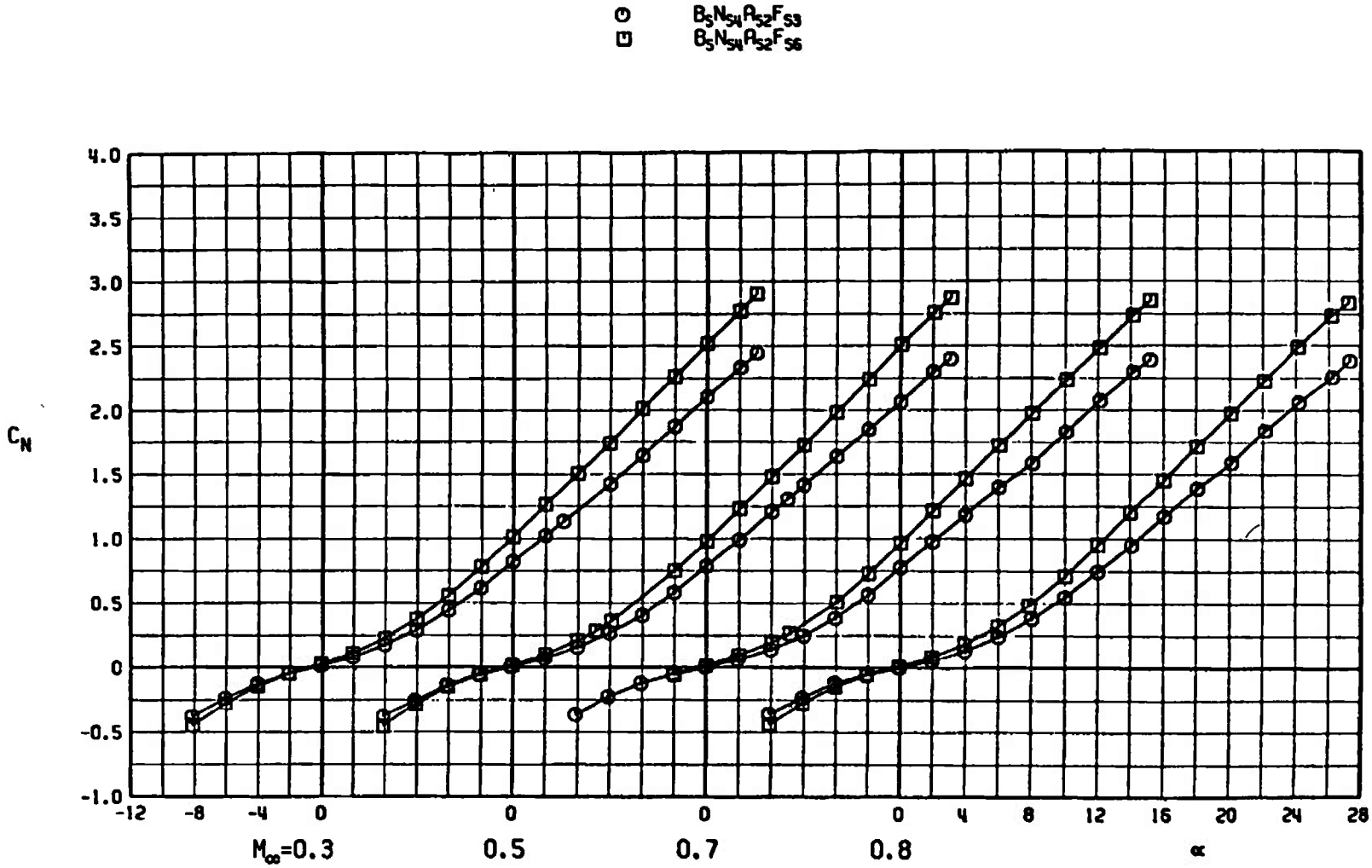

a. C_N versus α

Fig. 13 Effects of Fin Span on Longitudinal Characteristics of Model with Boattail Afterbody and Spherical-Segment Nose, $B_S N_{S4} A_{S2} F_{SX}$, $\phi = 0$

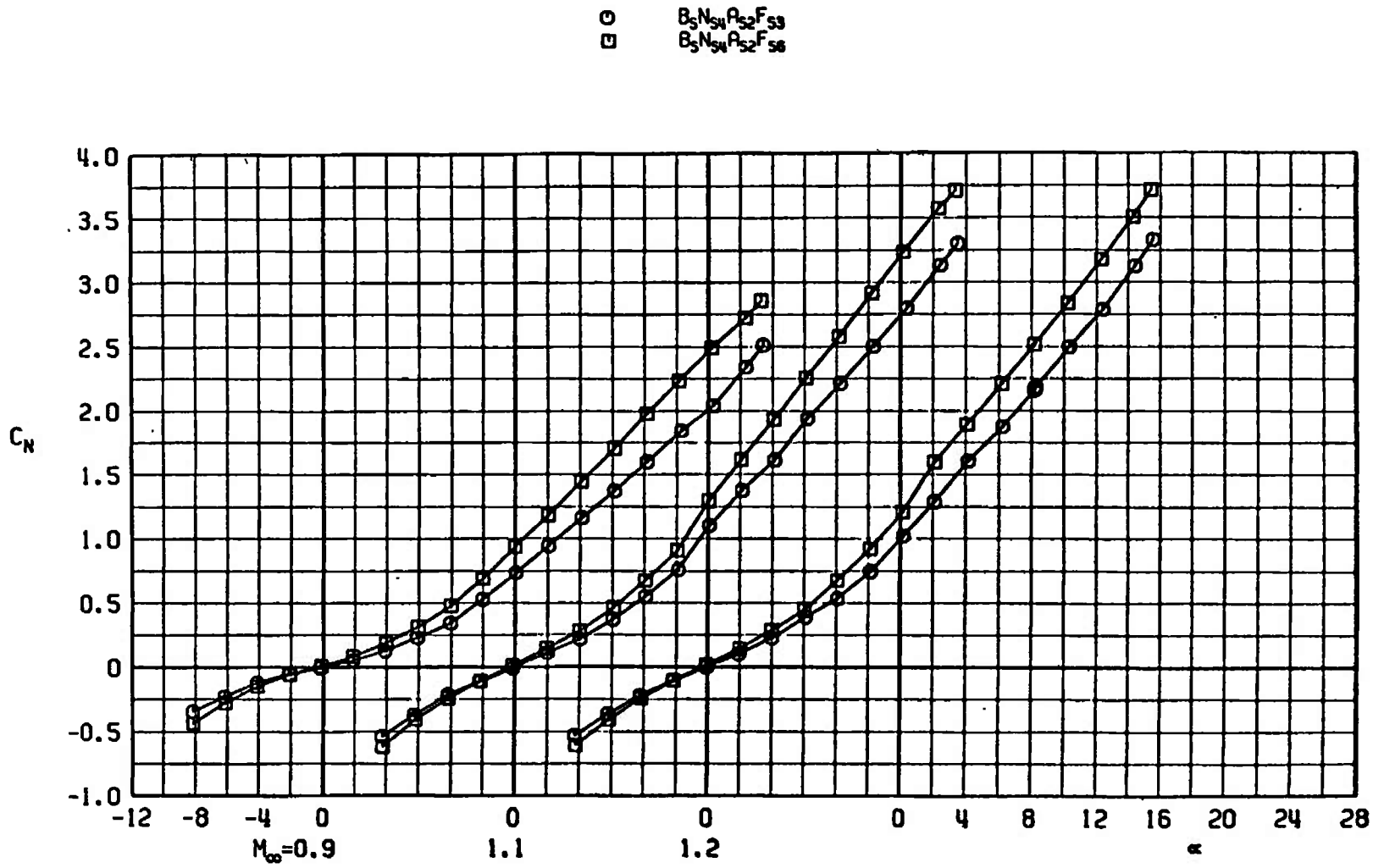

a. Concluded

Fig. 13 Continued

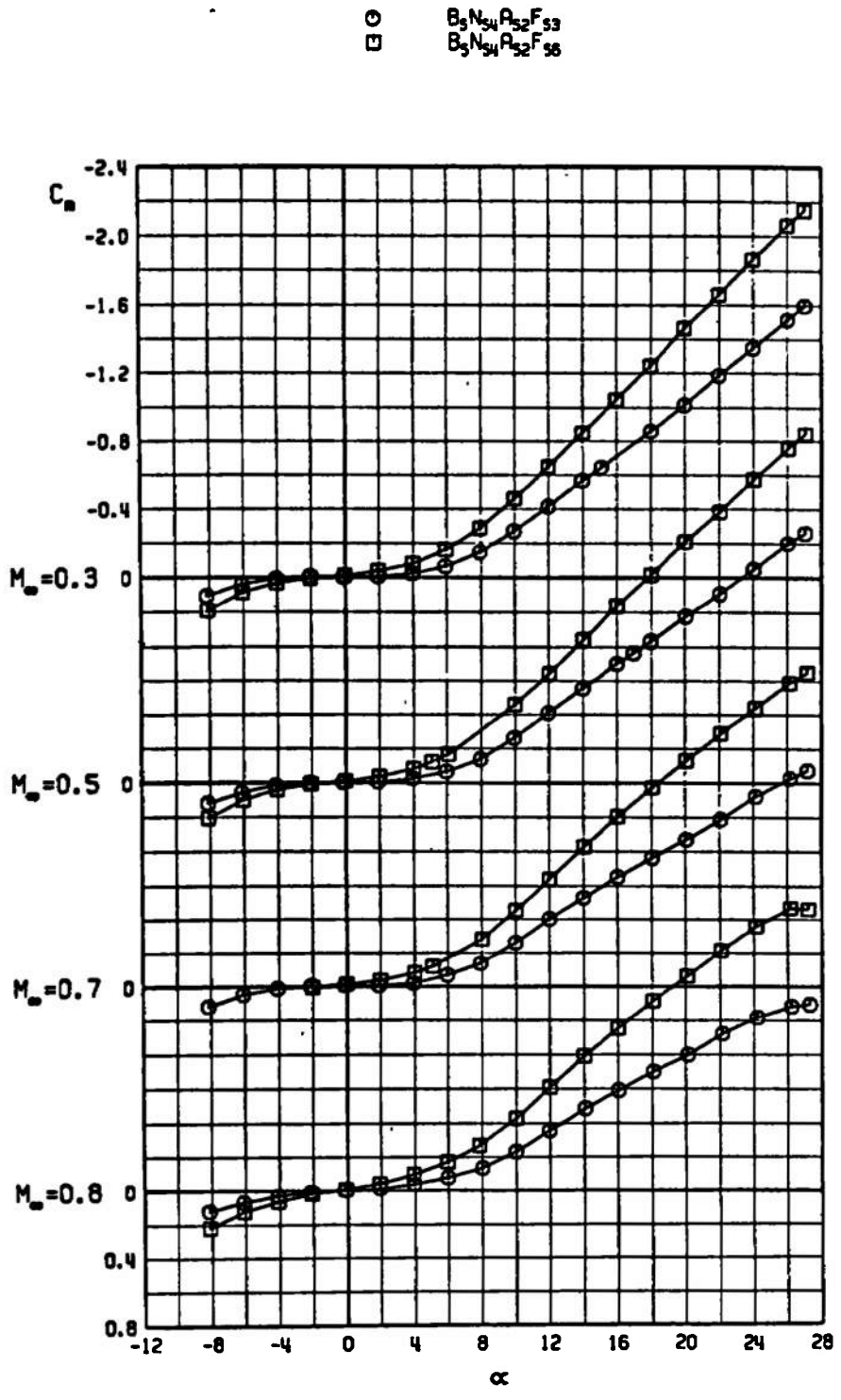

b. C_M versus α

Fig. 13 Continued

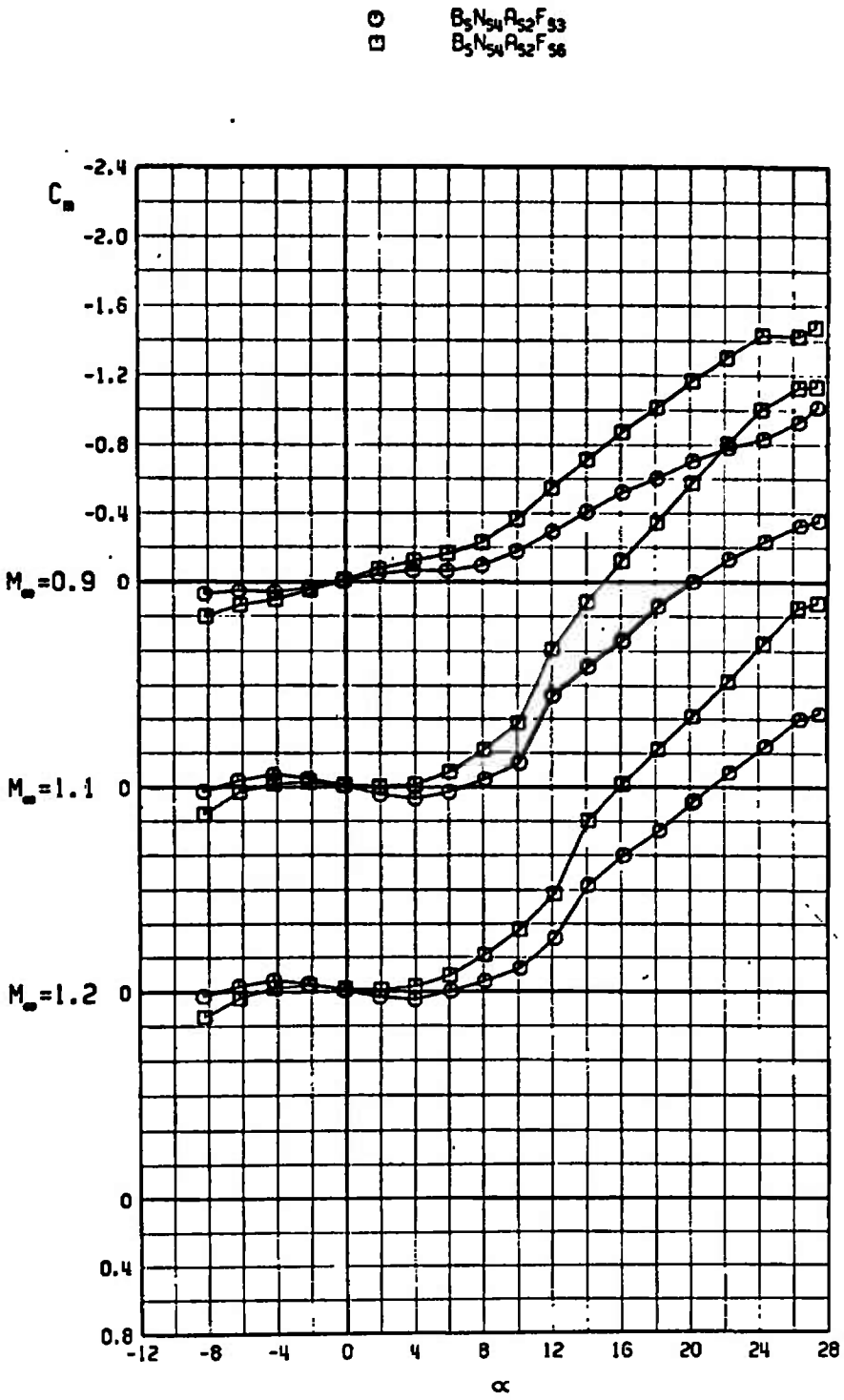

b. Concluded
Fig. 13 Continued

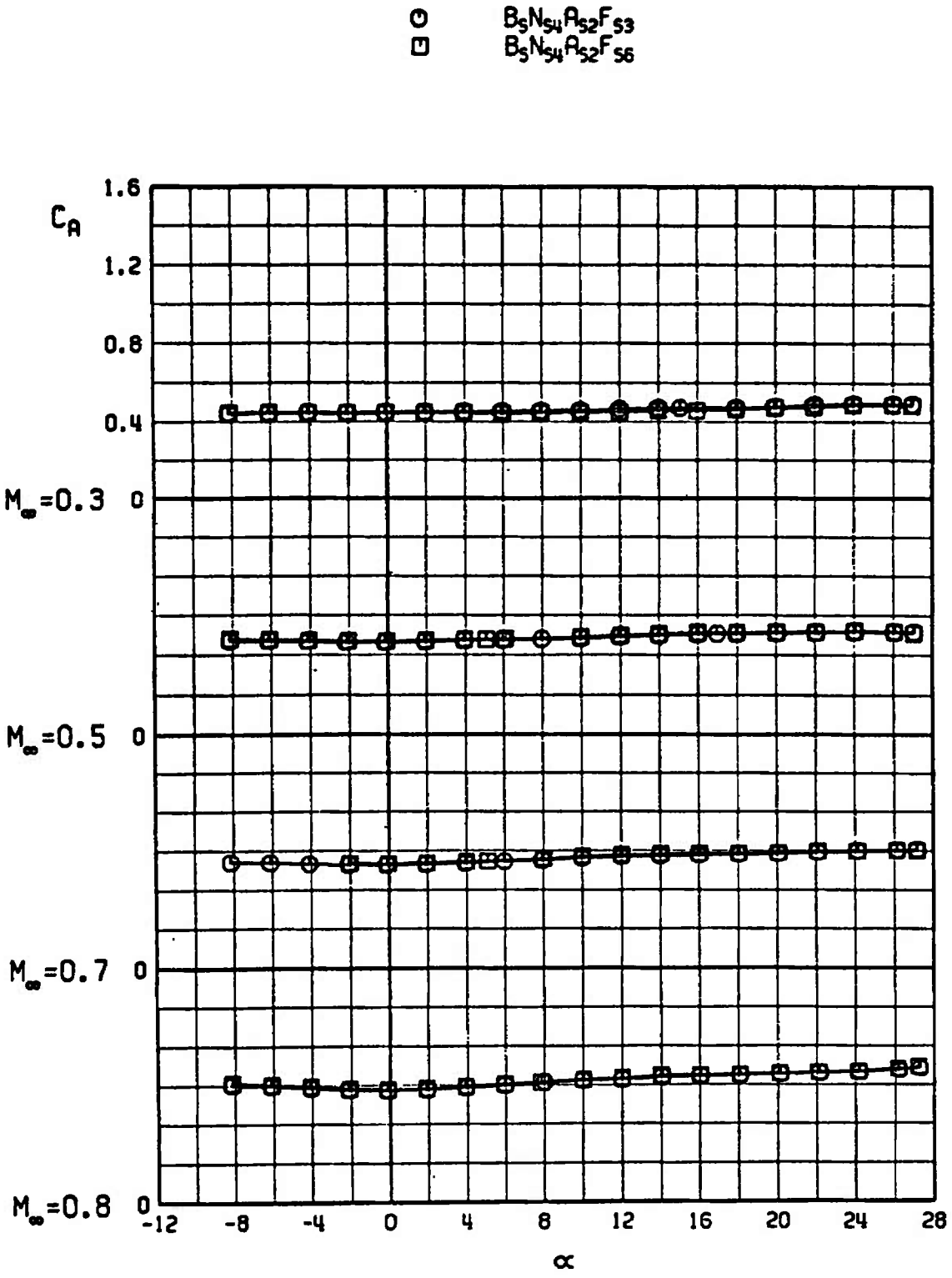

c. C_A versus α
Fig. 13 Continued

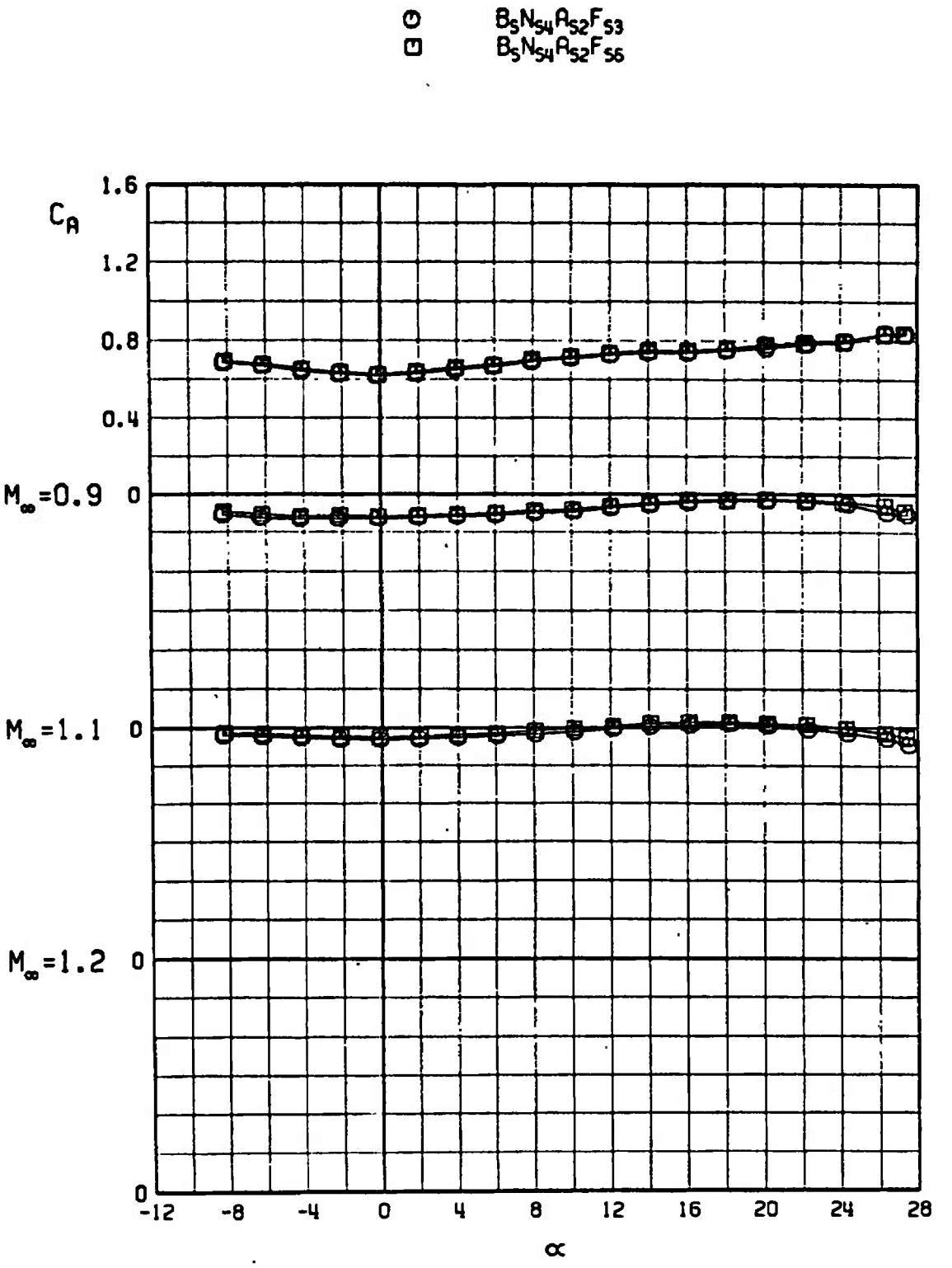

c. Concluded
Fig. 13 Concluded

UNCLASSIFIED

Security Classification

DOCUMENT CONTROL DATA - R & D

(Security classification of title, body of abstract and indexing annotation must be entered when the overall report is classified)

1. ORIGINATING ACTIVITY (Corporate author)	2a. REPORT SECURITY CLASSIFICATION
Arnold Engineering Development Center Arnold Air Force Station, Tennessee	UNCLASSIFIED
	2b. GROUP N/A

3. REPORT TITLE

TRANSONIC STATIC STABILITY CHARACTERISTICS OF BOMBLET MUNITION MODELS USED IN THE EVALUATION OF THE ZERO-CONING AERODYNAMIC DISPERSAL TECHNIQUE

4. DESCRIPTIVE NOTES (Type of report and inclusive dates)

September 16 and 17, 1971 - Final Report

5. AUTHOR(S) (First name, middle initial, last name)

T. O. Shadow, ARO, Inc.

6. REPORT DATE	7a. TOTAL NO. OF PAGES	7b. NO. OF REFS
November 1971	73	5

8a. CONTRACT OR GRANT NO.	9a. ORIGINATOR'S REPORT NUMBER(S)
b. PROJECT NO 2547	AEDC-TR-71-247 AFATL-TR-71-144
c. Program Element 62602F	9b. OTHER REPORT NO(S) (Any other numbers that may be assigned this report) ARO-PWT-TR-71-194
d.	

10. DISTRIBUTION STATEMENT Distribution limited to U.S. Government agencies only; this report contains information on test and evaluation of military hardware; November 1971; other requests for this document must be referred to Air Force Armament Laboratory (DLRA), Eglin AFB, Florida 32542.

11. SUPPLEMENTARY NOTES	12. SPONSORING MILITARY ACTIVITY
Available in DDC	AFATL (DLRA) Eglin AFB, Florida 32542

13. ABSTRACT

A wind-tunnel investigation was conducted in the Aerodynamic Wind Tunnel (4T) to determine the static stability characteristics of bomblet munition models designed for the evaluation of the Zero-Coning Aerodynamic Dispersal Technique. Force and moment data were recorded at Mach numbers from 0.3 to 1.2 at a constant Reynolds number of 2.2×10^6 per foot. Angle of attack was varied from -8 to 27 deg. Roll angle was varied from 0 to 30 deg on one configuration. The test results indicate that the configurations tested are marginally acceptable to achieve Zero-Coning dispersion.

Distribution limited to U.S. Government agencies only; this report contains information on test and evaluation of military hardware; November 1971; other requests for this document must be referred to Air Force Armament Laboratory (DLRA), Eglin AFB, Florida 32542.

This document has been approved for public release
its distribution is unlimited. Per TAB 74-11,
JTJ 24 May, 1974

DD FORM 1 NOV 65 1473

UNCLASSIFIED

Security Classification

14. KEY WORDS	LINK A		LINK B		LINK C	
	ROLE	WT	ROLE	WT	ROLE	WT
transonic flow						
bomblets						
dispersion						
fins						
roll						
static stability characteristics						
Reynolds numbers						
Mach numbers						

AFSC
Arnold AFS Tenn